Fall 2017

CRACKING IN ASPHALT PAVEMENTS: IMPACT OF COMPONENT PROPERTIES AND AGING ON FATIGUE AND THERMAL CRACKING

Reyhaneh Rahbar-Rastegar
University of New Hampshire, Durham

CRACKING IN ASPHALT PAVEMENTS: IMPACT OF COMPONENT PROPERTIES AND AGING ON FATIGUE AND THERMAL CRACKING

BY

REYHANEH RAHBAR-RASTEGAR

B.S. Civil Engineering, University of Guilan, 2005

M.S. Civil Engineering, University of Guilan, 2010

DISSERTATION

Submitted to the University of New Hampshire

in Partial Fulfillment of

the Requirements for the Degree of

Doctor of Philosophy

in

Civil Engineering

September 2017

This dissertation has been examined and approved in partial fulfillment of the requirements for the degree of Doctor of Philosophy in Civil Engineering by:

Dissertation Chair, Jo Sias Daniel,
Professor, Civil & Environmental Engineering, University of New Hampshire

Eshan V. Dave,
Assistant Professor, Civil & Environmental Engineering, University of New Hampshire

Majid Ghayoomi,
Assistant Professor, Civil & Environmental Engineering, University of New Hampshire

Geoffrey Rowe, Ph. D.
President of Abatec Inc.

Stacey Diefenderfer, Ph.D.
Senior Research Scientist, Virginia Department of Transportation

On August 8, 2017

Original approval signatures are on file with the University of New Hampshire Graduate School.

DEDICATION

To Afshin, my husband, for providing me help and encouragement that I needed in this journey. This work could not be accomplished without his support and love.

ACKNOWLEDGEMENTS

First and foremast, I would like to express my sincere gratitude to my advisor, Dr. Jo Daniel for believing in me, and her inspiring guidance and support over the last four years. Your patience, understanding, and trust motivated me to go forward in this journey. Your help and support will forever remain a major contributor behind my success and achievements.

My sincere thanks also goes to Dr. Eshan Dave. I am very grateful for your valuable advices, knowledge, and insightful discussions and suggestions. You have been an excellent mentor and a great inspiration for me. I have to thank the rest of my committee members, Dr. Stacey Diefenderfer, Dr. Geoff Rowe, and Dr. Majid Ghayoomi for their helpful comments and suggestions. Your involvement and guidance are truly appreciated.

I must also thank Dr. David Mensching who has helped me many times in providing advices as a friend. I would also like to acknowledge all the students and friends at UNH asphalt research group during my PhD program: Ashton Congalton, Dr. Yaning Qiao, Dr. Mohamed Elshaer, Mirkat Oshone, Jayne Knott, Chris Jacques, Chris Decarlo, Rasool Nemati, Saman Salari, and Katie Hasslett.

My thanks go out to Michelle Mancini and Kristen Parenteau in the Department of Civil and Environmental Engineering, and Kelly Shaw in the CEPS Business Center for their help and cooperation. I would also thank John Ahern for handling my endless lab equipment requests, and to all my friends at UNH who have been like family to me.

Last but not least, I would like to thank my beloved parents for being my first teachers and for supporting and encouraging me throughout this journey and my entire life, and to my brother, Ramin, who has always been there for listen and help.

Table of Contents

LIST OF TABLES

LIST OF FIGURES

ABSTRACT

CRACKING IN ASPHALT PAVEMENTS: IMPACT OF COMPONENT PROPERTIES AND AGING ON FATIGUE AND THERMAL CRACKING

By

Reyhaneh Rahbar-Rastegar

University of New Hampshire, September 2017

Cracking in asphalt pavements is one of the most common and critical pavement distresses. Cracks let the water penetrate from the surface to underlying layers resulting in shorter pavement service life and poor riding quality. There are various factors that affect the cracking potential of asphalt mixtures including the properties of asphalt components, mix design factors, loading time and loading mode, temperature, stress state, and aging. While several researchers have conducted studies investigating the cracking of asphalt mixtures, the effective parameters are not all well understood to allow engineers to design and construct more resistant pavements against cracking.

The work presented in this dissertation provides some additional insights into the effects of component properties and aging condition on asphalt cracking. The cracking susceptibility of hot mix asphalt (HMA) is evaluated through the experimental testing and numerical modeling on mixtures produced either in design (laboratory) or production (plant) stage. Various criteria and approaches for the prediction of cracking in asphalt binder and asphalt mixture are assessed and their correlation are discussed. Different levels of aging in laboratory are simulated, and the effects of long term oven aging (LTOA) on linear viscoelastic parameters, fatigue and

fracture characteristics of asphalt mixtures are explored. The uniaxial tensile fatigue testing based on simplified viscoelastic continuum damage (SVECD) approach is conducted to characterize fatigue behavior, and semi circular bending (SCB), disc-shaped compact tension (DCT) testing and cohesive zone model are used to evaluate thermal cracking in asphalt mixtures.

This dissertation makes a good contribution in improvement of available approaches for evaluation of cracking potential of asphalt pavements and allows for assessment of different mixtures at early stage of material selection. The results of this study can lead to develop a new parameter to predict fatigue and thermal cracking susceptibility of flexible pavements in performance-based specifications, resulting in a better ride quality and cost saving for contractors and taxpayers.

CHAPTER 1

INTRODUCTION

1.1 Statement of Problem

Annually, a lot of money is spent on maintenance and repair of pavements in the US. Cracking is one of the most common issues in flexible pavement structures which affects ride quality. Also, water penetration increases from the surface to underlying soil layers with the increase of cracking. Using recycled materials in asphalt mixtures which is a routine practice can produce stiffer mixtures which are less workable and more susceptible to cracking. The same issue occurs when the virgin mixtures age in asphalt pavements that makes the cracking assessment more complicated.

The necessity of research on cracking is well known. Fatigue (load associated) and thermal cracking (non-load associated) are two main types of cracking. A wide range of variables can impact on mixtures behavior against cracking. The fabrication method (lab versus plant), mixture combinations and volumetric design, environmental conditions, aging and recycled materials content, traffic loading volume, and pavement structure affect on both kinds of cracking. This dissertation investigates four crack-related subjects which impact on the evaluation of cracking, with the aim of a better prediction of cracking in asphalt pavements;

Plant versus lab production: The asphalt industry is moving towards the performance based methodologies. The prediction of asphalt performance and the evaluation of cracking properties in laboratory and mix design stage is desired. An important question is that how

accurate the laboratory production and testing can simulate and predict the actual cracking performance of asphalt mixtures in field. To answer to this question and investigate the correlation of lab results and actual field performance, this dissertation compares the cracking properties of similar mixtures which are produced in laboratory and plant.

Binder versus mixture parameters: In order to predict the cracking potential of asphalt mixtures in laboratory, asphalt binder and asphalt mixtures testing can be conducted. Many testing methods, approaches, and parameters have been developed to evaluate binder and mixture susceptibility against fatigue and thermal cracking. Some of the cracking criteria are developed based on the testing methods performed in linear viscoelastic modes, while the others might be designed for failure modes. Also, different loading modes (tension, tension-compression, bending, shear) might be used in testing methods. Therefore, the cracking potential of mixtures can be evaluated and ranked differently using different criteria. An extensive comparison on some of the commonly used cracking parameters is performed in this study. The results of this research aim to provide a correlation between binder and mixture cracking characteristics and help to improve the cracking performance of asphalt mixtures.

Fatigue versus thermal cracking: Although, many factors might have similar effects on two most prevalent types of cracks, fatigue and thermal cracking have different mechanisms in initiation and propagation. With this in mind, asphalt mixtures might have different behavior against fatigue and thermal cracking. While a mixture can perform very well against fatigue cracking, it might show poor performance in thermal cracking. A good understanding on the differences between fatigue and fracture mechanisms in asphalt mixtures and their evaluation is required. This study opened up a discussion on how different mixtures can behave against fatigue and thermal cracking using experimental testing and numerical modeling.

Effect of aging: Another important aspect which has a significant effect on the performance of asphalt mixtures is aging. The processes of volatilization over the mixing and compaction

of asphalt mixtures and oxidation over the pavement's service life change the properties of asphalt binder. Generally, the existence of aged binder in hot mix asphalt (HMA) increases the stiffness and decreases the ductility and relaxation capability, ultimately resulting in less cracking resistance. It might be because of either the existence of recycled materials (reclaimed asphalt pavement (RAP) and recycled asphalt shingles (RAS)) or the aging of virgin binder. The cracking assessment of asphalt mixtures in short term aging condition in laboratory is a routine practice, but the question is that how the performance of aged asphalt pavements in field can be predicted. The accelerated oven aging method helps to simulate the aging in laboratory and evaluate the properties of aged asphalt mixtures. This study provides the information on the variation of mixture properties with aging, and helps to improve the prediction of asphalt cracking.

1.2 Objectives

The main objectives of this research are:

- To compare linear viscoelastic properties and cracking behavior of mixtures produced in plant versus laboratory produced mixtures,
- To evaluate the available cracking parameters and criteria for asphalt binder and asphalt mixture and to investigate the correlation between them,
- To compare fatigue and thermal cracking behavior of different asphalt mixtures using experimental testing and numerical modeling,
- To evaluate the effect of long term aging on viscoelastic characteristics and cracking behavior of asphalt mixtures.
- To predict the cracking performance of HMA and develop a performance-based parameter by correlating binder and mixture testing results, and cracking specifications and measures

1.3 Structure of Work

This dissertation includes s series of published or publishable technical papers related to the general objective of this research which is the investigation of the effects of mixture properties on fatigue and thermal cracking behavior of asphalt mixtures.

Chapter 1 starts with an introduction about the problem statement and the necessity of research on cracking characterization, general objectives of the dissertation, and the format of work. Chapter 2 provides a comprehensive literature review on cracking related subjects such as cracking in lab produced versus plant produced mixtures, binder and mixture cracking parameters, testing and modeling of fatigue and thermal cracking, and the effect of aging on cracking.

Chapter 3 is in the form of a technical paper published by International Journal of Pavement Engineering (IJPE), entitled "Laboratory versus Plant Production, Impact of Material Properties and Performance for RAP and RAS Mixtures". In this study, 8 plant mixed, plant compacted, and 8 laboratory mixed, laboratory compacted mixtures are evaluated through binder and mixture testing. Mixture variables include aggregate gradation, binder grade and source, and recycled materials type and content. Performance grading on extracted and recovered binders, and complex modulus and SVECD fatigue testing on mixtures were conducted, and fatigue life was predicted using layered viscoelastic pavement analysis for critical distresses (LVECD) software.

Chapter 4 presents a technical paper accepted for Association of Asphalt Paving Technologists (AAPT) 2017 annual meeting and published in the International Journal of Road Materials and Pavement Design (RMPD). The title of this paper is "Comparison of Asphalt Binder and Mixture Cracking Parameters". The objective of this study is to compare binder and mixture parameters and evaluate the similarities and differences between the rankings and values

obtained. This study includes binder and mixture testing on 14 plant produced mixtures including three different binder grades, three binder sources, three aggregate gradations, and mixtures containing a range of RAP and/or RAS contents. Testing included PG grading and 4mm DSR testing on the extracted and recovered binders that were long-term aged. Mixture testing included complex modulus, SVECD fatigue, and DCT testing on short-term aged mixtures. Parameters evaluated included high and low PG temperatures, ΔT_{cr}, Glover-Rowe parameter (binder and mix-based), R value, dynamic modulus, phase angle, number of cycle to failure from SVECD and LVECD analysis, and fracture energy.

Chapter 5 of this dissertation is in the form of a technical paper submitted for American Society of Civil Engineers, Journal o Transportation Engineering (Part B: Pavements), entitled "Fatigue and Thermal Cracking Analysis of Asphalt Mixtures Using Viscoelastic Continuum Damage and Cohesive Fracture Models". This study evaluated fatigue and thermal cracking performances for nine asphalt mixtures using three approaches: simplified viscoelastic continuum damage model, thermal stress based cracking prediction and cohesive zone fracture model. The laboratory testing including SVECD uniaxial fatigue and disc shaped compact tension test were performed and the results are compared. To compare the fatigue and thermal cracking performance of the mixtures, Fatigue and thermal cracking performance predictions were conducted using LVECD, thermal cracking model used in Pavement ME and IlliTC thermal cracking simulation systems.

Chapter 6 is comprised of a manuscript to be submitted for publication entitled "Impact of Aging on Cracking Behavior of Asphalt Mixtures". The main focus of this chapter is how the fatigue and thermal cracking behavior of mixtures change as the asphalt mixtures undergo different levels of aging in laboratory. In this study, 10 plant produced, lab compacted mixtures are evaluated at different aging levels. The loose mix asphalt is age conditioned at three levels: 24 hr. @ 135°C, 5 days @ 95°C, & 12 days @ 95°C. The compacted specimens also are

exposed to aging for 5 days @ 85°C following AASHTO R-30. The mixtures contain a range of recycled materials, various virgin binder grades, binder sources, and nominal maximum aggregate size. Comparison between mixtures is conducted by constructing dynamic modulus master curves & Black space diagrams from complex modulus test data. Simplified Viscoelastic Continuum Damage testing, and Semi-Circular Bending fatigue testing are used to compare the fatigue behavior. The thermal cracking behavior is evaluated using Disc-shaped Compact Tension testing and cohesive zone modelling approach.

Chapter 7 provides a closing discussion on the objectives of this dissertation, and the author's progression on evaluation methods of cracking.

At the end, a master reference list and the appendix including the supporting figures and tables used in this dissertation work are presented.

Chapter 2

LITERATURE REVIEW

To satisfy the objectives of this study, a review on the relevant literature was conducted. As mentioned earlier, the format of this dissertation is a series of accepted or submitted journal papers with the scope of the evaluation of cracking in asphalt mixtures. Chapter 2 includes four sections related to differences in design and production stages, testing methods and parameters of asphalt binder, testing methods, models and parameters related to asphalt mixtures, and asphalt aging. The information provided in this chapter aim to identify and classify the findings and efforts related to the scope of this dissertation.

2.1 Asphalt Concrete Production in Plant and Laboratory

Agencies are moving towards the performance-based design methodologies for asphalt pavements, and different methods to evaluate the asphalt performance in the laboratory have been developed. The laboratory performance can be evaluated at the mix design and/or production stages. It is desired to predict the performance of asphalt mixtures in the mix design stage. Accordingly, a good understanding of differences in the behavior of mixtures produced in the laboratory and plant is required to assess anticipated field performance at the mix design stage. Figure 2.1. shows the asphalt production in laboratory and plant.

Earlier studies have been performed on the comparison of asphalt mixtures produced in laboratory and plant. Most studies show that the lab produced mixtures are stiffer than the

mixture produced in plant (Mogawer et al. 2012; Xiao et al. 2014). A recent study by Daniel et al. (2017) shows there is not a significant difference between the linear viscoelastic characteristics and fatigue cracking properties of a mixture produced in plant and lab (reheated and without reheating).

There are many factors that can cause differences in properties of plant versus lab produced mixtures, resulting in different behavior against cracking. Based on the scope of this study, this section is only focused on some of the factors that might be source of differences between the plant produced and lab produced asphalt mixtures.

Figure 2-1. Asphalt Production in Laboratory and Plant

2.1.1 Handling, Storage, and Sampling

One source of difference in the properties of plant produced and lab produced asphalt mixtures can be different types of handling of asphalt binder, aggregate, and recycled materials in plant and lab. The aging process of asphalt binder in lab and plant might take place differently. In the lab, asphalt binders are kept in small containers and at the room temperature that is not consistent, while all the tanks to maintain the asphalt binder in plant and asphalt pumps are enclosed systems in order to minimize the effect of aging. The storage condition after mixing is also different. The storage of asphalt mixtures in the silos in plant might result in an excessive age hardening of asphalt binder and mixture. Jacques et al. (2016) investigated the effect of

silo storage time on asphalt mixtures characteristics using different testing methods and found the short term aging condition in laboratory does not necessarily simulate the aging condition in plant.

The stockpiles of fine and coarse aggregates are made to store the aggregate in plant, while the aggregate are break down in more size fractions in laboratory and sorted in buckets to minimize the effect of segregation. Inclusion of recycled materials in the production of asphalt concrete is another parameter that can make differences between lab and plant produced mixtures (NCHRP report No. 673).

2.1.2 Mixing and Compaction

Different types and size of mixers and machines in laboratory and plant is definitely an important source of difference. The mixing operation in lab is performed by placing the aggregate, asphalt binder, and recycled materials or other additives in required amounts in a small mixing container and a mechanical mixing apparatus is used to mix the materials. In plants, the size and length of mixer, aggregate amount, the shape and size of flights, and many other factors might result in different aggregate breakdown and mineral fillers, different adhesion of thin film of binder to aggregate, and generally different mixture's properties (NCHRP report No. 673).

The performance of asphalt pavements is strongly influenced by the compaction level and the density of asphalt layer. Different compaction levels result in different air voids between lab and plant produced mixtures which can contribute to different cracking behavior. The compaction of asphalt samples in the lab is performed using Superpave gyratory compactor (SGC) machines following AASHTO T 312 "Preparing and Determining the Density of Hot-Mix Asphalt Specimens by Means of Superpave Gyratory Compactor" at a specific gyration level or height. The cylindrical molds and plates should be heated to the compaction

temperature. The compaction in field is completely different process than the compaction in lab.

2.1.3 Temperature

The properties of asphalt binder change significantly by temperature variation. Different temperatures during the process of asphalt production can make different levels of aging in asphalt binder. Lolly (2013) evaluated the effect of mixing temperature and exposure time on the aging and properties of different binders and mixtures. Mixing and compaction temperatures are calculated based on the viscosity of binder and can be determined from AASHTO T 245 section 3.3.1. The binder viscosity of 150 to 190 Pa-s and 250 to 310 are related to mixing and compaction temperatures, respectively. In the lab, materials are heated in ovens before mixing to get to the mixing temperature. The loose mix asphalt also is placed and heated in oven for about 2 to 4 hours at compaction temperature before being compacted. However, the temperature for lab produced samples vary with the actual time of heating in oven (depending on how long mixing and compaction takes for all the materials), types and amount of materials, and size and type of ovens (NCHRP report No. 673).

2.2 Binder: Testing and Cracking Parameters

Several researchers have been working on cracking index parameters that are determined from tests conducted on asphalt binders to assess cracking potential (Kandhal & Koehler, 1987; Bahia et al. 2001; Rowe et al. 2014; Anderson et al. 2014; Yao, et al. 2016;). In this section, only the parameters and approaches which are used in this study are discussed.

The first researches on asphalt binder cracking characterization was conducted under Strategic Highway Research Program (SHRP) program in 1990's. AASHTO binder specification M320 "Standard Specification for Performance-Graded Asphalt Binder" was developed based on the

results of this 5-year program. This standard includes a variety of binder testing to determine the binder grade considering the performance of binder against rutting and cracking.

G*sin δ is the binder rheology parameter suggested for fatigue cracking performance of asphalt mixtures at intermediate temperature, with a maximum value of 5000 kPa for asphalt binders subjected to long-term laboratory aging. The parameter is determined from testing on PAV residue, 25 mm diameter binder samples following AASHTO T315 using a dynamic shear rheometer (DSR). Although development of this parameter was an improvement in the evaluation of binder parameters, it is well recognized that it has many shortcomings and is not able to predict the fatigue properties of asphalt binders correctly (Hajj & Bhasin, 2017).

Another binder testing in Superpave binder specification is conducted using the bending beam rheometer (BBR), AASHTO T 313 "Determining the Flexural Creep Stiffness of Asphalt Binder Using the Bending Beam Rheometer (BBR)", to evaluate thermal cracking behavior of asphalt binder. This test is conducted at a temperature 10°C warmer than the binder low temperature grade on long term residue samples from PAV, to measure the creep stiffness and relaxation properties of asphalt binder.

Figure 2-2 shows a typical creep stiffness curve versus time obtained from a BBR test. The creep stiffness can be converted to thermal stress induced in asphalt binder because of thermal contraction, and the higher stiffness can be indicator of higher thermal stress. The slope of creep stiffness curve at 60 seconds (m value) shows the rate at which the thermal stress is relieved in binder. The maximum value of 300 MPa for creep stiffness (S) and the minimum value of 0.300 for the slope of creep stiffness curve (m) at 60 s are considered as measures of thermal cracking.

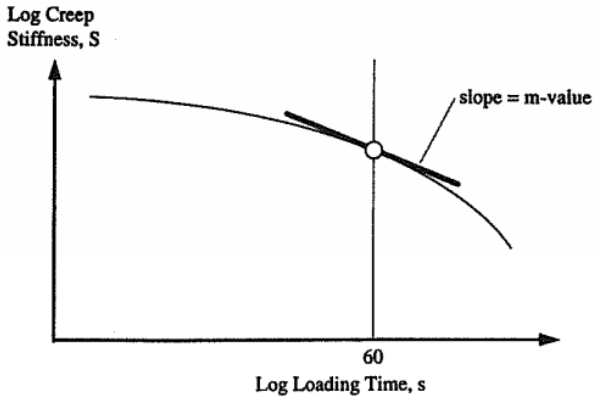

Figure 2-2. Creep Stiffness Curve (Brown et al. 2009)

It's well recognized that as the binder materials age, the difference between the critical temperatures predicted by S and m values widens. This difference is suggested by Anderson et al. (2011) as an index (ΔT_{cr}) to predict the thermal cracking potential of asphalt binders (Equation 2.1).

$$\Delta T_{cr} = T_{cr\,(stiffness)} - T_{cr\,(m\,value)} \quad 2.1$$

The cracking potential of asphalt binders is expected to be higher as the ΔT_{cr} value becomes more negative. Anderson et al. (2011) and Rowe (2011) recommended two minimum thresholds of -2.5 and -5 for ΔT_{cr} as cracking warning and cracking limit, respectively. Cracking warning is where the risk of crack should be identified and preventative action should be taken. Crack limit means the materials need the immediate remediation to prevent thermal cracking.

Christensen-Anderson model (CA model, 1993) is an asphalt binder rheological model that describes the complex shear modulus and phase angle by Equations 2.2 and 2.3, respectively.

$$G^*(\omega) = G_g \left[1 + \left(\frac{\omega}{\omega_0}\right)^{-\frac{\log 2}{R}}\right]^{-R/\log 2} \quad 2.2$$

$$\delta(\omega) = \frac{\pi}{2}\left[1 + \left(\frac{\omega}{\omega_c}\right)^{\frac{\log 2}{R}}\right]^{-1} \quad 2.3$$

where $G^*(\omega)$ = complex modulus, $\delta(\omega)$ = phase angle, G_g= glassy modulus, R= rheological index, ω= test frequency, and ω_c= crossover frequency. The R value is a parameter which describes the shape and skewness of shear modulus spectrum. It is defined as the difference between the log G* at crossover frequency and the log elastic asymptote of the master curve (Anderson et al., 1994). The Crossover frequency is the frequency at which the phase angle of binder is 45˚. As the asphalt binder ages, the shape of modulus master curve changes, resulting in changes in shape parameters. With increase of aged binder, the master curve tends to flatten. As a result, the crossover frequency decreases and rheological index (R value) increases (a wider relaxation spectra), (Jacques, et al., 2015). Mogawer et al. (2015) showed that crossover frequency versus R value plot can be an indicator of relative aging of mixtures. The Christensen-Anderson-and Marasteanu (CAM) model (2002) tried to modify the CA model for polymer modified binders especially at high and low frequencies.

The research conducted by Glover et al (2005) proposed a parameter in order to predict the cracking resistance of asphalt binders. This parameter, $G'/(\eta'/G')$, relates the storage shear modulus (G') and dynamic viscosity (η') to ductility at a combination of temperature and frequency (Glover et al., 2005). In a study on airport pavements, Anderson (2011) identified that the thermal cracking potential is correlated with the Glover parameter and ΔT_{cr} value. Later, in a discussion on Anderson study, Rowe presented an expression using some simplifications on the Glover parameter, as Glover-Rowe (G-R) parameter, to assess the cracking potential of asphalt binder. G-R parameter (Equation 2.4) captures the shear modulus and phase angle of binder in temperature-frequency combination of 15°C and 1 rad/s. Two boundary levels of 180 and 600 kPa are recommended as crack onset and significant cracking, by Rowe, and Anderson et al (2011), respectively.

$$\frac{G^*(Cos\ \delta)^2}{Sin\ \delta} \qquad 2.4$$

Where G* is complex shear modulus and δ is phase angle. Figure 2.3 shows two Glover-Rowe boundary levels in Black space diagram. Black space diagram is a rheological plot which represents the shear modulus versus phase angle, to evaluate the stiffness and relaxation of asphalt materials in one plot.

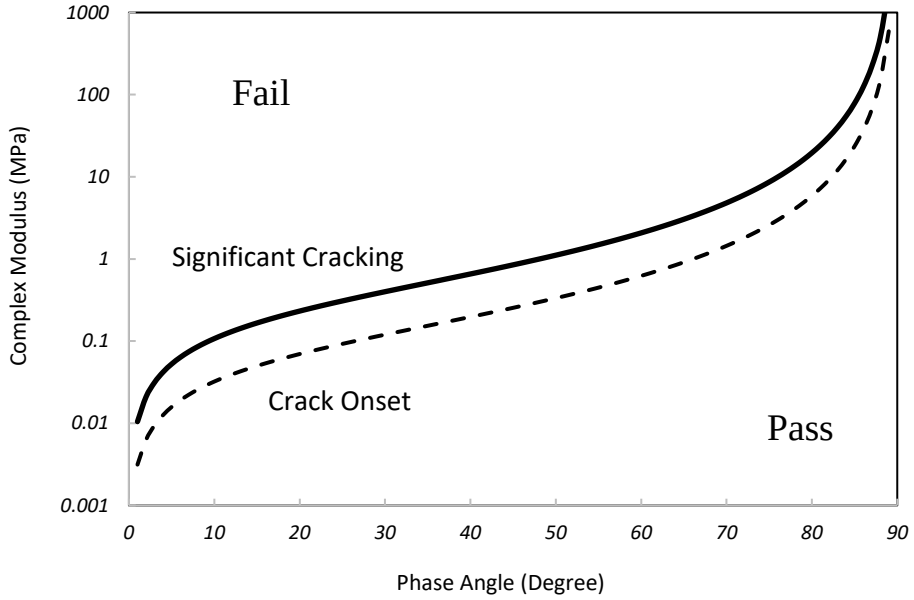

Figure 2-3. Glover-Rowe Black Space Diagram

Generally, the Black space diagrams capture both stiffness and relaxation properties together and make the interpretation of cracking performance more accurate. With the increase of complex shear modulus (G*) and decrease of phase angle (δ), the probability of cracking and being failed will increase. Accordingly, it's expected that as binder ages or the percent of recycled material in the mix increases, the location on the diagram goes to up and left and the mixture would be more prone to cracking. The shear modulus and phase angle values can be captured using a 4mm DSR device in a wide range of temperature and frequencies.

2.3 Mixture: Testing, Models and Cracking Parameters

Cracking is one of the main types of distresses in asphalt concrete pavements, categorized in two main groups: load associated (mainly fatigue cracking) and non-load associated cracking

(thermal cracking). The mechanism of initiation and propagation of these cracks is different. Fatigue cracking occurs when tensile strains in pavement exceed the tensile strength of material due to repetitive traffic loading, resulting in microcracks that grow and coalesce into macrocracks that lower pavement smoothness and integrity. Fatigue cracks can initiate at the bottom of the pavement layer (bottom-up) or near the pavement surface (top-down). Thermal cracking, common in cold climates, occurs when the thermal stress that builds up during cooling events in the pavement exceeds the tensile strength of the asphalt. Cracked pavements allow water to infiltrate to underlying pavement layers, further weakening the pavement and leading to a rougher ride and shorter service life.

In this section, some of the widespread in use and well known methods and models for testing and analysis of fatigue and thermal cracking used in this study are presented.

2.3.1 Fatigue Cracking

Fatigue cracking (also called alligator cracking) is a common type of distress in HMA pavements. Many researches have tried to characterize fatigue cracking by developing testing methodologies and approaches,

2.3.1.1 Testing Methods

It is undeniable that the complete simulation of filed condition in laboratory is impossible, due to the effect of some unpredictable variables. However, different researchers have put effort into developing the methods to be able to represent a more realistic condition of field in laboratory.

Beam Flexural Fatigue tests are the primary and widely used test methods to characterize fatigue cracking behavior of asphalt mixtures. The asphalt concrete beam is supposed to simulate the performance of asphalt pavement that is under bending load in field. The test can be performed in both stress- and strain-controlled modes.

Four-point bending tests on HMA beam is performed following AASHTO T 321 “Determining the Fatigue Life of Compacted Hot Mix Asphalt (HMA) Subjected to Repeated Flexural Bending”. In this test, small HMA beams are placed in device and subjected to repetitive flexural bending loads (Figure 2-4).

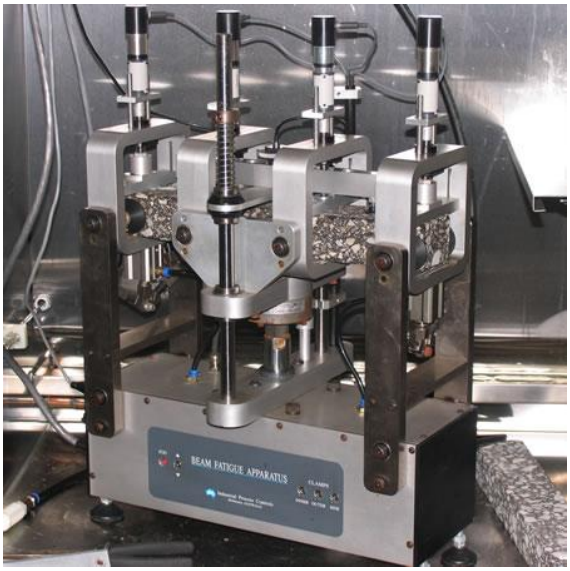

Figure 2-4. Flexural Fatigue Device Loaded with HMA Beam (pavementinteractive.org)

One of the fatigue tests developed in Europe is the Trapezoidal Cantilever Beam Test. In this test a trapezoidal beam is fixed on its larger end and the load is applied to the smaller end of cantilever beam (Figure 2-5). The test can be performed either in controlled stress or controlled strain modes. The sinusoidal load applies until the failure happens in the beam. The definition of failure criterion depends on the testing mode.

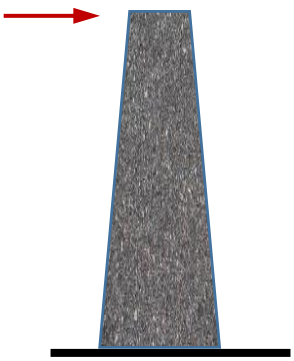

Figure 2-5. Typical Shape of Trapezoidal Cantilever Beam

Indirect Tensile (IDT) fatigue test is another testing method to evaluate the fatigue behavior of asphalt mixtures. At the beginning in 1970s, this test has been used by several researches (Moore and Kennedy, 1971; Navarro and Kennedy, 1975; Cowher, 1975). This test is conducted on cylindrical specimens compacted by Superpave gyratory compactor or cored from field, with a diameter of 150 mm (Figure 2-6). The specimen is subjected to a vertical load inducing an approximately uniform tensile stress in the specimen, and the horizontal and vertical strain values are measured.

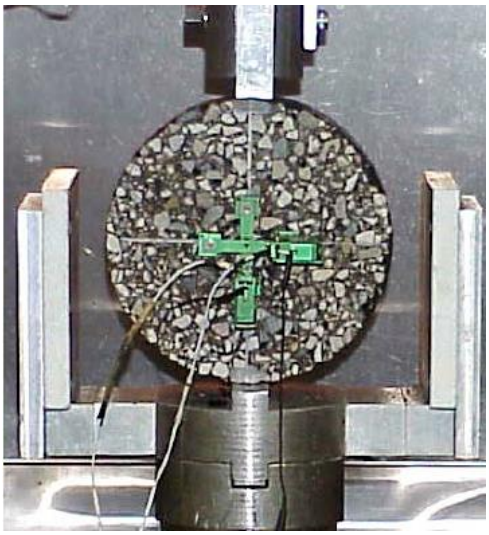

Figure 2-6. Indirect Tensile Fatigue Test Configuration

Uniaxial direct tension test is designed to evaluate the fatigue behavior of asphalt mixtures and is conducted following AASHTO TP 107 “Determining the Damage Characteristic Curve of Asphalt Concrete from Direct Tension Cyclic Fatigue Tests”. The specimens are cored from SGC samples in 100 mm in diameter and 130 mm in height. DEVCON® steel putty is used to glue the end plates to the specimens. Four LVDTs with a 70 mm gauge length are mounted to measure deformation. According to current protocol, testing temperature is supposed to determine based on virgin binder PG grade used in the mixture

Damage analysis for each mixture is performed and damage characteristic curves (DCC) are obtained using subroutines within the software and fatigue performance predictions are made

using the models available within the Alpha-F software. Also, the fatigue cracking resistance is assessed by fatigue failure criterion of asphalt mixtures versus number of cycles. Figure 2-7 shows a fatigue testing specimen and its configuration in AMPT.

Figure 2-7. Uniaxial Direct Tension Test Configuration

2.3.1.2 Models and Parameters

Simplified viscoelastic continuum damage, SVECD, model is a VECD approach that has been simplified for cyclic loading conditions using asphalt mixture performance tester (AMPT) to characterize the fatigue characteristics. Kim and Little (1990) initially presented a mechanistic approach resulted in Viscoelastic continuum damage (VECD) model. They applied the time-domain one dimension VECD model to asphalt concrete in cyclic domain and developed a uniaxial constitutive equation to predict the effects of loading (Kim and Little 1990). By applying Schapery (1984)'s elastic-viscoelastic correspondence principle, Kim and Lee 1998 presented a viscoelastic constitutive model with growing damage and healing.

The next step in VECD model timeline was taken by Daniel and Kim 2002. They indicated that viscoelastic material response under uniaxial tensile testing is independent of temperature,

loading type, and frequency. Accordingly, the results of a uniaxial tensile testing at a specific condition can be extended to different testing conditions. Also, the other researchers (Chehab et al. 2003 and Chehab et al. 2006) have studied on the other aspects of VECD such as the inclusion of viscoplasticity and application of three-dimension damage formulation.

Generally, viscoelastic continuum damage model relies on three important principles: elastic-viscoelastic correspondence, continuum damage mechanics, and time-temperature superposition with growing damage. Elastic-Viscoelastic correspondence principle developed by Schapery (1984) suggested the constitutive equations for viscoelastic materials are the same as those of elastic materials, by using pseudo variables instead of physical stain and stress (Daniel, 2001). Accordingly, the correspondence between linear elastic (LE) and linear viscoelastic (LVE) is shown in equation 2.5, where ε^R is pseudo strain (equation 2.6).

$$(LE) \quad \sigma = E\varepsilon \qquad \Leftrightarrow \qquad (LVE) \ \sigma = E_R\varepsilon^R \tag{2.5}$$

$$\varepsilon^R = \frac{1}{E_R}\int_0^t E(t-\tau)\frac{d\varepsilon}{d\tau}d\tau \tag{2.6}$$

The advantage of SVECD model is that both complex modulus and SVECD fatigue testing are compatible with AMPT and can be performed by one machine. In the other words, to identify the linear viscoelastic (LVE) characteristics of asphalt mixtures, first, dynamic modulus value |E*| is determined, and then the uniaxial fatigue testing is conducted to obtain the fatigue data. Also, the outcomes obtained from a single loading and temperature condition and be applied to any uniaxial fatigue testing in different loading and temperature conditions. Accordingly, using this method reduces the testing and analysis time.

Parameters

It is well recognized that the linear viscoelastic (LVE) characteristics of asphalt mixtures affect on cracking behavior of mixtures. Stiffness (dynamic modulus) and relaxation capability

(phase angle) are two parameters that should be considered while evaluating the cracking potential. Generally, it is expected to have higher cracking potential for the mixtures with higher stiffness and lower relaxation capability (Mensching et al. 2015). These parameters can be determined for asphalt mixtures from the results of complex modulus testing (AASHTO TP 342).

Using time temperature superposition principle (TTSP), the raw data obtained from complex modulus testing can be shifted and dynamic modulus master curve is produced. The sigmoidal models are used to model the dynamic modulus master curve of asphalt mixtures. Standard (ARA Inc., 2004) and the generalized (Rowe, 2009) sigmoidal equations are presented in Equations 2.7 and 2.8, respectively.

$$\log|E^*| = \delta + \frac{\alpha}{1+e^{\beta+\gamma\log(\omega)}} \quad 2.7$$

$$\log|E^*| = \delta + \frac{\alpha}{[1+\lambda e^{\beta+\gamma\log(\omega)}]^{1/\lambda}} \quad 2.8$$

where, $|E^*|$ is dynamic modulus, ω_r is reduced frequency, and α , β, δ, λ and γ are the fitting coefficients. The shape of dynamic modulus master curve can vary with changing the coefficients as follows: equilibrium modulus ($E_\infty = 10^\delta$) is the lower asymptote, glassy modulus ($E_g = 10^{\delta+\alpha}$) is the upper asymptote, and the frequency at inflection point can be calculated from $10^{-\beta/\gamma}$. The width of relaxation spectra and its non-symmetric property can be defined by γ and λ, respectively (Rowe et al. 2009, Mensching et al. 2016).

Mensching et al. (2016) discussed the impact of fitting parameters on the shape of dynamic modulus master curves. As materials age, the dynamic modulus master curve tends to be flatter, and the inflection points moves to the lower frequencies, resulting in an increase in γ and β values (the absolute values decrease). Crossover frequency parameter ($-\beta/\gamma$) versus relaxation spectra width parameter (γ) plot for mixtures is similar to crossover frequency versus R value plot for binders. This plot can be a criterion for cracking potential of asphalt mixtures.

However, this method is very new, and more investigation and efforts are required to develop a mixture cracking indicator based on this concept.

Mensching (2015) evaluated the combinations of $|E^*|$ and δ, to capture the effects of stiffness and relaxation together on low temperature cracking performance of mixtures, in 20°C- 1Hz and 20°C- 0.5Hz temperature-frequency for different data. This study was performed on a variety of lab and plant produced mixtures, and field cores. Four parameters of storage modulus, loss modulus, $|E^*| \tan \delta$, and $\frac{E^*(Cos\ \delta)^2}{Sin\ \delta}$ were considered in the study to determine a failure line in Black space diagram, but neither showed a very good correlation for the available data.

In another study, Mensching et al. (2016), developed an expression for asphalt mixtures similar to G-R parameter. Using the results of TSRST testing method, they employed stiffness and relaxation capability of asphalt mixtures ($|E^*|$ and δ) at the frequency of 0.01666 rad/s and temperature 10°C warmer than the PG low temperature of binder and suggested Equation 2.9 as a cracking criterion.

$$|E^*|(\cos\delta)^2/(\sin\delta) \leq 3.68E4\ MPa \qquad 2.9$$

Several laboratory testing have been developed to characterize cracking behavior of asphalt mixtures. Some of the methods will be discussed in section 2.3. In this section, a number of criteria and parameters developed for mixture laboratory testing are presented.

Considering the nature of fatigue cracking which is the result of repetitive loading, fatigue life or the number of cycles to failure (N_f) is one of the common criteria for the evaluation of fatigue cracking in asphalt mixtures testing. It is clear that the higher number of cycles shows a better resistance against fatigue cracking. This parameter is used in many laboratory fatigue testing. However, the definition of failure point at which the number of cycles is measured is not unique.

Generally, the failure criteria in controlled strain testing methods is widely supposed to be 50% of reduction in initial modulus, but for controlled strain tests, the number of cycles at 10% of initial stiffness is considered to be the fatigue life. Another criterion to determine the fatigue failure is when the phase angle starts to decrease. It happens when a crack appears in the specimen (Artamendi & Khalid, Brown et al., 2009, Li & Mensching, 2017, Tayebali, 1977, van Dijk & Visser, 1977).

Fatigue Endurance Limit (FEL) is another material property to evaluate the fatigue behavior. The main concept goes back to 1970, when Monismith (1970) identified that the variation of relationship between the number of cycles to failure and the tensile strain at the bottom of asphalt layer is significant at the low strain levels. The endurance limit is defined as a strain level below which there is no cumulative damage over an indefinite number of load cycles (NCHRP report No. 646). This parameter can be used for relative comparison of cracking behavior of asphalt mixtures.

The main results of S-VECD method can be presented in the format of damage characteristic curve (DCC), the energy-based fatigue failure criterion versus number of cycles ($G^R - N_f$), and tensile strain versus number of cycles (ε_t - N_f).

Although the analysis of S-VECD fatigue testing is conducted using the Alpha fatigue software by Instrotek, the equations 2.10 to 2.13 are the primary relationships used to analysis obtained data and determine DCC (Underwood, 2011).

$$\varepsilon_R = \begin{cases} \varepsilon_R = \frac{1}{E_R}\int_0^{\xi} \int E(\xi-\tau)\frac{d\xi}{d\tau} & \xi \le \xi_P \\ \varepsilon^R_{0,ta_{cycle\,i}} = \frac{1}{E_R}\frac{\beta+1}{2}\left(\left(\varepsilon_{0,pp}\right)_i |E^*|_{LVE}\right) & \xi > \xi_P \end{cases} \quad 2.10$$

$$C = \begin{cases} C = \frac{\sigma}{\varepsilon^R DMR} & \xi \le \xi_P \\ C^* = \frac{\sigma_{0,ta}}{\varepsilon^R_{0,ta} DMR} & \xi > \xi_P \end{cases} \quad 2.11$$

$$dS = \begin{cases} (dS_{transient})_{timestep\ j} = \left(-\frac{DMR}{2}(\varepsilon^R)_j\,\Delta C_j\right)^{\frac{\alpha}{1+\alpha}}\left(\Delta\xi_j\right)^{\frac{1}{1+\alpha}} & \xi \le \xi_P \\ \left(dS_{cyclic}\right)_{cycle\ i} = \left(-\frac{DMR}{2}\left(\varepsilon^R_{0,ta}\right)^2\,\Delta C_j\right)^{\frac{\alpha}{1+\alpha}}\left(\Delta\xi_p K_1\right)^{\frac{1}{1+\alpha}} & \xi > \xi_P \end{cases} \quad 2.12$$

$$K_1 = \frac{1}{\xi_f - \xi_i}\int_{\xi_i}^{\xi_f}\left(f(\xi)\right)^{2\alpha}\,d\xi \quad 2.13$$

Where $\varepsilon^R_{0,ta}$= Tension amplitude of pseudo strain for given cycle, β = quantity to determine proportion of tensile loading in cycle, C^* = pseudo secant modulus in cycle portion, DMR = dynamic modulus ratio from LVE testing, $\varepsilon_{0,pp}$= peak to peak strain for given cycle, ξ_P= pulse time, $\sigma_{0,ta}$ = tension amplitude of stress for given cycle, and $f(\xi)$ = loading function.

One of the energy based fatigue failure criteria developed by North Carolina State University is G^R. G^R is the rate of change of the averaged released pseudo strain energy (per cycle) throughout the entire history of the test, and calculated from the Equation 2.14.

$$G^R = \frac{\int_0^{N_f} W_C^R}{N_f^2} \quad 2.14$$

Where W^R_C is total released pseudo strain energy, and N_f is the number of cycles before failure (Sabouri and Kim, 2014).

2.3.2 Thermal Cracking

Thermal cracking mechanism is totally different from that of fatigue cracking. This kind of cracking that is common in cold climates occurs when the pavement temperature drops significantly, and the thermal stress in the pavement exceeds the tensile strength of asphalt. Various testing methods are developed to assess this kind of cracking, but some common and recent tests are discussed in the following section.

2.3.2.1 Testing Methods

The indirect tension (IDT) testing method is discussed in the previous section (2.3.1) to characterize fatigue cracking. This test can also be conducted at low temperature to assess the thermal cracking properties of asphalt mixtures, following AASHTO T 322 “Determining the Creep Compliance and Strength of Hot-mix Asphalt (HMA) Using the Indirect Tensile Test Device”.

This method includes two parts of measuring creep compliance and determining tensile strength and strain at failure. In the first part (creep compliance), a static load is applied on diametral axis of the sample at three low temperatures. The tensile creep compliance function can be determined using the vertical and horizontal deformation measured near the center of specimen, where the stress distribution is approximately constant. In the second part of the test (tensile strength and strain at failure), a vertical deformation with the constant rate of 0.5 inches/min is applied to the specimen until it fails (Brown et al. 2009)

Thermal Stress Restrained Specimen Test (TSRST) is another method to evaluate the thermal cracking potential of asphalt mixtures. Several researchers used TSRST to characterize asphalt concrete (Monismith et al., 1965; Fabb, 1974; Sugawara et al., 1982; Carpenter, 1983; Arand, 1987; and Janoo, 1989). Later, the test method was developed as a part of SHRP by OEM and Oregon State University and specified by AASHTO TP 10 “Standard Test Method for Thermal Stress Restrained Specimen Tensile Strength”. Figure 2-8 shows a TSRST sample in the test configuration.

Figure 2-8. TSRST Test Configuration (Asphalt Research Consortium, 2007)

The specimens are glued to two platens using epoxy Devcon steel putty in proper alignment. The temperature drops 10°C per hour during the test. The LVDTs record the tensile strain and a load cell indicates the tensile load on the specimen. The testing might take a couple of hours to failure.

The Asphalt Thermal Cracking Analyser machine by University of Wisconsin-Madison (Tabatabaee et al., 2012) and Asphalt Concrete Cracking Device (ACCD) (Kim et al. 2009) are two other test methods to measure thermal stress in asphalt concrete. In addition to the test methods mentioned here, two common fracture tests of disk-shaped compact tension (DCT) and Semi-Circular Bending (SCB) are used in this dissertation.

At present, disk-shaped compact tension (DCT) fracture test is specified as ASTM D7313 for low temperature fracture characterization of asphalt mixtures. A typical test set-up and test specimen is shown in Figure 2-9. In the test procedure a notched disk shaped specimen is initially pre-loaded with 0.1 kN of seating load, thereafter the test control is switched over to achieve a constant crack mouth opening displacement (CMOD) rate of 0.167 mm/s. As with any fracture test, the load initially increases as the stress concentration and formation of a non-

linear fracture process zone (FPZ) occurs near the notch tip (Anderson 2005). Once the FPZ is fully formed and the level of micro-cracking at the crack tip reaches the point where cracks begin to coalesce to form a macro-crack, the required force capacity of the specimen begins to decrease and crack propagation starts to occur. The test is continued until the load decreases to the seating load level of 0.1 kN, at which point the test ends.

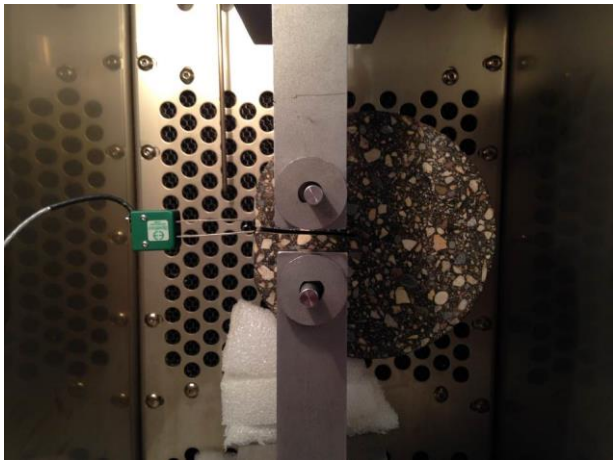

Figure 2-9. Disk-shaped Compact Tension (DCT) Fracture Test Set-up

Semi-Circular Bending (SCB) fracture is a testing method to evaluate the fracture energy of asphalt mixtures at intermediate temperatures. As shown in Figure 2-10, the test is a three-point bending test on a semi circular asphalt specimen with a notch in the middle and bottom. Many researchers have used this test (Wu, Mohammad et al. 2005, Li and Marasteanu 2009, Huang et al. 2013, Aragao and Kim 2012, Al-Qadi, Ozer et al. 2015, Haslett et al. 2017). The test is conducted following AASHTO TP 105, by applying a load which causes a cross head deformation with constant rate till fracture failure. The common procedures for the SCB test are suggested by University of Illinois, University of Louisiana, and University of Minnesota. The differences between the methods are in the number and length of notch, the rate of displacement, and thickness (Nsengiyumva et al. 2015). In this study, the Illinois method of

SCB testing is used and IFIT software is employed to analyze the data and calculate the fracture energy and flexibility index.

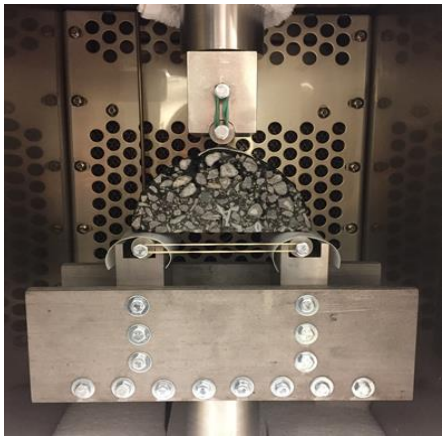

Figure 2-10. Semi-Circular Bending (SCB) Test Configuration

Zofka and Braham (2009) compared the results of IDT, DCT, and SCB testing on field cored samples from 10 pavement sections and concluded that the SCB testing has the best correlation with the cracking condition observed infield.

2.3.2.2 Models and Parameters

Two types of empirical and mechanistic models are used to model the thermal cracking of asphalt mixtures. The empirical models are based on the data indicating the thermal cracking in field, while the principals of mechanics of materials are used in developing the mechanistic models. Fromm and Phang's model (1972) and airport pavement model by Haas et al. (1994) are two empirical models that are developed using the regression analysis on the results of laboratory testing on field cores and data collected from different sites in Canada.

One of the primary studies on a mechanistic model for thermal cracking is performed by Hills and Brien (1966). They predicted a fracture temperature at which the asphalt mixture fails by measuring thermal stress and thermal strength of materials and validated their findings with laboratory testing. Some other studies were conducted by Christison et al. (1972) which predicted the thermal stress using experimental work in two fields in Canada, and Finn et al.

(1977) which developed COLD computer program based on Hills and Brien research to determine the thermal cracking potential of asphalt mixtures.

Use of energy based approaches for fracture characterization of quasi-brittle materials such as asphalt mixtures have been extensively discussed (Roque et al. 2004, Wagoner et al. 2005a). Two well documented mechanistic models for thermal cracking used in this study are the Cohesive Zone Fracture (CZF) model (also called fictitious crack model) and Thermal Cracking (TC) model.

The Cohesive Zone Fracture (CZF) Model is a well established approach to model the cracking development in brittle, quasi- brittle, and ductile materials and an efficient way for computational modeling of fracture. The earliest studies on the concept of CZ approach started in 1960s by Barenblatt. Several researches have been working on CZM such as Dugdale (1960), Camacho and Ortiz (1996), Xu and Needleman (1994), Bazant and Planas (1998), Song et al. (2005). Park (2009) investigated the nonlinear fracture process using CZ model and devided the process into four stages, as shown in Figure 2-11. The four stages include no damage in materials, crack initiation, nonlinear material softening (damage evolution), and failure. The constitutive relations of CZ model and the application of model to the computational methods are presented comprehensively in the literature (Kim 2011, Song et al. 2006).

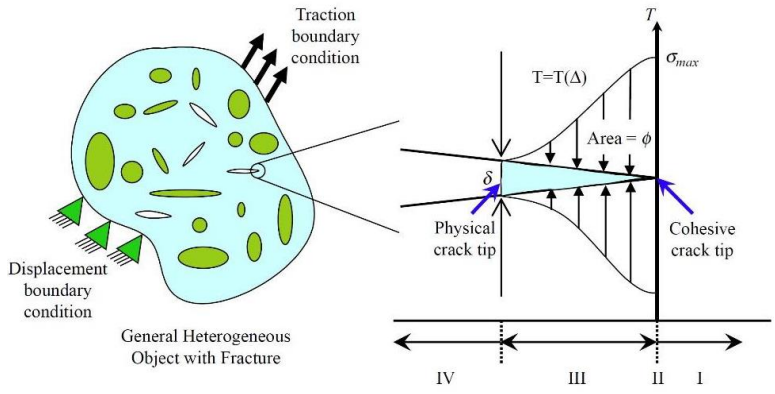

Figure 2-11. Schematic Illustration of the Cohesive Zone Model (Kim, 2011)

Parameters

Use of energy based approaches for fracture characterization of quasi-brittle materials such as asphalt mixtures have been extensively discussed (Roque et al. 2004, Wagoner et al. 2005a). The fracture energy of material is defined as the energy needed to create a new unit fracture surface in the body (Anderson 2005). Following the ASTM D7313 procedure, the fracture energy denoted as "G_f" is determined by first calculating the work of fracture, W_f. Work of fracture is defined as the area under the load-CMOD curve. Fracture energy can be calculated by normalizing the fracture work by the area of fracture surface that is generated during the test. This area can be estimated as a product of the thickness of the specimen (t) and the length of new crack formed during the test. This crack length is often referred to as ligament length (a). Fracture energy calculation is shown in Equation 2.15.

$$G_f = \frac{W_f}{t \times a} \quad 2.15$$

DCT fracture energy or total DCT fracture energy (G_f) has been extensively studied for its application to reflective cracking in asphalt overlays (Wagoner et al. 2006) and thermal cracking in asphalt pavements (Marasteanu et al. 2006 and 2012, Dave et al. 2016). This parameter has been compared with field thermal cracking performance and threshold values have been developed through field calibration and validation efforts. After an extensive multi-laboratory repeatability and reproducibility campaign, Minnesota Department of Transportation (MnDOT) has moved to pilot implementation of G_f as a thermal cracking performance parameter (Van Deusen et al. 2015, McCarthy et al. 2016). In the pilot implementation phase, a minimum G_f value of 400 J/m^2 is required for mix design acceptance and verification testing is conducted during the mix production and pavement construction phases.

A potential drawback of G_f or $G_f^{Post\text{-}peak}$ as an asphalt mixture low temperature cracking performance parameter is the inability of energy measurement to distinguish between mixtures with high peak load and steep post-peak slope (commonly referred to as high strength low toughness materials) and mixtures with low peak load and shallow post-peak slope. This topic has been a motivational factor behind development of normalized energy indices such as the Illinois flexibility index parameter (Al-Qadi et al. 2015).

A comprehensive discussion on different available parameters is conducted by Zhu et al. 2016. Table 2-1 shows a summary of parameters for evaluation of quasi-brittle material.

Table 2-1. Summary of various fracture indices (Zhu. Et al. 2017)

Fracture Indices		**Symbol**	**Physical Interpretation / Definition**
Energy Indices	Fracture energy	G_f	Energy needed to create a new unit fractured surface in the material.
	Pre-peak fracture energy	$G_f^{Pre\text{-}peak}$	Energy during thepre-peak part of the load-CMOD curve. Typically associated with energy needed to initiate crack.
	Post-peak fracture energy	$G_f^{Post\text{-}peak}$	Energy during the pre-peak part of the load-CMOD curve. Typically associated with energy necessary to propagate a crack.
Fracture Strength and Stress-Intensity Factor	Fracture strength	S_f	Measure of peak load in fracture test that is normalized for specimen geometry.
Normalized Fracture Energy Indices	Toughness index	TI	Post-peak fracture energy weighted by the displacement between maximum load and 50% of maximum post-peak load.
	Initial post-peak slope flexibility index	$G_f/m_{initial}$	$m_{initial}$ is defined as the average slope of load-CMOD curve between 90% and 70% of peak load.
	Average post-peak slope flexibility index	$G_f/m_{average}$	$m_{average}$ is defined as average of tangent slopes along each point on the softening curve.
	Flexibility index using difference between initial and final post-peak slopes	$G_f/(m_{initial} - m_{final})$	m_{final} is defined as average slope over the latter 20% CMOD.
	Fracture strain tolerance	FST	G_f/S_f, normalized fracture energy with respect to fracture strength.

2.4 Aging

Hot mix asphalt pavements undergo aging during mixing and compaction processes, and also over the service life. Generally, the aging process is the change of binder chemistry due to two processes of volatilization and oxidation of binder. Volatilization is the evaporation of light oils and hydrocarbons (carbon and hydrogen) resulting in the increase of asphalt specific gravity. Volatilization occurs primarily during asphalt mixing and compaction that the binder temperature is very high (about 150° C). The volatilization rate increases dramatically with the increase of temperature (Lavin 2003, Fernandez et al. 2013).

Oxidation that is the most dominant cause of aging in asphalt concrete pavements occurs due to the chemical reaction of asphalt hydrocarbons with oxygen. The interaction of hydrocarbons with hydroatoms like oxygen causes imbalance electrochemical forces and the polarity increases in binder molecules. More polarity results in stronger intermolecular forces, and accordingly, asphalt elastic modulus and viscosity increase. It is well known that the increase of temperature has a significant effect on aging rate. Also the other parameters like environmental conditions (e.g. pressure and moisture) and traffic loading affect on aging process.

It has been well recognized by many researchers (Kim et al. 2003, Glover et al. 2009, and Daniel et al. 1998) that binder aging has serious effects on asphalt mixture performance. These changes can impact on asphalt binders in different ways:

- Stiffness: Aging process results in excessive stiffness in asphalt mixtures. With the increase of aging, asphalt modulus grows. Although, it improves the bearing characteristics of mixture, stiffer mixtures are more prone to cracking.
- Relaxation: As the asphalt aging increases, the relaxation capability decreases. The researches show oxidation has a significant negative effect on asphalt binder phase

angle. With decrease of phase angle, binder viscosity reduces and the elastic characteristics of asphalt binder increases.

- Fracture: the other effect of age hardening on asphalt binder is the increase of brittleness. The aged asphalt binders and mixtures are less ductile, and therefore the cracking potential increases.

Consequently, the cracking performance of aged mixtures is supposed to be worse than virgin mixtures. Also, high percentages of RAP or RAS that contain aged binder is expected to decrease the cracking resistance.

Asphalt aging in field- It has been well established that the age hardening of asphalt concrete pavement in the field can be divided in two significant stages. Short term aging occurs during asphalt production and compaction, and continues in 2-3 years after placing the asphalt. Short term aging contains both volatilization and oxidation age hardening. Then, oxidation process continues as long term aging at a much slower rate during pavement service life (Brown et al. 2009).

Asphalt aging in lab- To recognize the behavior of aged asphalt in field, the age hardening should be simulated in lab. Both binder and mixture can be simulated to short term and long term aged conditions. The accelerated laboratory aging methods for binder and mixture are summarized in the following sections.

2.4.1 Binder Aging

The accelerated testing methods have been developed to age asphalt binder in the laboratory. Generally, by accelerating the oxidation process can enhance the aging, and this fact is used in the lab to simulate the long term binder aging in field. Therefore, increasing temperature, increasing the surface area of binder exposed to air, decreasing binder film thickness, passing

more air flow, and increasing pressure might be the techniques employed in the lab to accelerate the aging process.

During the Strategic Highway Research Program (SHRP), two procedures were developed for short term and long term aging of asphalt binders in laboratory, which are the most commonly used standards in the US.

2.4.1.1 Short term aging

The Rolling Thin-Film Oven (RTFO) is used to simulate the short term aged condition on asphalt binders in the lab following AASHTO T 240. This process happens during mixing and replacement of asphalt mixture in the field. The asphalt binder samples are placed in cylindrical glass bottles in a rotating carriage. By elevating the temperature, unaged asphalt binder samples are exposed to air flow and heat at the temperature of 325° F (163°C) for 85 minutes. One of the RTFO problems is that it is not applicable well for the highly viscous binders like polymer modified binders, since they do not flow easily in RTFO bottles. The RTFO aging method is also standardized in Australia/New Zealand (AS/NZS 2341.10:2015), the United Kingdom (Hill et al. 2008), and South Africa.

There are some other methods, mainly developed in Europe, for short term conditioning of asphalt mixtures. Thin Film Oven Test (TFOT), EN 12607-2 or ASTM D 1754) is one of these methods. 50 ml binder is poured in a cylindrical pan (140 mm diameter and 9.5 mm depth) and the pan is placed in a convention oven at 163°C for 5 hours. Considering the dimensions of pan, the thickness of binder layer would be more than 3 mm. The main concern in this method is that the thick binder film may limit the aging to the surface of binder layer (Airey 2003). That is why the Modified Thin Film Oven Test (MTFOT) was developed which the binder film thickness and the aging time were changed to 100 micron and 24 hours, respectively.

As mentioned, one of the issues with RTFO (AASHTO T 240 or EN 12607-1) is that this highly viscous binders or polymer-modified binders do not flow well in the bottles. The modified Rolling Thin Film Oven Test (MRTFOT) was developed to solve this problem, using the still rods inside the glass bottles. The rods were supposed to make shearing force in viscous binder to spread asphalt binder into thin layers, but since the next research works showed the rods does not help, this method is not a common technique.

The Rotating Flask Test (RFT), EN 12607-3, is another test developed in Europe to simulate short term aging on binder. In this method, the binder sample rotates in a rotating spherical flask of the rotary evaporator at 165°C for 150 minutes and air flow. Comparing two methods of RTFO and TFOT, Airy 2003 expressed that RTFO makes approximately three times higher aging than RFT.

2.4.1.2 Long term aging

long term aging on asphalt binders in the lab is performed by the Pressure Aging Vessel (PAV) which simulates 7 to 10 years oxidation of asphalt in service based on AASHTO R 28. The combination of heat and pressure is used in this method. PAV samples are placed under pressure of 300 psi (2070 kPa) and temperature of 194°, 212°, 230° F (90°, 100°, or 110° C) for 20 or 40 hours. Different temperatures are used to simulate different climate conditions. Verhasselt and Vanelstraete (2000) found that at higher temperatures, some segregation might happen in the polymers available in polymer modified binders.

RTFO (AASHTO T 240) and PAV (AASHTO R 28) are common in the Europe as well, called EN 12607-1 and EN 14769, respectively.

Another accelerated long term aging test is Rotating Cylinder Ageing Test (RCAT), EN 15323, developed by Belgian Road Research Center. In this procedure, a large cylinder containing binder is rotating (1 revolution per min) in oven at 90° C for 140 hours and oxygen flows.

2.4.2 Mixture Aging

There are several methods available in the literature for conditioning of asphalt mixture in the lab. NCHRP report 815, entitled “Short Term Laboratory Conditioning of Asphalt Mixtures” and the interim NCHRP reports of “Long Term Aging of Asphalt Mixtures for Performance Testing and Prediction” discuss different methods on short term and long term aging of asphalt mixtures, respectively. These works are summarized in following;

2.4.2.1 Short Term Aging

AASHTO R30 is the current standard practice for aging of hot mix asphalt mixtures to simulate both short and long term aging conditions. based on the standard, the pans of loose mix asphalt are placed in a forced-draft oven for 4 hours ± 5 min at a temperature of 275 ± 5° F (135 ± 3° C). The loose mix asphalt should be stirred after 1 hour to obtain confirm conditioning. It is the outcome of a study conducted by Bell et al. (1994) as a part of SHRP project.

The previous researchers have tried to simulate short term aging in the lab by applying different temperatures during different time duration. One of the oldest works was conducted by Aschenbrener and Far (1994). They compared the theoretical maximum specific gravity (G_{mm}) values and the Hamburg wheel-tracking test (HWTT) results of short term oven aged (STOA) specimens and the corresponding mixtures in the field. The conditioning time of STOA specimens varied between 0 to 8 hour at the field compaction temperature. The results related to the specimens with 2 to 4 hours aging matched best with the field results.

In 2000, Brown and Scholz used short term oven aging (135° C) on compacted specimens and compared their stiffness with the stiffness of unaged mixtures. The results indicated 9% to 24% increase the stiffness per hour aging. The other main studies during the last decade were conducted on the effect of different parameters on short term aging. The effect of silo storage

time was investigated by Daniel et al. (2014). The silo storage time is found to have an important effect on aging level and asphalt mixture properties.

Some other studies are performed about short term aging on warm mix asphalt (WMA) in the recent years. Estakhri et al. (2010) compared the performance of WMA and HMA mixtures that were subjected to STOA in different time and temperatures using the HWTT. The results recommended a 4-hour oven aging at 275° F (135° C) for WMA with Evotherm DAT. Two NCHRP projects (Project 9-43 by Bonaquist, 2011 and Project 9-49 by Epps Martin et al. 2014) were also investigated the appropriate aging time and temperature on WMA. Project 9-43 evaluated the effect of STOA protocol using the comparison of maximum specific gravity and indirect tensile (IDT) test results, and it recommended 2-hour oven aging for WMA at the compaction temperature. Project 9-49 suggested the STOA protocol of 2 hours at 240° F (116° C) for WMA and 275° F (135° C) for HMA, using the evaluation of moisture susceptibility of mixtures.

2.4.2.2 Long term aging

The procedure of long term aging of asphalt mixture in the lab is more complicated than that o short term aging. Long term aging may be conducted on compacted specimens or loose mix asphalt. There is more variety in time and temperature of LTOA in literatures. Also, in some studies the combination of heat and pressure is used to obtain higher levels of aging in a short time.

Based on the AASHTO R 30 (2002) that is the current aging protocol for asphalt, a compacted mixture of aggregate and binder should be conditioned in a forced-draft oven for 5 days (120 ± 0.5 hour) at 85 ± 3°C for long term mixture conditioning, preceded by short term mixture conditioning in a forced-draft oven for 4 hour ± 5 min at 275 ± 5° F (135 ± 3° C). The mixture

conditioning for short term aging applies to loose mixture only, while the conditioning for long term aging applies on compacted specimens (compaction according to AASHTO T 312).

But there are some shortcomings in AASHTO R 30 that show the necessity of a revision on this standard.

- Although 5-day forced-draft oven aging in the lab simulates the aging of asphalt mixtures after about 2-3 years of service in field, it is well accepted that 5-day is not sufficient to simulate the field long term aging behavior.
- Only one temperature is used as conditioning temperature in AASHTO R 30, while the various climate conditions and mean temperatures over the United States do not seem to make the same aging levels in a specific time.
- The effect of air void on aging is not considered in AASHTO R 30.

AASHTO R 30 standard is based on a research conducted by Bell et al. (1994) as a part of SHRP A-003A. They compared the volumetric properties and modulus testing results of laboratory specimens and field cored samples. 1 to 8 days conditioning at 185° F (85° C) to 212° F (100° C) was considered to simulate long term oven aging in the lab on compacted specimens, proceeded by short term aging on loose mix. The temperature of 85° C was recommended for long term aging in the lab, while 100° C was found to damage the samples and make unreliable data. Also, 4 to 8 days aging at 85° C was suggested to represent more than 3 years aging.

Another study is conducted by Brown and Scholz (2000) to simulate the long term aging of asphalt mixtures in the lab. They used oven aging method on compacted specimens with continuous and gap-graded aggregate gradation. Comparing the stiffness modulus of aged specimens and field cored samples, 5 days aging at 85°C is the recommended time and temperature for UK.

Several researches (Muglar 1970, Hayicha et al. 2003, and Collop et al. 2004) have been performed in Europe also about the appropriate duration and temperature of long term aging in oven on compacted samples. Generally, the older studies suggested higher temperatures (more than 100°C) in a shorter aging duration (in hour scale), while the recent studies preferred the lower temperatures (60 – 85°C) in longer duration of time (5 to 20 days).

The mentioned studies investigated the effect of long term aging on compacted asphalt samples. Some issues are reported in literatures about aging of asphalt mixtures on the compacted specimens. Aging gradient is one of the problems that might happen during long term aging. The aging gradient can affect the testing results and behavior of samples; for example, failure in long term aged compacted specimens in the SVECD fatigue testing is almost different from that of un-aged specimens. Another issue is slump that occurs due to the high temperature during the aging of compacted mixtures. It causes different air voids in the specimens resulting in inconsistency of the results. Therefore, some researchers tried to conduct the long term aging process on loose mix asphalt. However, loose mix asphalt need more shear force and gyration numbers to be compacted.

Most of the studies about aging on loose mix asphalt are conducted in Europe. The objectives of these researches were not necessarily the evaluation of long term aging, but they aimed to produced RAP in their studies. Van Gooswilligen (1989), Such et al. (1997), Read and Whiteoak (2003), and De la Roche et al. (2009) used long term oven aging on loose mix asphalt.

Another study by Reed (2010) compared the dynamic modulus of compacted and loose mix of rubber modified asphalt mixtures. The conditioning time and temperature for both loose mix and compacted samples were 5 and 14 days at 85°C. Also, the dynamic modulus and beam fatigue testing were conducted on the 7 years old field pavement samples. The author believed the results of compacted samples are more ideal than the loose mix state. The results indicated

lower dynamic modulus at low temperature and more stiffness at higher temperature for laboratory aged samples. Although Reed (2010) suggested aging of compacted specimens, some other studies (Mollenhauer and Mouillet 2011, and Van den Begh 2011) recommended long term aging of loose mixtures instead of compacted samples.

Elwardany, et al. (2016) presented the results of an active NCHRP project (09-54) to date. They performed the temperature conditioning of asphalt for both compacted and loose mix with and without pressure. The samples were in two different sizes, and oven aging and pressure aging vessel (PAV) were used for conditioning of asphalt mixtures. They compared airvoids, and the results of dynamic modulus and SVECD fatigue testing for different mixtures. Based on the results to date, the oven aging on loose mix asphalt is preferred, because of uniformity of aging.

Chapter 3

LABORATORY VERSUS PLANT PRODUCTION: IMPACT OF MATERIAL PROPERTIES AND PERFORMANCE FOR RAP AND RAS MIXTURES

3.1 Introduction

The asphalt industry has been moving towards performance based design, reinforced by federal legislation under the Moving Ahead Progress for the 21st Century Act. Many different methods and approaches have been developed over the last several decades to evaluate the performance of asphalt mixtures in the laboratory. Originally, most laboratory testing was performed on laboratory fabricated specimens; more recently, the differences between laboratory and plant production methods have been recognized. An understanding of differences between the properties and performance measured on specimens fabricated in different ways is important for implementation of performance based approaches. There are different methods to fabricate asphalt mixture test specimens; the most common ones are:

- Laboratory mixed, laboratory compacted (LMLC): the specimens are mixed and compacted in the laboratory using conditioning methods that are intended to simulate what happens in the plant and are generally used for mix design purposes (Kim, et al. 2002)
- Plant mixed, laboratory compacted (PMLC): the specimens are fabricated in the laboratory by reheating and compacting the loose mix produced at the plant
- Plant mixed, plant compacted (PMPC): the specimens are compacted in a laboratory at the plant immediately following production without reheating of the loose mixture

- Field cores: the specimens are taken from the asphalt pavement and are the best representation of in-place mixture conditions

These specimen fabrication methods use different handling, mixing, and compaction methods that can potentially impact the properties measured from the resulting specimens. The handling and storage condition of asphalt binder in plant and lab are different. The asphalt binders in the lab are kept in small containers at room temperature, while the asphalt is handled in enclosed systems at the plant and may result in differences in stiffness (NCHRP No. 673). Another potential source of difference is the breakdown of aggregates that occurs during plant production and differences in mineral filler amounts that are added in the plant [NCHRP No. 673]. The temperatures to which the asphalt and aggregate are subject are different in the plant versus the laboratory and the method of compaction is different from lab to field as well.

Most studies conducted on plant and lab produced mixtures show the lab produced specimens are stiffer than plant produced specimens. Johnson et al. (2010), evaluated asphalt mixtures containing reclaimed asphalt pavement (RAP) and recycled asphalt shingle (RAS) and showed that the dynamic modulus ($|E^*|$) of plant produced specimens are lower than those of lab produced mixtures. However, the research did not evaluate the impact of RAP/RAS on the difference between plant and lab produced mixtures. A pooled fund study on high RAP mixtures (Mogawer, et al 2012), indicated that the reheating effect in PMLC mixtures causes them to be significantly stiffer than PMPC ones. Research performed on plant-foamed asphalt mixtures containing RAP (Xiao, 2014) showed the rut depth of PMLC specimens are lower than PMPC, indicating higher stiffness of the PMLC specimens. Researchers believe the reason is the effect of reheating in the lab, resulting in aged binder and stiffer materials. Also, the binder testing on recovered asphalt binder indicates the failure temperature of lab produced specimens are higher than that of plant produced ones (Xiao, 2014). On the other hand, the results of frequency sweep testing (AASHTO TP7-94) on Michigan, Missouri, and Indiana

mixtures (McDaniel et al. 2002) show that the stiffness of plant and lab produced mixtures of Michigan and Missouri are similar, while a higher stiffness (G*) is observed for plant produced mixtures of Indiana.

There are many variables that affect the performance of asphalt mixtures such as binder grade, binder source, gradation, volumetric properties, and recycled content and it is important to understand how these may potentially impact differences in measured properties of laboratory and plant produced specimens. The scope of this paper is to evaluate PMPC versus LMLC mixtures to compare the material properties that would be measured during the mix design phase and during production. This study provides new information on properties measured on binders and mixtures that has been rarely discussed in the literature. It is anticipated that the findings of this research will lead to a better understanding of differences between laboratory and plant produced mixtures and would be a basic work for future investigations.

The main objectives of this study are to:

- compare the measured properties of plant produced and lab produced specimens
- evaluate the impact of mixture variables on the differences between properties measured on PMPC and PMLC specimens
- evaluate the impact of differences in measured properties on predicted fatigue performance

3.2. Materials and Test Methods

3.2.1 Materials

This study includes testing on 11 plant produced (PMPC) and 11 lab produced (LMLC) mixtures. The PMPC specimens were fabricated at two different drum plants in Lebanon, NH, and Hooksett, NH. The raw materials were collected for fabrication of the LMLC specimens. The Lebanon mixtures were placed in the field along New Hampshire (NH) State Route 12

near Westmoreland during the 2013 construction season. The mixtures are varied in binder PG grade (PG 52-34, PG 58-28, PG 64-28), binder source, nominal maximum size of aggregate (NMAS) (9.5, 12.5 and 19 mm), recycled material type, and binder replacement (16% – 32% RAP or RAP/RAS). Table 3-1 shows the combinations evaluated, mix design volumetric information and actual binder replacement values. Table 3-2 shows the aggregate gradation of different mixtures. The RAP binder used in Lebanon plant had a continuous grade of 81.3-19.3° C; this is a typical value for RAP materials in NH. The stiffness of the Hooksett RAP was not measured, but is likely similar to the Lebanon RAP. The RAS material is primarily tear-off shingles and could not be graded in the laboratory.

3.2.2 Binder Testing

The asphalt binder from each of the mixtures (both plant and laboratory mixed) was extracted in accordance with AASHTO T 164 procedure 12 using a centrifuge extractor and toluene solvent and recovered based on ASTMD 7906-14 using a rotary evaporator. Performance grading of the virgin binders and the extracted and recovered binders was conducted following AASHTO MP1-93.

Table 3-1. Mixtures Properties and Volumetric Information

Plant	Virgin Binder PG Grade	Binder Source	NMAS (mm)	%Total Asphalt (P_{be})	VMA (%)	(VFA) (%)	%Total Binder Replacement (% RAP/ % RAS)	Average % air PMPC Specimens	Average % air LMLC Specimens
Lebanon	58-28	1	12.5	5.3	15.5	74.9	18.9 (18.9/0)	7.7	6.4
		1	12.5	5.3	16.2	75.8	28.3 (28.3/ 0)	7.4	6.5
		2	19	4.8	15.0	71.3	20.4 (8.2/	6.3	5.7
		2	19	4.7	14.1	75.9	31.3 (31.3/ 0)	6.0	5.6
	52-34	1	12.5	5.3	15.5	74.9	18.9 (18.9/0)	6.3	6.8
		1	12.5	5.3	16.2	75.8	28.3 (28.3/ 0)	6.9	6.4
		3	19	4.8	15.0	71.3	20.4 (8.2/	5.7	5.6
		3	19	4.7	14.1	75.9	31.3 (31.3/ 0)	6.1	5.7
Hooksett	58-28	2	12.5	5.8	15.9	79.5	22.4 (22.4/0)	5.3	5.6
		2	9.5	6.1	16.5	78.9	21.3 (21.3/0)	5.7	6.0
	64-28	2	9.5	6.1	16.5	78.9	16.4 (16.4/0)	5.9	6.0

Table 3-2. Gradation Information for Different mixtures

Sieve Size (mm)	12.5 mm 28.3% RAP	12.5 mm 18.9% RAP	19 mm 31.3% RAP	19 mm, 20.4% RAP RAS	12.5 mm Hooksett	9.5 mm Hooksett
	% Passing					
37.5	100	100	100	100	100	100
25	100	100	100	100	100	100
19	100	100	99	99	100	100
12.5	98.6	98.6	83.4	83.4	98.9	100
9.5	86.9	86.3	70	70.3	86.5	98
4.75	60	59.2	47.2	46.3	57.9	78
2.36	41.7	41.5	32.4	32	44.0	62
1.18	30.7	30.7	23.5	23.3	34.3	49
0.6	21.1	21.3	16.2	16	25.2	35
0.3	11.4	11.4	9.3	9	15.9	22
0.15	6.1	5.9	5.2	4.7	8.0	12
0.075	3.9	3.9	3.3	3.1	4.68	8.5

3.2.3 Mixture Testing

Complex modulus testing is a way to determine two important mixture properties: dynamic modulus and phase angle. Complex modulus testing was performed on three replicate cylindrical specimens of each mix following AASHTO TP-79. The testing was conducted using asphalt mixture performance tester (AMPT) equipment in unconfined compression using four LVDTs with a 70 mm gage length to measure deformations. The complex modulus data were analyzed using Abatech RHEA® software, and the results are presented in the form of dynamic modulus master curves represented using a generalized sigmoid format (Equation 3.1) and phase angle diagrams to evaluate the relaxation capability of the mixtures.

$$\log|E^*| = \delta + \frac{\alpha}{\left[1+\lambda e^{\beta+\gamma\log(\omega)}\right]^{\frac{1}{\lambda}}} \quad 3.1$$

Where $|E^*|$ is dynamic modulus, α, β, δ, λ, and γ are fit coefficients and ω is reduced frequency. Reduced frequency is equal to frequency used in the test multiplied by shift factor, a_T, obtained from Equation 3.2.

$$log a_T = a_1 T^2 + a_2 T + a_3 \quad 3.2$$

Where a_1, a_2, and a_3 are shift factor coefficients, and T is temperature (Rowe, 2009).

Uniaxial tensile fatigue testing and analysis using the simplified viscoelastic continuum damage (S-VECD) approach was conducted on four specimens of each mixture following AASHTO TP 107.

Damage analysis for each mixture was performed and damage characteristic curves (DCC) were obtained using models available within ALPHA-Fatigue software. Also, the fatigue cracking resistance was assessed by fatigue failure criterion of asphalt mixtures versus number of cycles (G^R-N_f). G^R is the rate of change of the averaged released pseudo strain energy (per cycle) throughout the test, and is calculated from the Equation 3.3.

$$G^R = \frac{\int_0^{N_f} W_C^R}{N_f^2} \quad 3.3$$

Where W^R_C is released pseudo strain energy, and N_f is the number of cycles before failure. (Sabouri & Kim, 2014)

3.2.4. Pavement Evaluation

Layered Viscoelastic Pavement Design for Critical Distresses (LVECD) is a program developed by North Carolina State University to calculate responses and predict the fatigue and rutting behavior of asphalt pavements (Eslamnia et al. 2012). To assess the fatigue behavior, this 3D finite element based software employs simplified viscoelastic continuum damage (SVECD) approach. A damage characteristic curve (DCC) from SVECD is used in this model. Since DCC is developed by removing the bulk viscoelastic response of material from the constitutive response, it can be used to evaluate the mixture's response to any uniaxial loading history and temperature combination (Chehab et al. 2003, Daniel & Kim, 2002)

3.3 Results and Discussion

3.3.1 Binder Testing and Analysis

The continuous high and low PG temperatures for the different virgin and extracted and recovered binders are shown in Figures 3-1 and 3-2, respectively. The high PG temperatures from the lab produced mixtures are greater than those from the plant produced mixtures and there are slight differences with the different binder sources. The two PG 52-34 virgin binders did not quite meet the required performance grade on the low side. The binders extracted and recovered from Hooksett plant and lab mixtures show higher difference in high temperature PG grade than Lebanon mixtures. The difference between PMPC and LMLC mixtures is less pronounced on the low temperature side and all of the low grades are controlled by the m-value. In most cases for both 12.5 and 19 mm Lebanon extracted binders, PMPC mixtures show colder temperatures, while two PG 58-28 binders extracted from Hooksett LMLC mixtures have colder temperatures than PMPC mixtures.

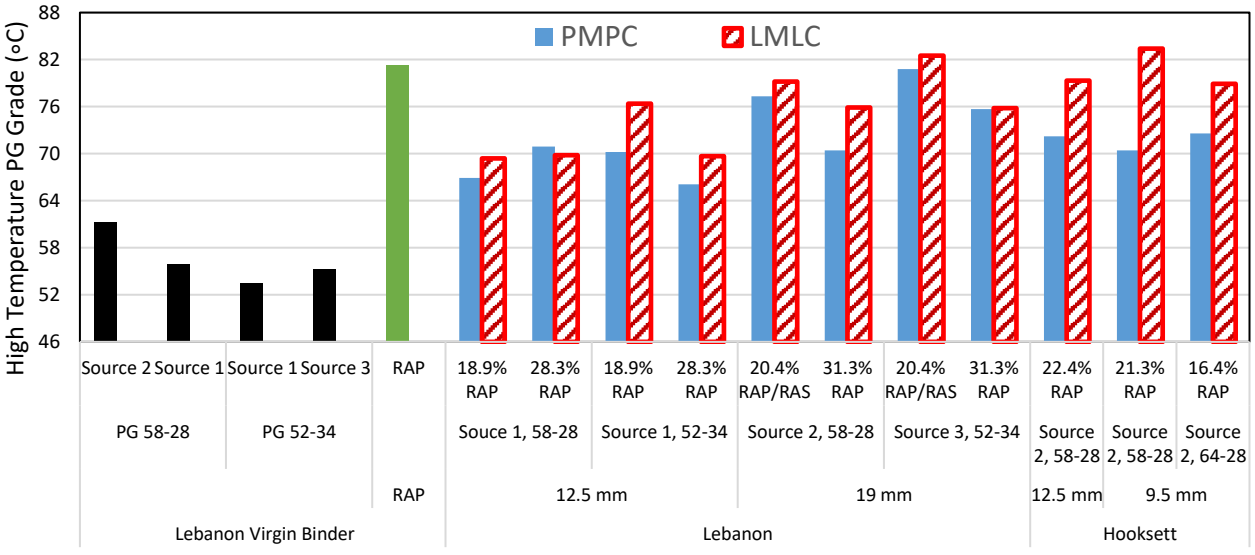

Figure 3-1. High PG Temperature for Different Binders

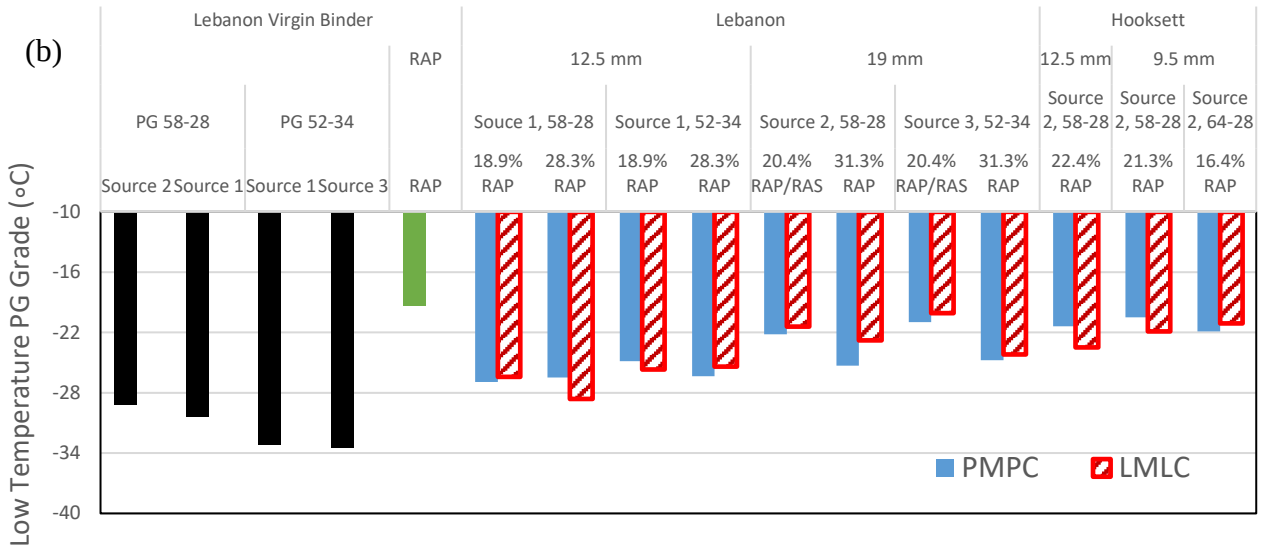

Figure 3-2. Low PG Temperature for Different Binders

The mixtures containing RAS have warmer temperatures than 31.3% RAP mixtures and the binders extracted from the 19 mm mixtures have warmer temperatures than those extracted from the 12.5 mm mixtures for the same recycled material content. The different binder sources for 12.5 mm and 19 mm may cause the difference in high and low temperature PG grade of extracted and recovered binders, so that warmer high temperatures of virgin binders from sources 2 and 3 used in 19 mm mixtures result in warmer high temperature of extracted and recovered binders from 19 mm than 12.5 mm. The slightly higher actual binder replacement for the 19 mm mixture (20.8% versus 18.9% for 12.5 mm) may contribute to the warmer temperatures, as well.

The results of the performance grading analysis indicate that the most of the LMLC materials are more highly aged than the PMPC materials and that the difference between the two depends on the mixture recycled content, effective binder content, virgin binder grade, and possibly binder source.

The difference between continuous low temperature binder determined from creep stiffness (S-value) and the log-log slope of creep curve (m-value), ΔT_{cr}, is presented in Figure 3-3 for

the different extracted binders The ΔT_{cr} value is negative for all binders, indicating they are m-controlled. In most cases, the LMLC recovered binders show larger ΔT_{cr} values than the PMPC recovered binders. The recovered binders from 19 mm and PG 52-34 mixtures show larger values than the 12.5 mm and PG 58-28 mixtures, respectively, but there is no trend in the difference between PMPC and LMLC mixtures with NMAS or binder grade. An interesting point observed is that the trend of plant versus lab produced mixtures opposite for ΔT_{cr} as compared to the low temperature PG grade. This indicates that the aging which the asphalt is experiencing in the laboratory is changing the relaxation capacity (m-value) of the binder more than it is changing the stiffness (S value).

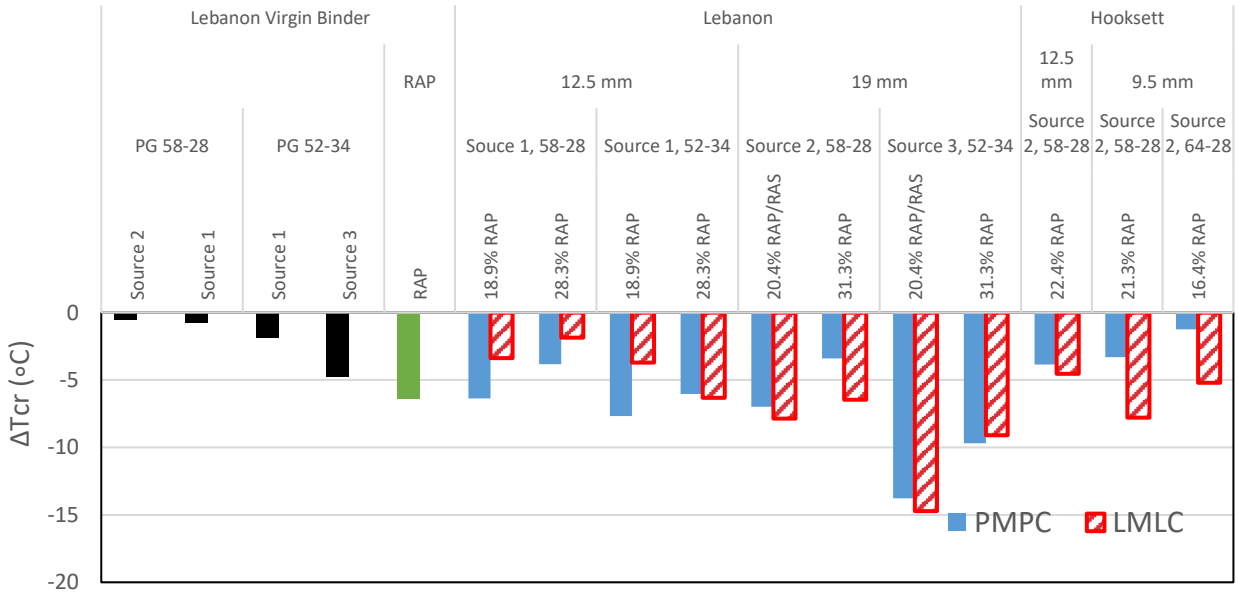

Figure 3-3. ΔT_{cr} Binder PG Grade

3.3.2 Mixture Testing Analysis and Results

3.3.2.1 Stiffness - Dynamic Modulus

Figures 3-4 and 3-5 compare the average dynamic modulus master curves of lab produced mixtures versus those of plant produced mixtures for Lebanon and Hooksett mixtures, respectively. All of the lab produced Lebanon mixtures higher dynamic modulus than the

corresponding plant produced mixtures over the entire frequency range, except the PG 58-28, 30% RAP mixtures for both 12.5 and 19 mm (28.3% RAP and 31.3% RAP). For these two cases, plant produced mixtures tend to be stiffer at low temperatures/high frequency; the PG temperatures for these two plant mixtures were also warmer than the corresponding lab mixtures. The difference between LMLC and PMPC dynamic modulus master curves is greater for 19 mm mixtures and the PG 58-28 base binder mixtures. Larger differences with a PG 58-28 base binder mixture were also observed in another project [NHDOT, SPR 15680B].

Unlike the Lebanon mixtures, the lab produced Hooksett mixtures mostly show higher dynamic modulus than plant produced mixtures. The higher stiffness of two PG 58-28 plant mixtures at low temperatures is in accordance with warmer low PG temperature of extracted binders from these plant produced mixtures (Figure 3-2). Although, both Lebanon and Hooksett are drum plants, but the results show different plants can produce different effects on asphalt mixtures' properties; this could be due to any number of production factors such as temperature, mixing time, storage and handling conditions. It should be noted that the lower air voids of lab produced Lebanon mixtures than plant produced ones, and slightly higher air voids of lab produced Hooksett mixtures might have affected the stiffness of these mixtures.

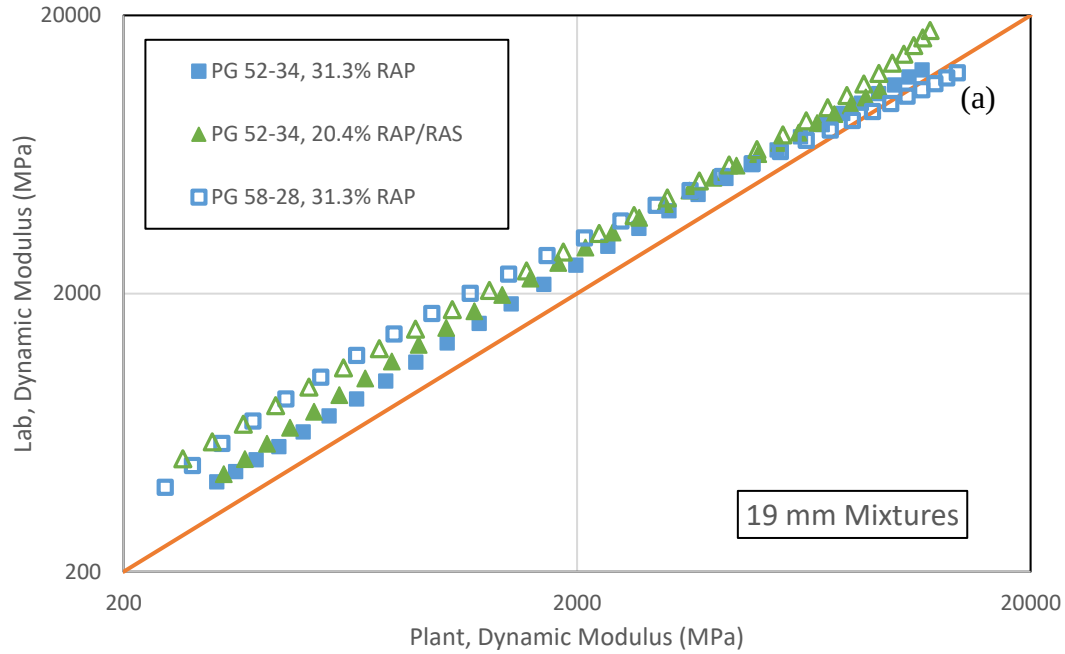

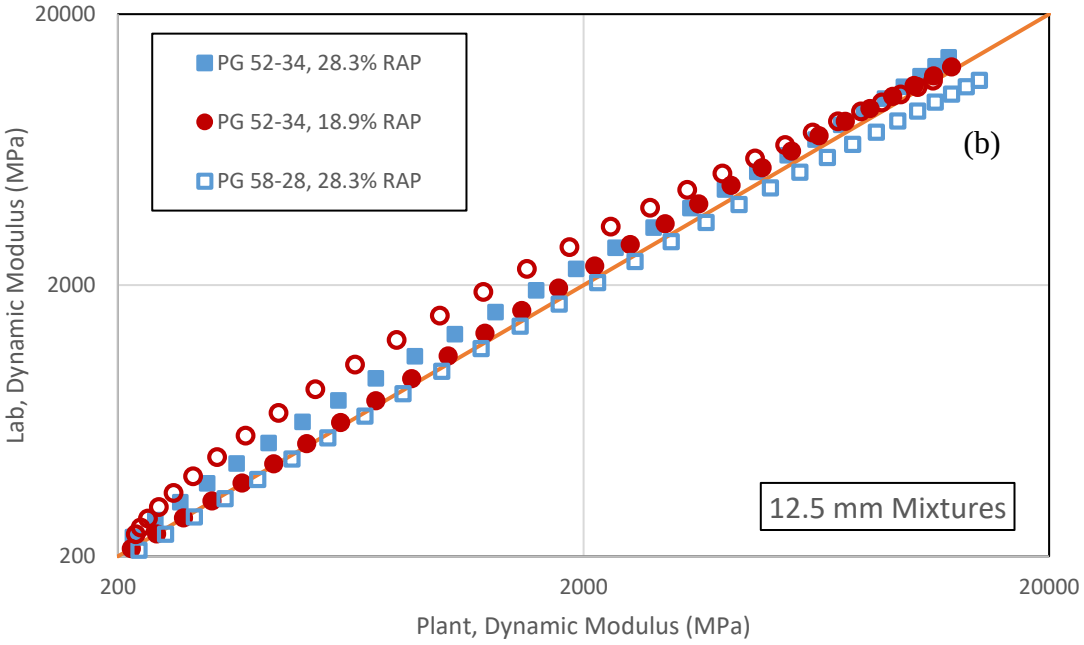

Figure 3-4. Dynamic Modulus Master curves of Lab versus Plant Produced Mixtures for a) 19 mm b) 12.5 mm, Lebanon Mixtures

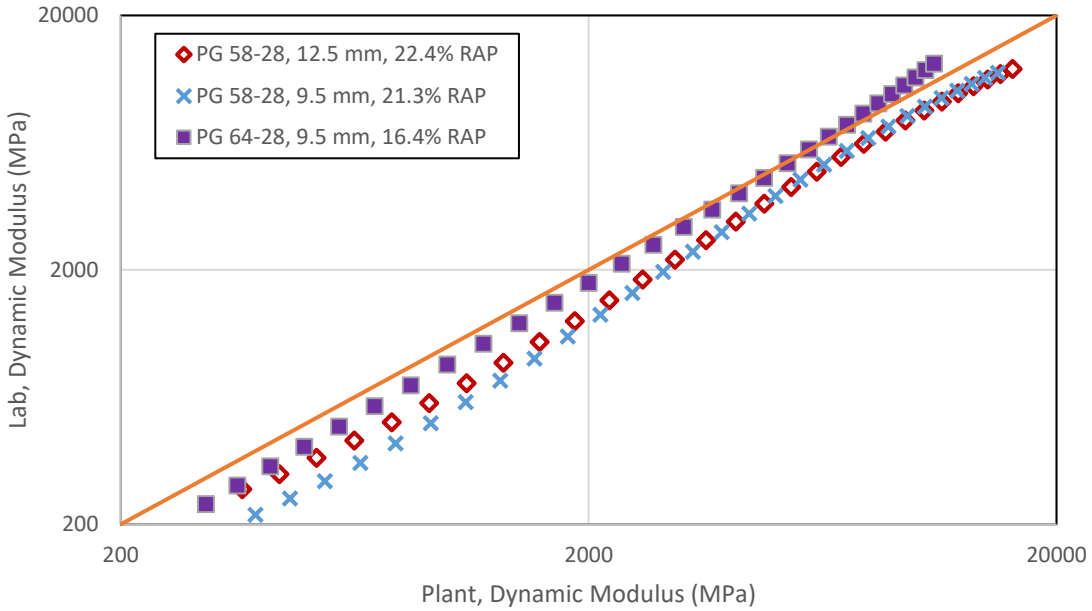

Figure 3-5. Dynamic Modulus Master curves of Lab versus Plant Produced Mixtures for Hooksett Mixtures

3.3.2.2 Relaxation – Phase Angle

The relaxation capacity of mixtures plays an important role in cracking behavior. The higher phase angle indicates the higher viscosity of asphalt materials, resulting in a better resistance to cracking. Figures 3-6 and 3-7 show the phase angle values of lab produced mixtures versus those of plant produced mixtures for Lebanon and Hooksett mixtures, respectively. Similar to the dynamic modulus results, the difference in phase angle values of plant and lab produced mixtures is different for Lebanon and Hooksett mixtures. Except 19 mm PG 52-34, the Lebanon plant produced mixtures are higher (showing more elastic behavior) than the corresponding lab produced mixtures, while the phase angle values of Hooksett lab produced mixtures are higher. The results of statistical analysis (t-test) for dynamic modulus and phase angle show that there was not a significant difference (at 95% confidence level) between dynamic modulus and phase angle of plant and lab produced mixtures, except for the PG 58-28, 12.5 mm, 18.9% RAP Lebanon and PG 58-28, 9.5 mm, 21.3% RAP Hooksett mixture.

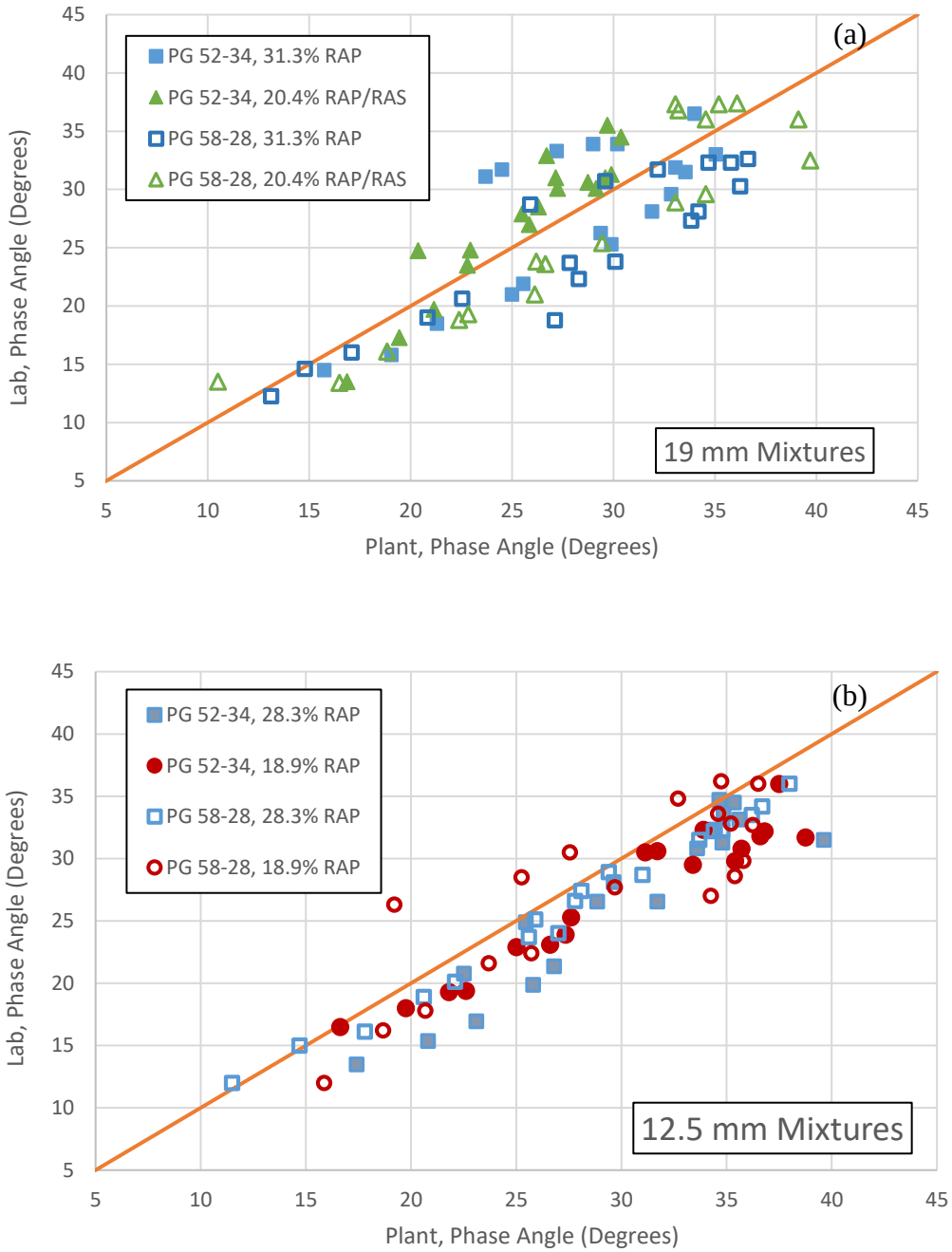

Figure 3-6. Phase Angle Values of Lab versus Plant Produced Mixtures for a) 19 mm, b) 12.5 mm, Lebanon Mixtures

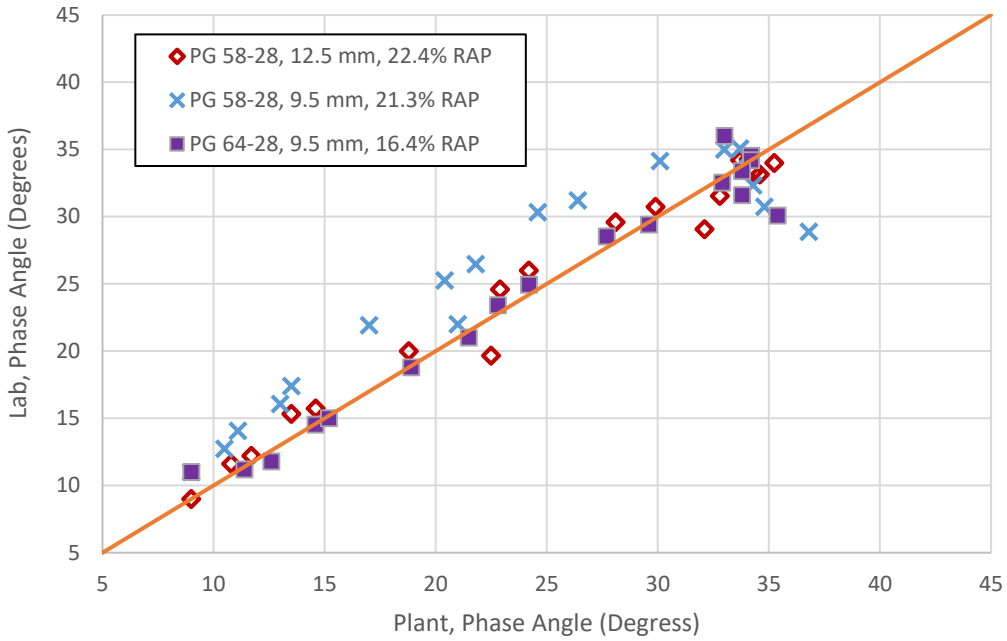

Figure 3-7. Phase Angle Values of Lab versus Plant Produced Mixtures for Hooksett Mixtures

3.3.2.3 SVECD Fatigue

Figures 3-8 and 3-9 compare the damage characteristic curves (DCC) of the different plant and lab produced mixtures for Lebanon and Hooksett, respectively. Generally, DCC curve shows how the material integrity of the specimen decreases as damage is growing. The mixtures that have DCC curves further up and to the right would be expected to perform better, since they are able to maintain their integrity better during the test. However, the cracking performance of a mixture in the field depends on pavement structure as well.

The DCC curves of lab produced mixes are very close to, or higher than plant produced ones for all Lebanon, 12.5 mm mixtures, indicating lab produced specimens might show better performance during the fatigue cyclic test, while most of the 19 mm plant produced mixtures have slightly better fatigue resistance than lab produced mixtures with showing higher pseudo stiffness in a same amount of damage.

One interesting point is that there is not a significant difference between the damage characteristic curves of 19 mm mixtures, while 12.5 mm mixtures show a larger distinction between mixtures. 18.9% RAP mixtures show a more rapid decrease in material integrity compared to 28.3% RAP mixtures, while the material integrity of RAP/RAS mixtures decreases with a lower slope in most cases.

Another observation is that in most cases, the last point of the DCC curve, which represents the pseudo stiffness at failure (C_F), increases with higher percentage of RAP. As can be seen in Figure 6, C_F also increases by using stiffer binder (PG 58-28) instead of PG 52-34 in asphalt mixtures. The increase of C_F with higher percentage of RAP is observed in other studies, as well (18, 19).

For Hooksett mixtures, two plant produced, PG 58-28 mixtures have higher DCC curves than lab produced mixtures, while the curves of PG 64-28 are very close. The highest difference is observed in two PG 58-28 mixtures, which agrees with dynamic modulus and phase angle results.

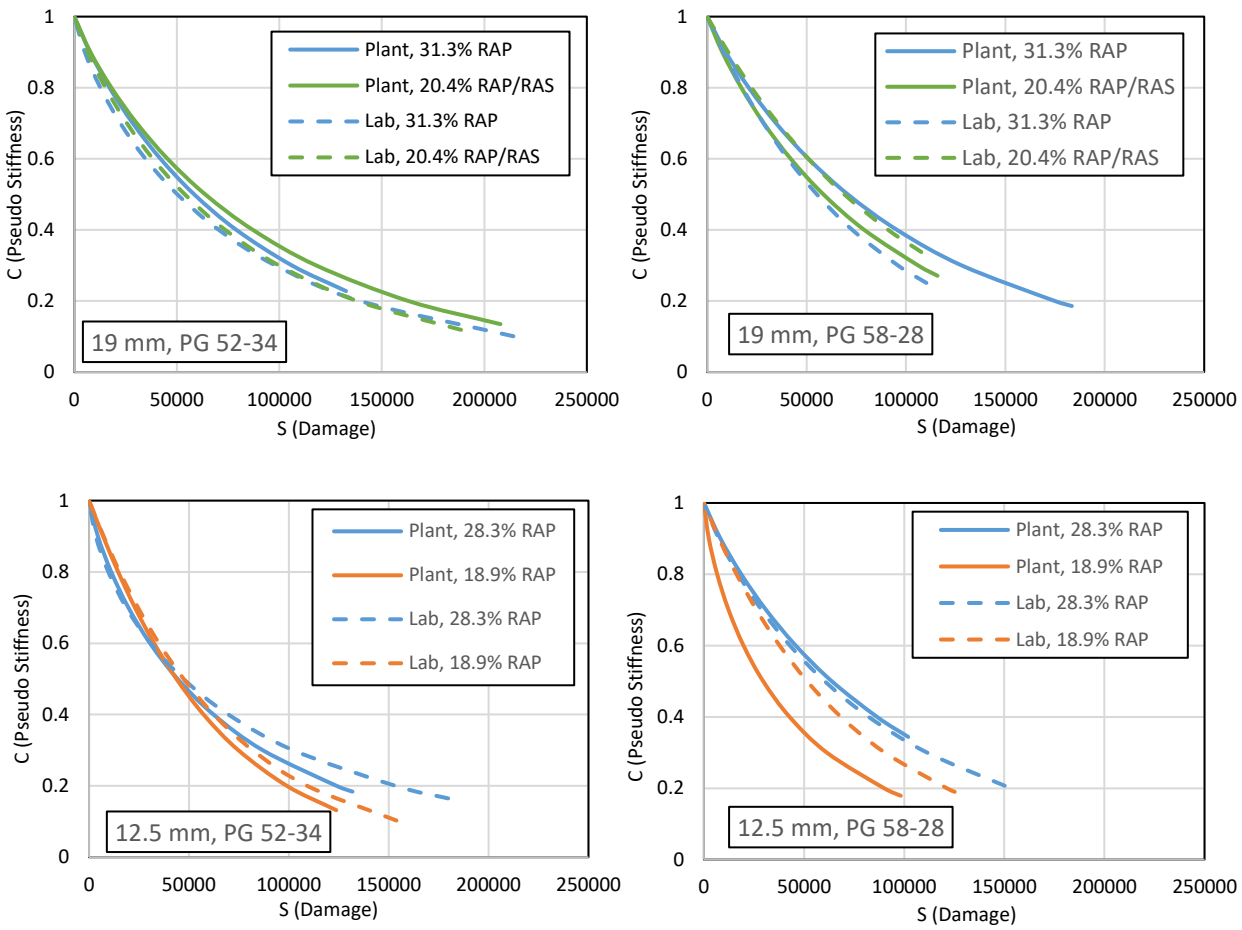

Figure 3-8. Damage Characteristics Curves of Lebanon Mixtures

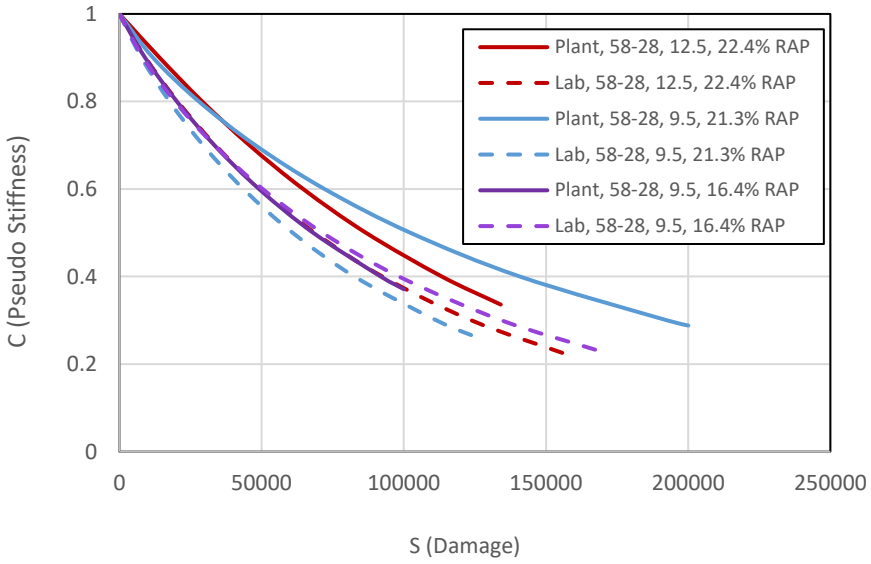

Figure 3-9. Damage Characteristics Curves of Hooksett Mixtures

Figures 3-10 and 3-11 compare the fatigue failure criterion (G^R) versus the number of cycles (N_f) of plant produced and lab produced mixtures for Lebanon and Hooksett, respectively. Generally, the higher G^R values at the same number of cycles (N_f) indicates better fatigue performance.

In most cases, there is a strong relationship (high coefficient of determination, R^2) between fatigue failure criterion (G^R) and the number of cycles to failure (N_f). The 30% RAP plant produced mixtures (31.3% RAP for 19 mm and 28.3% RAP for 12.5 mm) have slightly better fatigue performance than the lab produced mixtures and the lab produced RAP/RAS mixtures show better fatigue life.

The mixtures containing only RAP (18.9% to 31.3%) with both 12.5 and 19 mm NMAS show a similar behavior, while incorporating RAS improves the asphalt fatigue life. However, adding RAS might result in a more brittle mixture and sudden failure at high G^R values, as occurred in 19 mm, PG 52-34 mixture.

The trend of G^R versus N_f diagrams for Hooksett mixtures is similar to DCC curves. The plant produced PG 58-28 mixtures show better fatigue behavior than the corresponding lab produced mixtures, while it is the reverse for the PG 64-28 mixture.

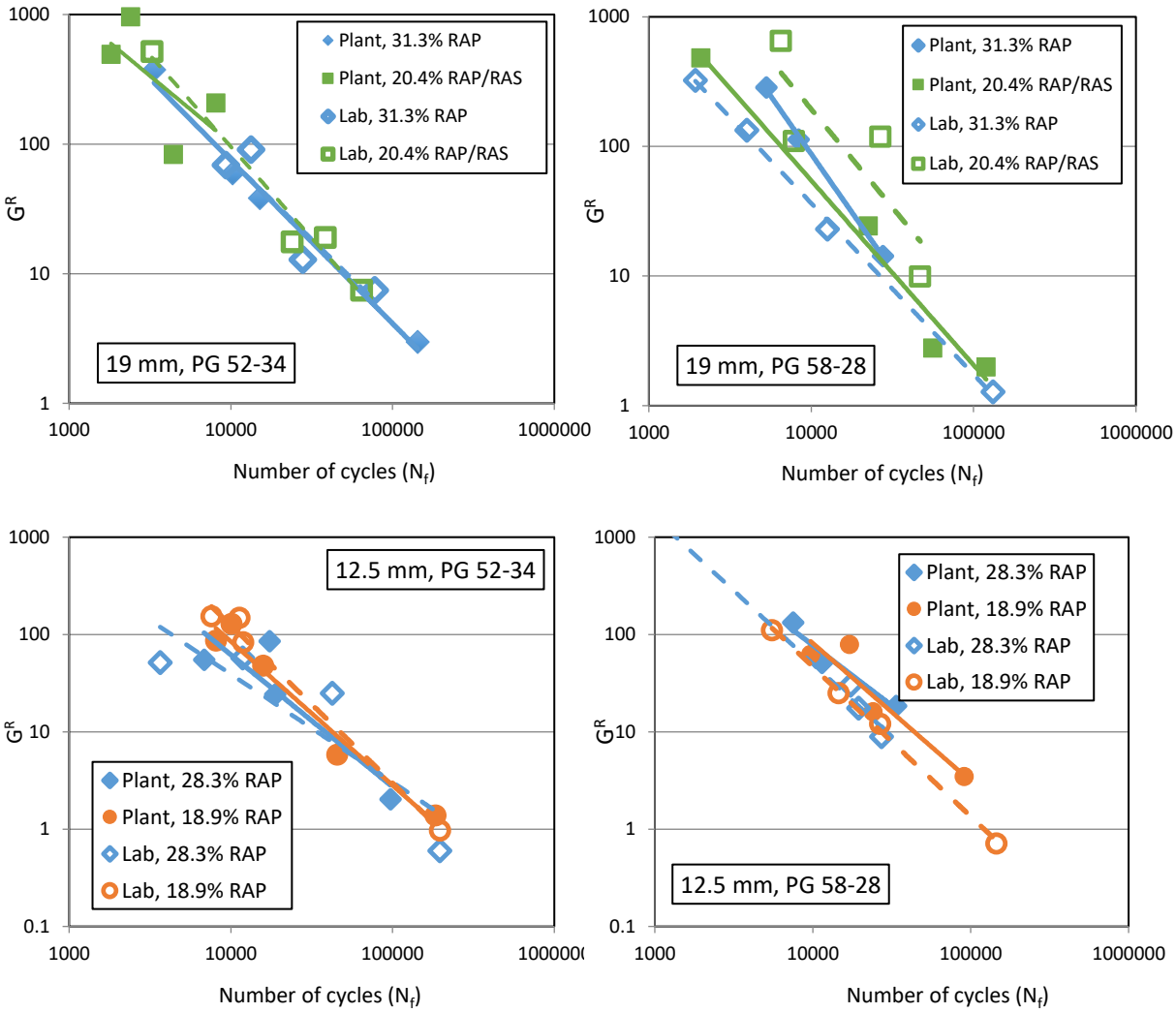

Figure 3-10. Fatigue Failure Criterion versus Number of Cycles for Lebanon Mixtures

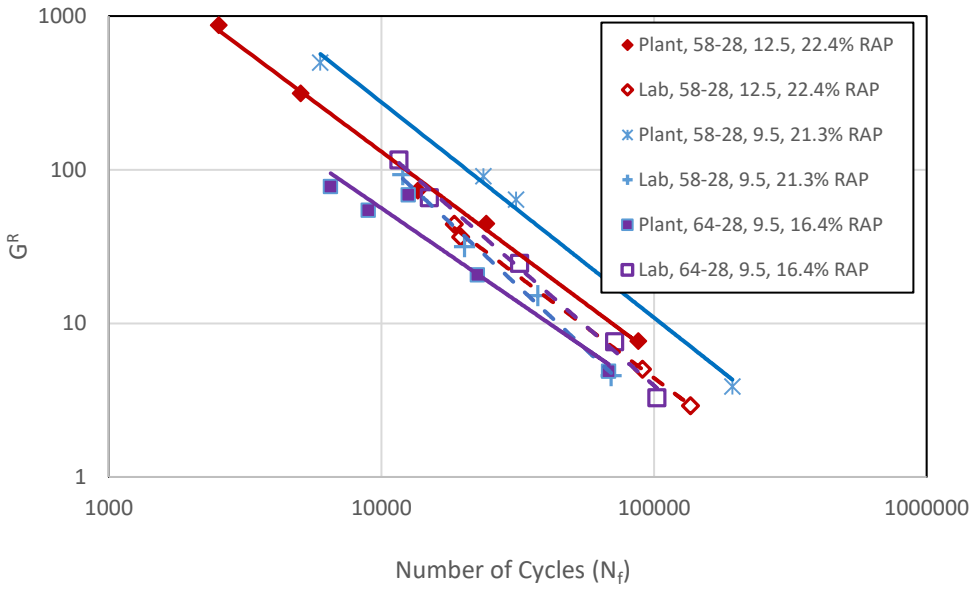

Figure 3-11. Fatigue Failure Criterion versus Number of Cycles for Hooksett Mixtures

3.3.3 Pavement Analysis

The mixtures produced in the Lebanon plant were placed in the field along New Hampshire (NH) State Route 12 near Westmoreland during the 2013 construction season. Figure 3-12 shows the cross section of the pavement that is used in the LVECD program to simulate the fatigue performance of mixtures in the field. Other critical inputs for running the analysis include:

Vehicle speed: 96.5 km/h (60 mph)

Tire load: single axle, 40 kN (8992 lbf)

Tire pressure: 759 kPa (110.1 psi)

Tire imprint shape: rectangular

Average annual daily truck traffic: 1800 vehicles per day

Growth rate: Linear at 2.8% per year

LVECD model predicts pavement responses and damage evolution (fatigue and rutting) in both spatial distribution and time history modes. One of the most useful outputs of this program is damage factor (N/N_f) which is calculated on the basis of cumulative damage model and Miner's

rule. The damage factor varies in magnitude from 0 (no damage) to 1 (completely damaged element) (20).

Figures 3-13 and 3-14 compare the percentage of the asphalt layer that has failed for lab and plant produced mixtures over the service life of pavement (20 year) for Lebanon and Hooksett mixtures, respectively. This parameter is calculated by dividing the number of failed points (N/N_f =1) in each section by the total number of elements. Some of the mixtures do not show any failure points, indicating that fatigue cracking would not be a primary concern in this pavement structure with these mixtures.

Generally, there is not a consistent trend in the fatigue life evaluation of plant versus lab produced mixtures. Totally, there are zero failure points for 2 lab produced and 4 plant produced mixtures. PG 52-34, 19 mm, plant produced, RAP/RAS mixture shows the worst fatigue performance, followed by PG 58-28, 19 mm, lab produced, RAP/RAS mixture.

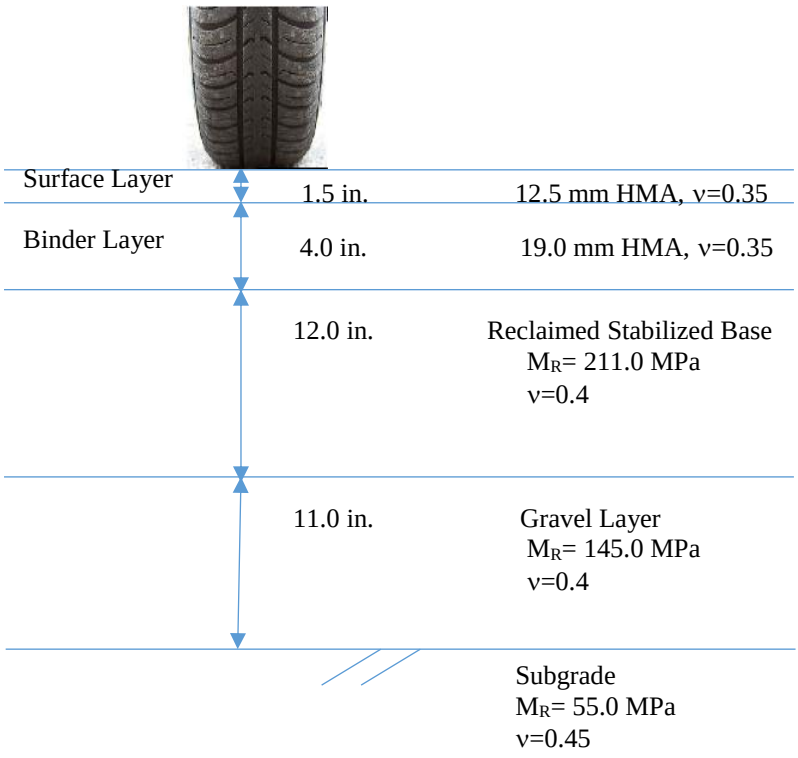

Figure 3-12. Pavement Cross Section and Materials Used in LVECD Analysis

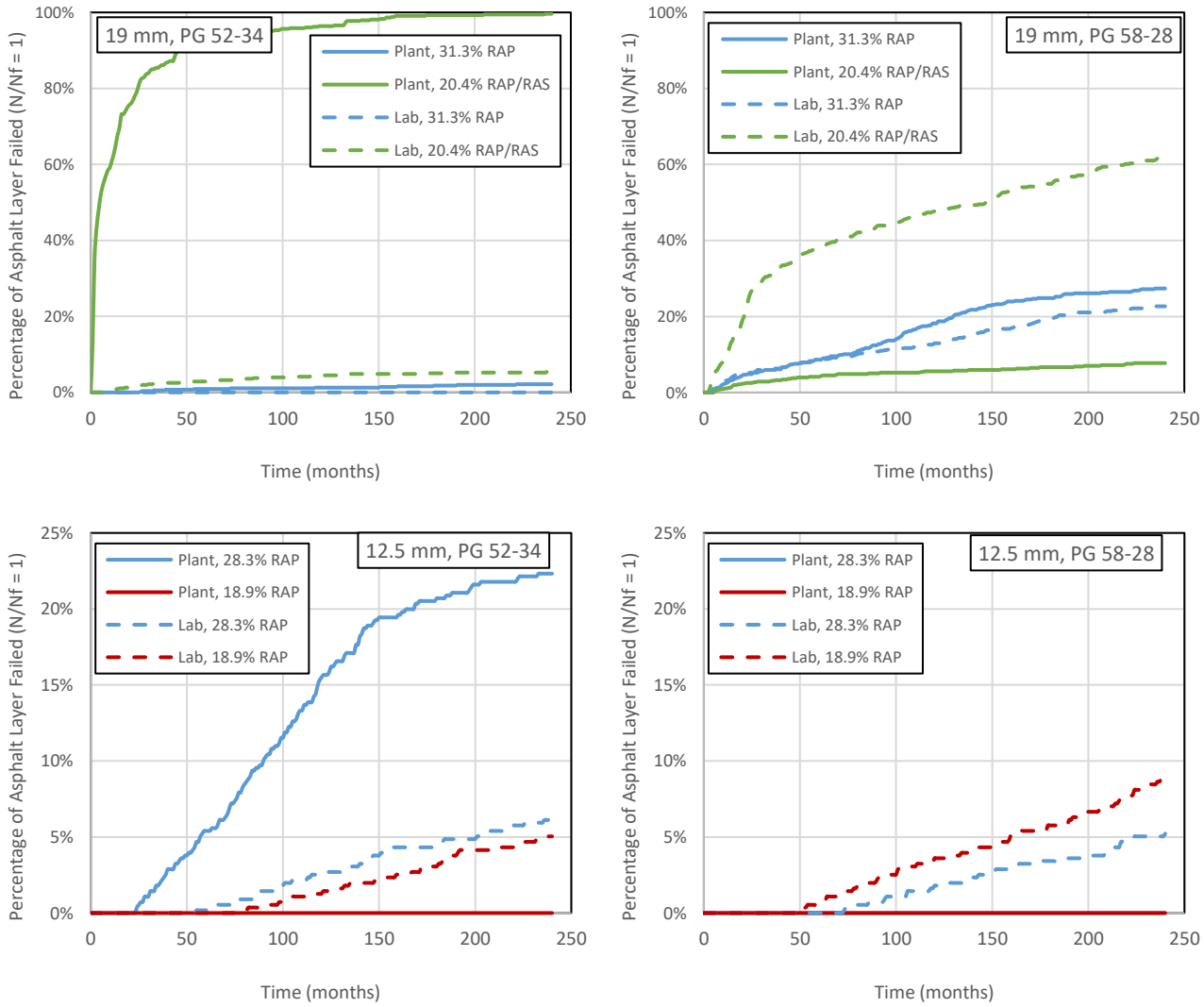

Figure 3-13. Number of Failure Points for Lebanon Mixtures Using LVECD

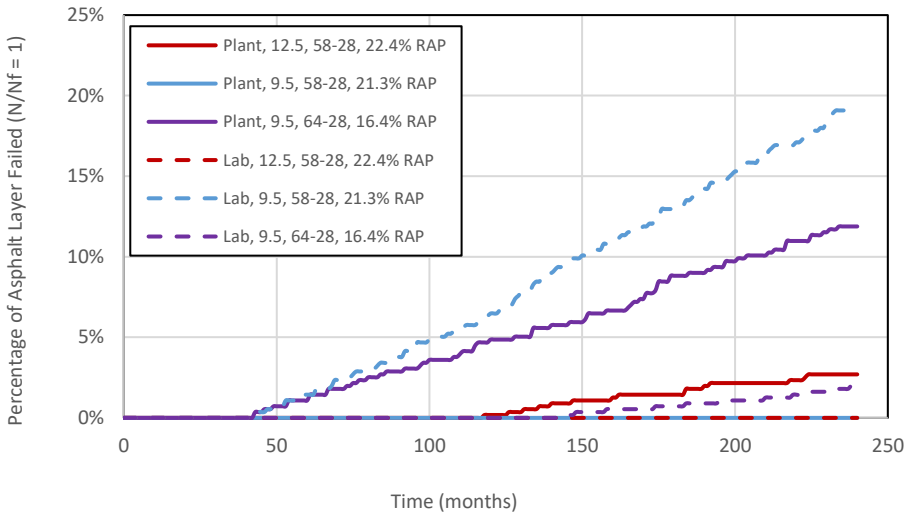

Figure 3-14. Number of Failure Points for Hooksett Mixtures using LVECD

3.4 Summary and Conclusions

The main objective of this research was to compare laboratory measured properties and cracking behavior of plant and laboratory produced specimens and the impact of different mixture variables including NMAS, RAP and RAS content, PG binder grade, and binder source. The study included the evaluation of 11 plant produced mixtures and 11 laboratory produced mixtures. Performance grading was conducted on extracted and recovered asphalt binders, and mixture testing including complex modulus and SVECD fatigue were performed on asphalt mixtures. LVECD software was also used for pavement structure evaluation. The following conclusions were drawn from the results of testing and analysis:

- The binder testing results generally show warmer high and low PG temperatures for laboratory produced mixtures, indicating the laboratory production method results in material that is more aged than the plant produced material.
- The binders extracted from the 19 mm mixtures have warmer temperatures than those extracted from 12.5 mm mixtures. Slightly higher actual binder replacement values in

the 19 mm mixtures also may contribute to the warmer temperatures. The rheological properties of virgin binders from different sources reflect on PG temperatures of extracted and recovered binders.

- The results show all binders used in this study are m-controlled. In most cases, ΔT_{cr} values are higher for the laboratory produced mixtures. Generally, ΔT_{cr} of the mixtures containing RAS are larger than those for the mixtures with RAP only, suggesting the inclusion of RAS makes the material more susceptible to cracking.
- The results of complex modulus testing were not consistent for different plants. For Lebanon mixtures, dynamic modulus of laboratory produced mixtures are typically higher than that of plant produced mixtures, with greater difference observed with 19 mm and PG 58-28 mixtures, which is in agreement with the binder testing results. While for Hooksett plant, higher dynamic modulus is observed for plant produced mixtures.
- The results of phase angle diagrams show the comparable phase angles for lab and plant mixtures, but in most cases the phase angles of lab produced specimens are slightly lower than plant produced, indicating less relaxation ability for lab mixtures.
- Generally, the difference between DCC curves for lab produced mixtures is less than those for plant produced ones. Also, most 12.5mm lab produced mixtures show more integrity than their corresponding plant produced mixes during the fatigue testing, while the integrity of 19 mm plant produced mixtures are higher.
- Different plants may produce different effects on the properties and behavior of asphalt mixtures. The reason can be different production factors such as temperature, mixing time, storage and handling conditions.
- There is no evident trend between fatigue life evaluation of plant and lab produced mixtures. The variation of fatigue damage prediction is much higher for plant produced mixtures. The worst predicted fatigue life is related to the mixtures with RAS/RAS.

Overall, the results of this study demonstrate that specimens produced in the laboratory and plant can result in measured material properties that are significantly different. There is not a constant shift between the properties measured on laboratory and plant produced specimens, with differences being influenced by virgin binder grade, aggregate gradation (perhaps due to effective binder content/film thickness), and virgin binder source. This study only included investigation of short term aging condition; future work is needed to investigate the impact of long term aging as well. Also, evaluation of the impact of changing material properties on thermal cracking and rutting performance needs to be assessed for application in performance based approaches. The variation of aggregate gradation can also be compared for lab and plant produced mixtures as a future work through sieve analysis after the binder extraction.

Chapter 4

COMPARISON OF ASPHALT BINDER AND MIXTURE CRACKING PARAMETERS

4.1 Introduction

Cracking is one of the main types of distresses in asphalt pavements. The two major types of cracking, fatigue and thermal cracking, have different mechanisms in terms of crack initiation. Fatigue cracking is a load associated type of cracking which occurs when the number of load repetitions exceeds the fatigue life of pavement, and the average temperature of the pavement layer in the field is considered as the critical temperature for fatigue cracking. Thermal cracking occurs at low temperatures, when the thermally induced stress at the top of the pavement exceeds the tensile strength of the asphalt mixture.

Asphalt concrete is a non-homogenous viscoelastic material, and its behavior depends on the properties of the asphalt binder and the aggregate skeleton. Cracking in asphalt pavement is not only dependent on the properties of the asphalt mixture itself, but also on other factors such as climate, pavement structure, and traffic loads. Asphalt binder plays an important role in asphalt mixture performance. Changes in stiffness, relaxation capability, and aging condition of the binder can alter the cracking resistance of the mixture. The relationship between binder properties and mixture properties is complicated and is still not completely understood. Many studies have been conducted on the binder and mixture properties that are associated with the cracking performance of asphalt mixtures. Safaei, et al. (2016) compared the asphalt binder

and mixture models for fatigue cracking using the simplified viscoelastic continuum damage (SVECD) approach and showed there is a good agreement between them. Fatigue performance of asphalt binder versus asphalt mixture and full-scale pavements was studied by Al-Khateeb et al. (2008). In terms of thermal cracking, Moon et al., (2013) measured the thermal stresses calculated from asphalt binder and mixture creep data and demonstrated that there is a significant difference between the results. A study by Reinke et al. (2016) showed only a moderate correlation of ΔT_{cr} with thermal cracking ($R2 \approx 0.6$), compared to the correlation of ΔT_{cr} with only fatigue or to total cracking (including thermal cracking) with a $R2 > 0.9$.

Researchers have developed various cracking index parameters to evaluate the cracking potential of asphalt binders and mixtures, but there is still a question of how mixture properties change with changes in binder characteristics and how the binder and mixture parameters may differentially rank expected performance of materials with respect to cracking. The primary objective of this study is to directly compare several common and recently developed asphalt mixture and asphalt binder index parameters to determine if correlations exist with respect to fatigue and thermal cracking.

4.2 Cracking Parameters and Criteria

4.2.1 Binder; Methods and Parameters

It is well known that the binder rheology has an impact on asphalt cracking resistance. For the first time, Strategic Highway Research Program (SHRP) developed a new measure of binder rheology ($G^* \sin \delta$) as a criterion for fatigue cracking performance of asphalt mixtures at intermediate temperature. The maximum value of 5000 kPa is considered for asphalt binders subjected to long-term laboratory aging. Although introducing this measure by combining stiffness and relaxation of binder was progress, it is accepted that $G^* \sin \delta$ is not able to

adequately represent the fatigue cracking behavior (Rowe et al. 2014).

In this study, performance grading was conducted to obtain high and low PG temperatures. Thermal cracking evaluation in the Superpave specification was conducted using the bending beam rheometer (BBR), AASHTO T 313, at a temperature 10°C warmer than the binder low temperature grade. The creep stiffness (S value) and the slope of creep stiffness curve (m value) were measured and the temperature at which the material meets the maximum value of 300 MPa and the minimum value of 0.300 for the S and m value criteria, is determined. It is believed that the binders that show greater difference between the critical low temperatures of S=300 MPa and m=0.300 are more prone to thermal cracking. Based on this idea, Anderson et al., (2011) developed the ΔT_{cr} parameter which is defined as the difference between two low temperatures T (S=300 MPa) – T (m=0.3). A crack warning value of -2.5°C was suggested by Anderson (2011), and a cracking limit value of -5°C was suggested by Rowe (2011).

DSR testing using 4 mm geometry (WRI, 2010) over a range of temperatures and frequencies was conducted and allows for the development of both complex shear modulus and phase angle master curves to describe the stiffness and relaxation capability, respectively. Black space diagrams are used to capture both stiffness and relaxation together to assess the relative cracking behavior of binders.

Two useful parameters that can be calculated from the results of 4 mm DSR testing are R value and Glover-Rowe (G-R) parameter. R value, is a rheological parameter determined from the complex modulus master curve and, as can be seen in Figure 4-1, it is the difference between the log G* at crossover frequency and the log elastic asymptote of the master curve (Anderson et al., 1994). As aging or RAP content increases, the master curve tends to flatten, resulting in an increase in R value. Crossover frequency decreases with increase in binder aging (Jacques, et al., 2016). Based on this concept, Mogawer et al. (2015), suggested that crossover frequency versus R can show the relative aging of mixtures.

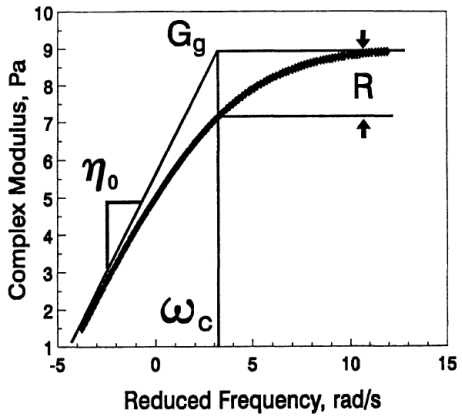

Figure 4-1. Schematic of definition of the rheological index

The Glover-Rowe parameter can be used to assess the cracking resistance of an asphalt binder. The basis of this approach was originally put forth by Glover et al. (2005). They suggested a correlation between a new DSR function with ductility using a temperature-frequency combination of 15°C and 1 rad/s. Studying airfield pavements, Anderson et al. (2011) identified that both the Glover parameter, G'/(η'/G'), and the ΔT_{cr} parameter quantify the loss of relaxation in asphalt binder during the aging process and can be used to assess non-load associated cracking in asphalt pavements.

Rowe (2011) rearranged the Glover criterion and using some simplifications, suggested a new expression to evaluate low temperature cracking performance. Glover-Rowe (G-R) parameter (Equation 4.1) captures the complex shear modulus (G*) and binder phase angle (δ) at temperature-frequency combination of 15°C - 0.005 rad/s. At the frequency of 0.005 rad/s, G-R parameter gives a boundary value of 0.18 MPa, which is considered as the onset of cracking, while a value of 0.60 MPa or more is suggested as an indicator of significant cracking. These values at this temperature-frequency combination were developed for a PG 58-28 climate region; current work is ongoing to determine how these should be adjusted to other climactic conditions.

$$\frac{G^*(\cos\delta)^2}{\sin\delta} \quad 4.1$$

4.2.2 Mixture; Methods and Parameters

Asphalt linear viscoelastic (LVE) properties have always played an important role in investigation of cracking performance of asphalt mixtures. In this study, an Asphalt Mixture Performance Tester (AMPT) was used to perform the complex modulus testing (AASHTO TP-79) on different mixtures. Dynamic modulus and phase angle results were obtained as two main components of LVE characterization.

To determine dynamic modulus master curves, the average data were shifted using time-temperature superposition principle, and a standard sigmoidal function was used to fit the dynamic modulus data (Equation 4.2).

$$\log|E^*| = \delta + \frac{\alpha}{1+\exp(\beta+\gamma(\log\omega))} \quad 4.2$$

where, $|E^*|$ is dynamic modulus, ω_r is reduced frequency, and α , β, δ, and γ are the fitting coefficients. δ is lower asymptote, α is the difference between the upper and lower asymptote values, and, β and γ define the shape of master curve; γ is related to the width of relaxation, and β affects the location of inflection point (the frequency of inflection point = $10\text{^}(\beta/\gamma)$), (Rowe et al. 2009). Like |G*| and phase angle for binder, the |E*| and phase angle are indicators of mixture stiffness and relaxation capability that can impact on cracking.

Mensching et al. (2016) discussed the impact of fitting parameters of β and γ on the shape of dynamic modulus master curves. Figure 4-2 shows how the shape of master curve changes with varying two parameters of γ and β. As asphalt materials age, the master curve tends to flatten, and γ value increases (the absolute value decreases). The inflection point position is controlled by the β parameter. The inflection point moves to the left (lower frequencies) with increase in RAP or aging of asphalt materials (Mensching et al. 2015). Crossover frequency parameter (–

β/γ) versus relaxation spectra width parameter (γ) plot for mixtures is similar to crossover frequency versus R value plot for binders.

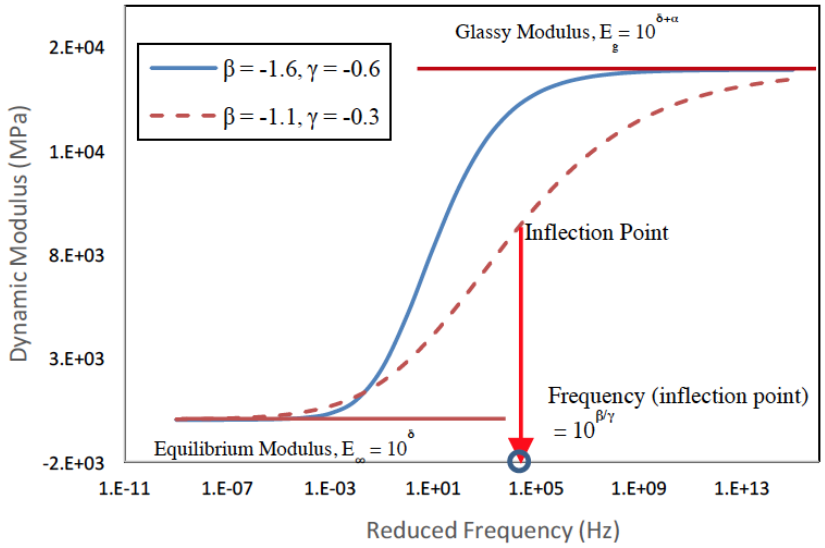

Figure 4-2. Schematic of |E*| Master Curve with Varying β and γ Parameters

Mensching et al. (2016) developed a mixture based Black space parameter with the same format of the Glover-Rowe parameter. This parameter employs stiffness and relaxation of mixture (|E*| and δ) instead of complex modulus and phase angle of binder. The suggested parameter by the authors can be calculated from Equation 4.3 at the frequency of 0.01666 rad/s and temperature 10°C warmer than the PG low temperature of binder.

$$|E^*|(\cos\delta)^2/(\sin\delta) \leq 3.68E4\ MPa \quad 4.3$$

To evaluate the fatigue behavior of asphalt mixtures, uniaxial fatigue testing was conducted on different mixtures following AASHTO TP-107 procedure. The simplified viscoelastic continuum damage (SVECD) approach to cracking, developed by Underwood and Kim (2010), models the constitutive response of asphalt concrete over cyclic loading in uniaxial tensile mode. It is a mechanistic model that predicts fatigue cracking performance under different

stress/strain amplitudes at various temperatures. Damage characteristic curves in terms of C (pseudo stiffness) versus S (damage parameter) and an energy-based failure criterion curve of G^R versus number of cycles to failure (N_f) are developed in this approach. G^R (Equation 4.4) is defined as the rate of change of averaged released pseudo strain energy throughout the test. Sabouri and Kim (2014) developed G^R and showed it is strongly correlated with the number of cycles to failure (N_f).

$$G^R = \frac{\int_0^{Nf} W_C^R}{N_f^2} \quad 4.4$$

Where W^R_C is released pseudo strain energy and N_f is the number of cycles before failure. The corresponding fatigue cracking in the field will depend on both the pavement structure and mixture properties. An index parameter defined as the number of cycles at G^R= 100, suggested by Sabouri et al. (2015), is used in this study to compare fatigue life of different mixtures. Generally, higher N_f value at the same G^R indicates better fatigue resistance.

The Disc-shaped Compact Tension Test (DCT) was conducted on several mixtures to characterize the low temperature cracking behavior in asphalt mixtures. Fracture energy (G_f) is an engineering property that can be determined from the DCT testing. The fracture work is defined as the area under the load versus crack mouth opening displacement (CMOD) curve. Fracture energy is determined by normalizing the fracture work for specimen thickness and ligament length. The fracture energy is considered to be the amount of energy required to develop a unit surface fracture of the asphalt mixture. Furthermore, the initial post peak slope (m) was used to characterize the material response past the peak load. The fracture energy normalized by the initial post peak slope (G_f/m) was also studied for different specimens (Al-Qadi et al. 2015).

Pavement fatigue life evaluation for all of the mixtures was conducted using Layered Viscoelastic Critical Distresses (LVECD) software developed by Eslaminia et al. (2012). To

assess the fatigue behavior, this 3D finite element based software employs the SVECD approach.

4.3 Materials

This study includes testing on 14 mixtures that were produced in drum plants in Lebanon, NH, and Hooksett, NH. The mixtures produced at Lebanon were placed in the field along New Hampshire (NH) State Route 12 near Westmoreland during the 2013 construction season. The Hooksett mixtures were produced during the 2014 construction season; the field location of these mixtures is unknown. The mixtures are varied in PG binder, binder source, nominal maximum size of aggregate (NMAS), recycled material type, and binder replacement amount. Table 4-1 shows the combinations evaluated, mix design volumetric information, and actual binder replacement values. The RAP binder had a continuous grade of 81.3-19.3°C. The RAS material is primarily tear-off shingles and could not be graded in the laboratory.

Table 4-1. Mixtures Information and Properties

Plant	Virgin Binder PG Grade	Binder Source	NMAS (mm)	%Total Asphalt (P_{be})	VMA (%)	(VFA) (%)	% Binder Replacement (% RAP/ % RAS)
Lebanon	58-28	Source 1	12.5	5.3 (4.7)	15.5	74.9	18.9 (18.9/0)
				5.3 (4.7)	15.1	76.6	18.5 (7.4/ 11.1)
				5.3 (5.0)	16.2	75.8	28.3 (28.3/ 0)
			19	4.7 (4.2)	14.1	74.4	20.8 (20.8/0)
		Source 2	19	4.8 (4.4)	15.0	71.3	20.4 (8.2/ 12.2)
				4.7 (4.4)	14.1	75.9	31.3 (31.3/ 0)
	52-34	Source 1	12.5	5.3 (4.7)	15.5	74.9	18.9 (18.9/0)
				5.3 (4.7)	15.1	76.6	18.5 (7.4/ 11.1)
				5.3 (5.0)	16.2	75.8	28.3 (28.3/ 0)
		Source 3	19	4.8 (4.4)	15.0	71.3	20.4 (8.2/ 12.2)
				4.7 (4.4)	14.1	75.9	31.3 (31.3/ 0)
Hooksett	58-28	Source 2	9.5	6.1 (5.7)	16.5	78.9	21.3 (21.3/0)
			12.5	5.8 (5.5)	15.9	79.5	22.4 (22.4/0)
	64-28		9.5	6.1 (5.7)	16.5	78.9	16.4 (16.4/0)

4.4 Results

4.4.1 Binder Results

The continuous high and low PG temperatures for the Lebanon RAP and virgin binders and all extracted and recovered binders are shown in Figure 4-3. The high PG temperatures for the RAP/RAS mixtures are greater than those for all of the RAP only mixtures, even at higher RAP binder replacement values. Higher RAP only content generally shows slightly warmer high PG temperatures. The mixtures made with source 3 PG 52-34 virgin binder do not show the benefit of the softer binder on the high PG temperature. The binder testing results on this virgin binder show elevated zinc levels, indicating that re-refined engine oil bottoms (REOB) may have been used in the production of this virgin binder.

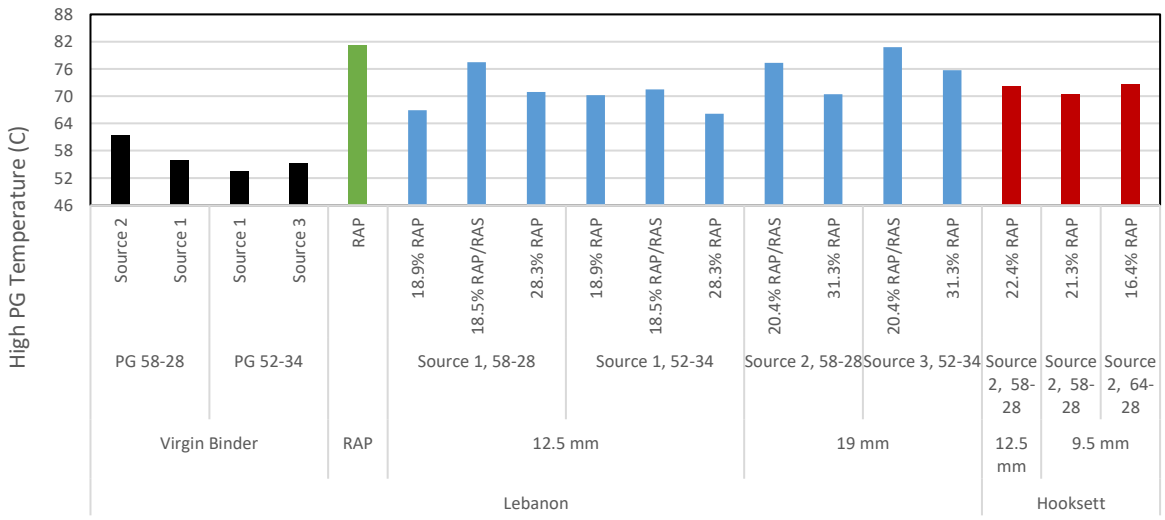

Figure 4-3. High PG Temperatures for Virgin and Extracted and Recovered Binders

Figure 4-4 shows the low PG temperatures for the different virgin and recovered binders. None of the extracted and recovered binders meet the required low temperature criteria for the region (all are warmer than -28°C). The mixtures with RAP and RAS show the warmest temperature, indicating that these mixtures might be more prone to cracking at the low temperatures than other materials. The materials containing the source 3 PG 52-34 virgin binder do not show the

benefit of the softer binder. As mentioned in the results of high PG temperature, the reason might be the presence of REOB in this binder. It should be noted that the process of binder extraction and recovery has been similar for all the binders. However, the impact of the extraction and recovery process on different binders from different sources may have been different that might influence on the binder grading results.

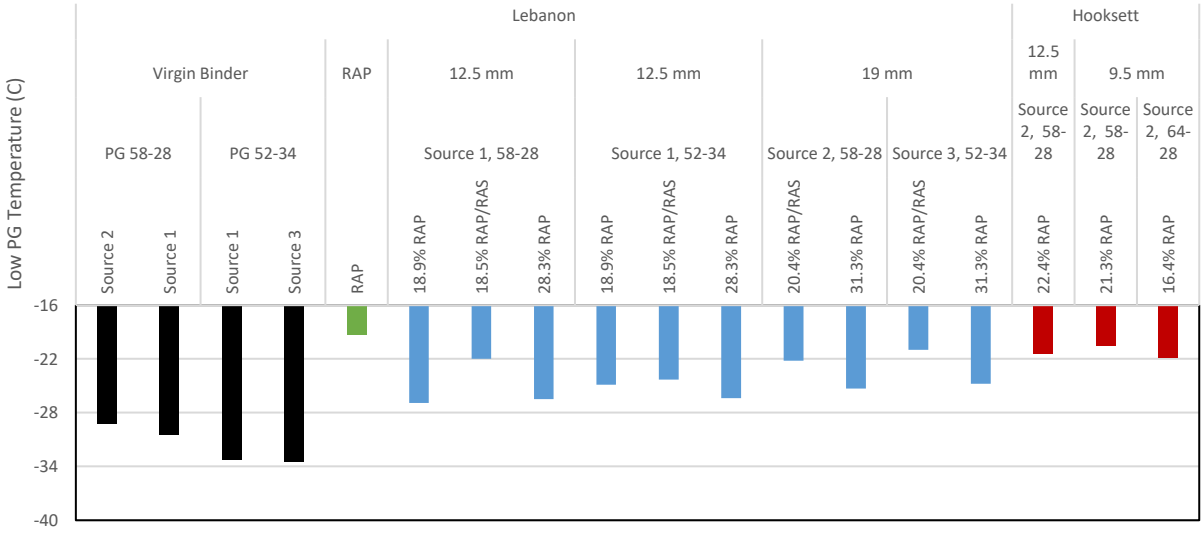

Figure 4-4. Low PG Temperatures for Virgin, and Extracted and Recovered Binders

Figure 4-5 shows the ΔT_{cr} values at 20-hour PAV aging level for all of the binders and also at 40-hour PAV for virgin binders and source 3 extracted binders; others are not shown due to the lack of sufficient materials for testing. The crack warning value (-2.5°C) and cracking limit (-5°C) are also shown on the plot. All of the virgin and recovered binders, except the source 1 PG 58-28, are m-controlled at the 20-hour PAV aging level. The 40-hour PAV aging further decreases the ΔT_{cr} values, with larger changes observed for the PG 52-34 virgin binders. The binders extracted and recovered from RAP/RAS mixtures all exceed the crack limit with ΔT_{cr} values less than -5°C. The use of softer binder grades did not improve the ΔT_{cr} values for the extracted and recovered materials, and in the case of source 3, produces values that are significantly worse than the corresponding materials with the PG 58-28 virgin binder.

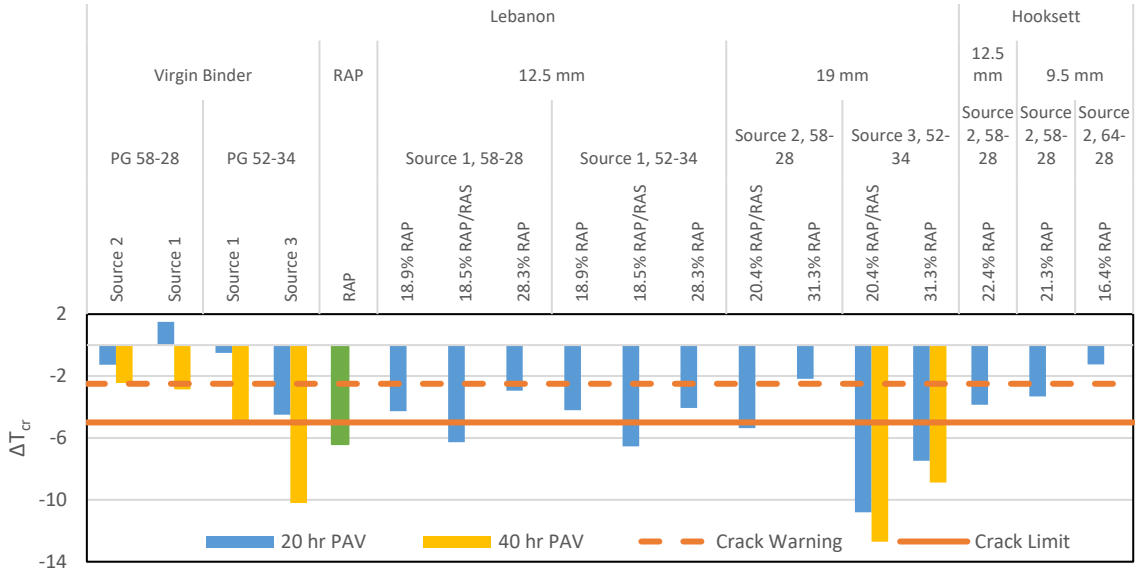

Figure 4-5. ΔT_{cr} Values for Virgin, and Extracted and Recovered Binders

The complex modulus master curves and Black space plots for the different extracted and recovered binders were developed using the results of 4 mm DSR testing and can be found in Daniel and Rahbar-Rastegar, (2016). All binders extracted and recovered from RAP/RAS mixtures show higher stiffness at higher temperature. The RAP/RAS mixtures have lower phase angles, or more elastic behavior, while PG 58-28, 19 mm, 31.3% RAP shows the highest phase angles.

Figure 4-6 shows the crossover frequency versus R value for different Lebanon recovered binders. Generally, materials that are further towards the lower right corner of the graph would be more likely to have cracking issues and materials move that direction with aging. The source 3 binders and binders extracted and recovered from RAP/RAS mixtures show the highest R values and lower crossover frequencies. Plotting R value versus ΔT_{cr} (Figure 4-7) is another way to represent how binder rheology changes as materials age. The results show that there is a strong relationship between R value and ΔT_{cr}, and the trends are is similar to those observed with R value versus crossover frequency.

Figure 4-8 shows the Glover-Rowe parameter for the various binders. Two curves of damage onset (G-R = 180 kPa) and significant cracking (G-R = 600 kPa) are added to the plot to evaluate which mixtures may potentially have cracking issues. The Glover-Rowe results are in a good agreement with the results of crossover frequency versus R-value. Two 19 mm, RAP/RAS mixtures have the highest G-R values. As with the PG parameters, use of the softer PG binder is not showing expected benefits with respect to cracking indices.

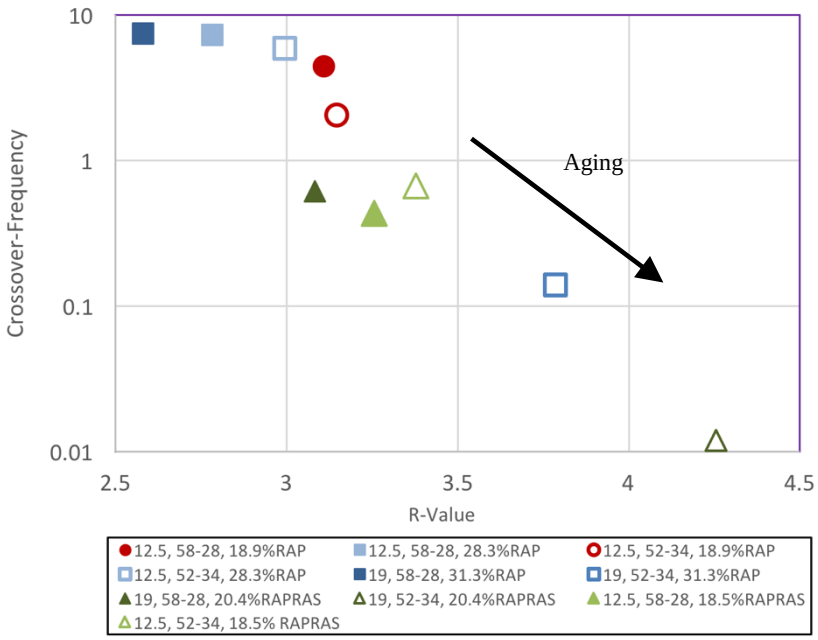

Figure 4-6. Crossover Frequency versus R-value for Extracted and Recovered Binders

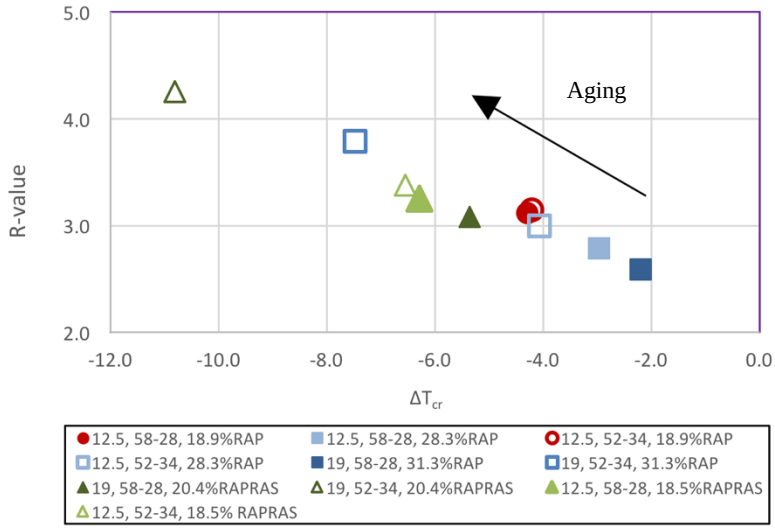

Figure 4-7. R value versus ΔT_{cr} for Extracted and Recovered Binders

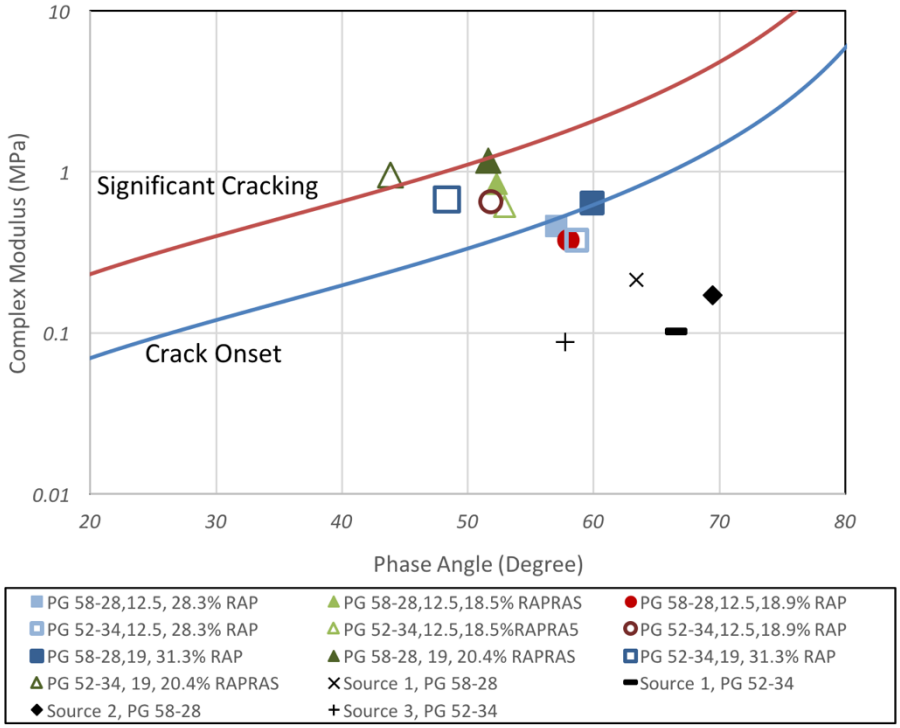

Figure 4-8. Glover-Rowe Parameter for Virgin and Extracted and Recovered Binders at 15°C and 0.005 rad/sec

4.4.2 Mixture Results

The average dynamic modulus master curves for all of the mixtures are shown in Figure 4-9.

Generally, the results are as expected with higher dynamic modulus curves for stiffer binders, coarser aggregate structure, and higher recycled content for Lebanon mixtures. The Hooksett mixtures have higher dynamic modulus values than the Lebanon mixtures. Similar to the G* master curves, the PG 52-34, 19 mm, RAP/RAS mixtures show the lowest dynamic modulus at the low temperatures and highest at the high temperatures.

To capture the stiffness and relaxation capability of mixtures together, the Black space diagrams are plotted in Figure 4-10. Generally, the lower dynamic modulus (stiffness) and higher phase angle (relaxation capability) are expected to improve the cracking resistance of mixtures. The phase angles generally decrease with increasing RAP content, and the RAP/RAS mixtures have the lowest phase angles. The phase angles are similar across the different gradations.

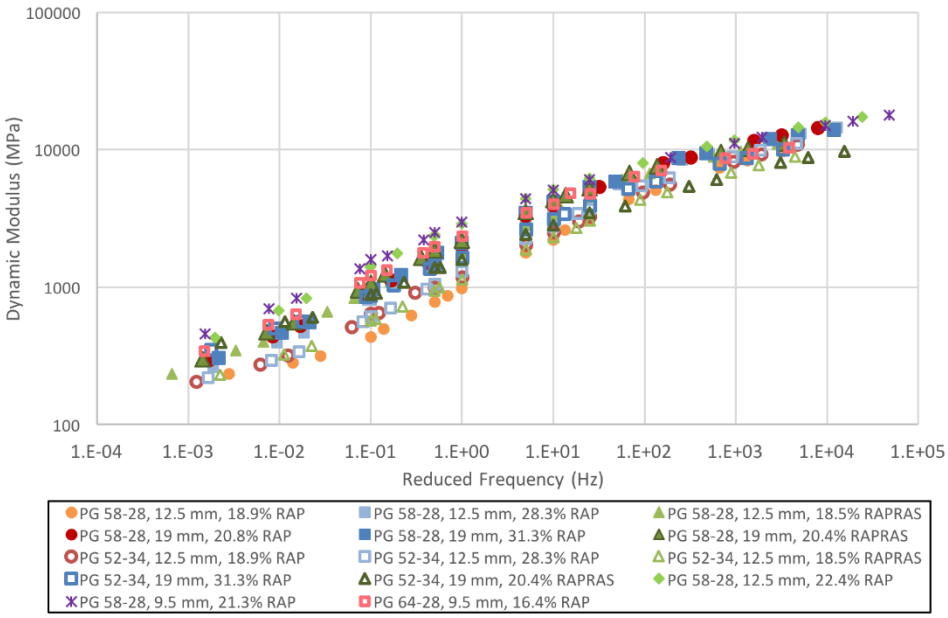

Figure 4-9. Average Dynamic Modulus Master Curves for All Mixtures

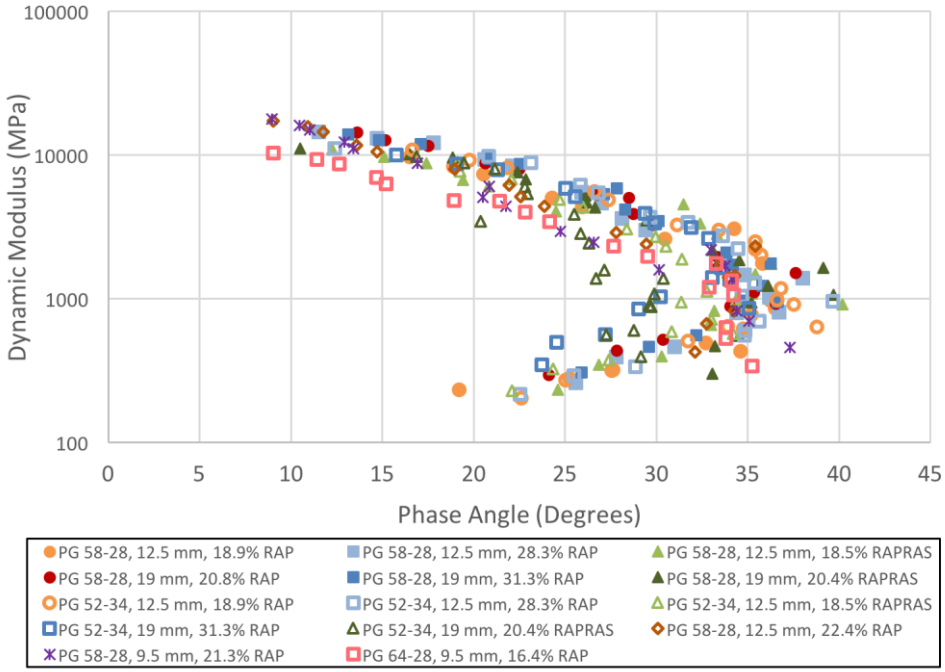

Figure 4-10. Black Space Diagrams for All Mixtures

After the dynamic modulus master curve is constructed, the data is fitted using a sigmoidal function (Equation 2). Figure 4-11 shows the cross-plot of the -β/γ and γ values for all of the mixtures. The expected relative positions of mixtures with different recycled content are generally not seen in this comparison. However, the relative positions of the softer binder grades (showing worse performance) do agree with what has been observed with other parameters. Comparing Figure 4-11 with Figure 4-6 (the equivalent binder plot), there are some relative similarities in mixture ranking but there is not a consistent trend in ranking of the two measures.

The mixture-based Glover-Rowe parameters (Mensching et al., 2015) for the mixtures are presented in Figure 4-12. In this study, the mixture-based G-R parameter is calculated at 15˚C and the frequency of 0.005 rad/s. There is not a threshold for this parameter, but materials that are further towards the upper left corner of the graph are expected to be more prone to cracking. As mixtures age, their response moves from the lower right to the upper left in this plot. The relative positions of various mixtures in this space are different than their relative positions in

the Glover-Rowe binder space. Two PG 58-28 Hooksett mixtures show higher mix-based Glover-Rowe values, indicating that they are expected to be more susceptible to cracking. Two PG 52-34, Lebanon mixtures have the lowest Glover-Rowe mix-based values. However, the mix-based Glover-Rowe parameters do show that using a softer binder grade is not effective in all cases. This is similar to the results obtained using other parameters.

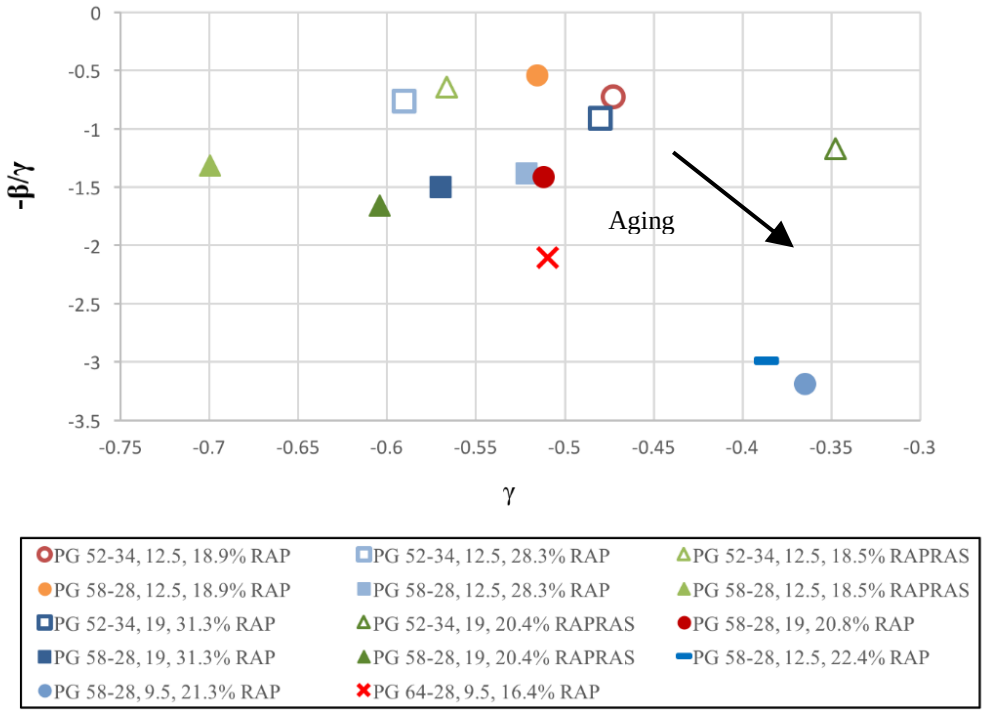

Figure 4-11. Mixture Crossover Frequency Parameter vs. Relaxation Spectra

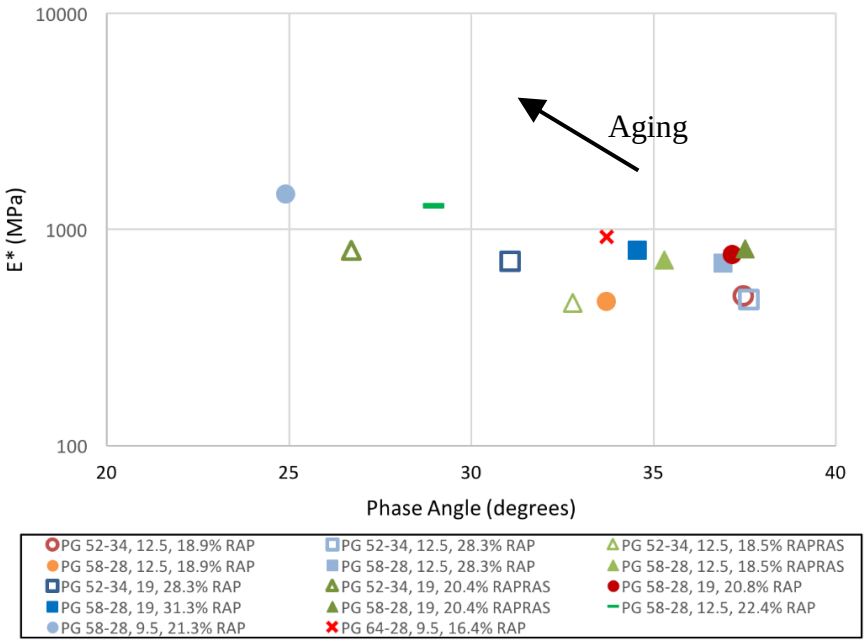

Figure 4-12. Mixture-based Glover-Rowe Modified Parameter at 15ºC and 0.005 rad/sec

Figure 4-13 shows the number of cycles to failure for different mixtures at G^R=100. For 12.5 mm, Lebanon mixtures, RAP/RAS mixtures have the higher number of cycles, but for 19 mm mixtures, 31.3% RAP mixtures show better fatigue life. The lowest N_f is observed with the Hooksett mixture that has the stiffest type of binder in this study. Again, the benefit of a softer binder with the higher recycled content levels is not observed in some cases with this parameter.

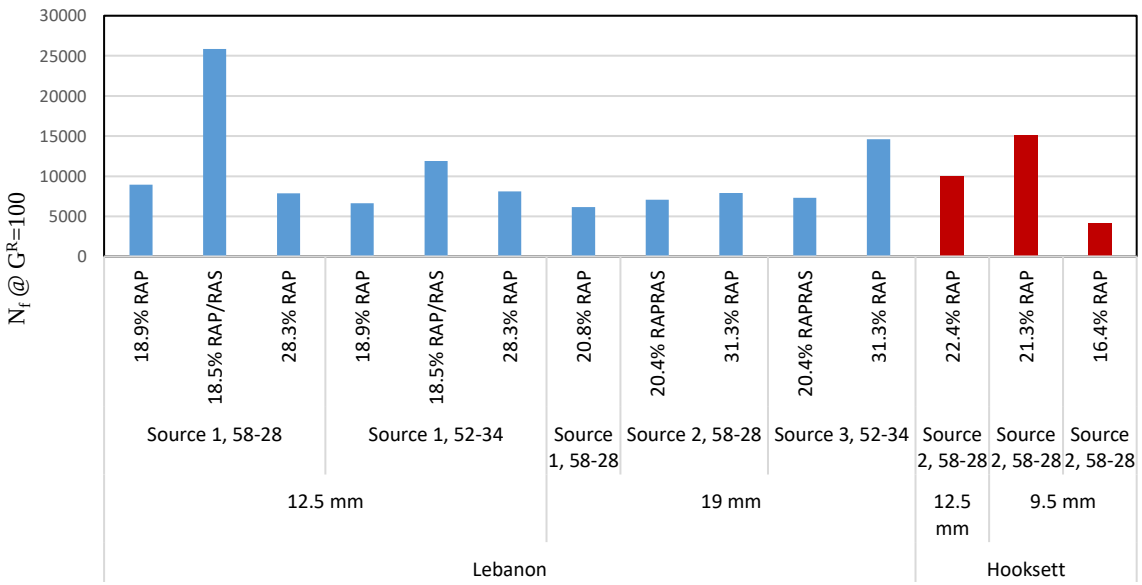

Figure 4-13. Number of Cycles to Failure at G^R=100

The appropriate low temperature PG grade for Westmoreland was determined to be -28°C using the LTPPBind software. DCT testing was performed at -18° C (10 degrees warmer than low PG temperature) for mixtures that had sufficient material available for DCT testing. Figures 4-14 and 4-15 show the fracture energy and G_f/m parameters, respectively, for all of the mixtures. The Lebanon and Hooksett mixtures are distinguished by solid and hashed colors, respectively. The error bars indicate the standard deviation. As can be seen, the variation of fracture energy for the mixtures is limited to 10%, except for PG 58-28, 9.5 mm, 21.3% RAP and PG 58-28, 19 mm, 20.4% RAP/RAS mixtures. According to Figure 14, the mixtures with finer aggregate show higher fracture energy before failure, meaning the finer mixtures are more resistant to cracking and require more energy to fail. The reason is probably the higher binder content of finer mixtures which make them more ductile.

Fracture energy is calculated as the area under load-CMOD curve. Accordingly, for different mixtures with similar fracture energies, this parameter may not capture the ductility of mixture in the post peak region if the mix exhibits a very high peak load. For better understanding of asphalt mixtures' behavior at low temperature, the G_f/m parameter is calculated and results are shown in Figure 4-15. This parameter is defined as the measured fracture energy divided by the post peak slope (m) of load-CMOD curve. The higher G_f/m is favorable for better performance in low temperature cracking.

The general trend is in accordance with fracture energy values, except for PG 52-34, 19 mm, RAP/RAS mixture. Surprisingly, the mixtures having highest and lowest G_f/m contain the softer PG 52-34 binder, indicating that only using binder with a lower low temperature grade may not be sufficient in prevention against thermal cracking.

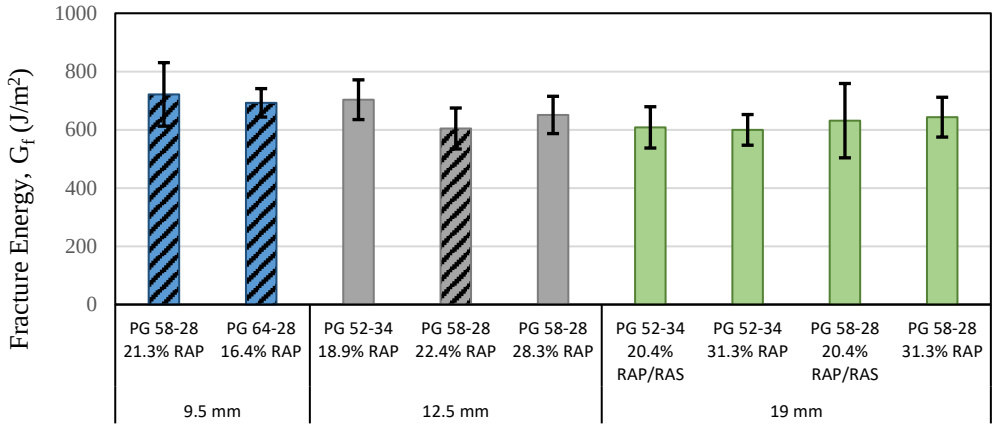

Figure 4-14. Fracture Energy for Different Mixtures

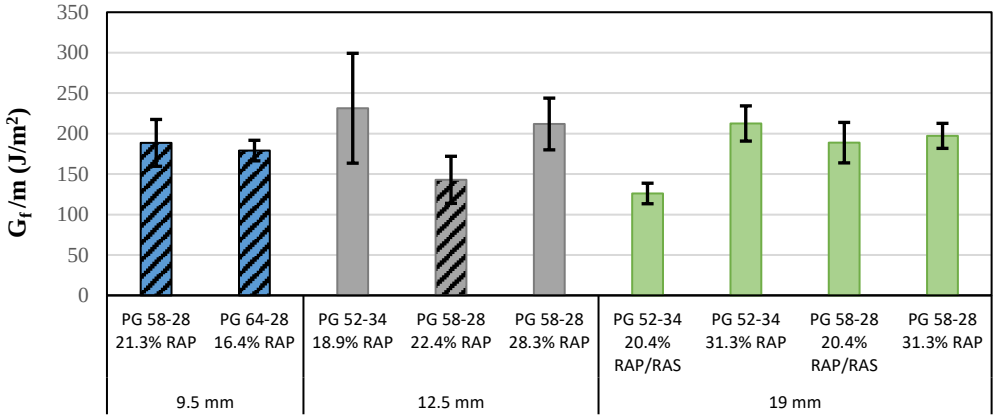

Figure 4-15. G_f/m for Different Mixtures

In the LVECD analysis, if the number of repetitions equals the number of cycles to failure ($N/N_f=1$), the element is considered to be failed. Figure 4-16 shows the percentage of failed elements in a pavement section at the end of a 20-year analysis. The mixtures can be ranked in three groups: 1- the mixtures with very low failure percentage (less than 5%), 2- mixtures with the failure percentage of 10-30%, and 3- two RAP/RAS mixtures with very high percent of failure.

Seven of the mixtures do not show any failure points, with the LVECD analysis indicating that fatigue cracking would not be a primary concern in this pavement structure with these mixtures. To evaluate potential differences in the fatigue behavior of these mixtures, the maximum damage factor value at the end of the 20-year analysis for these mixtures is shown in Figure 4-17. Although the performance of all seven mixtures are reasonable, more damage occurs in the

PG 52-34, 12.5 mm, 18.9% RAP mixture. The other mixtures all have N/N_f ratios less than 0.35.

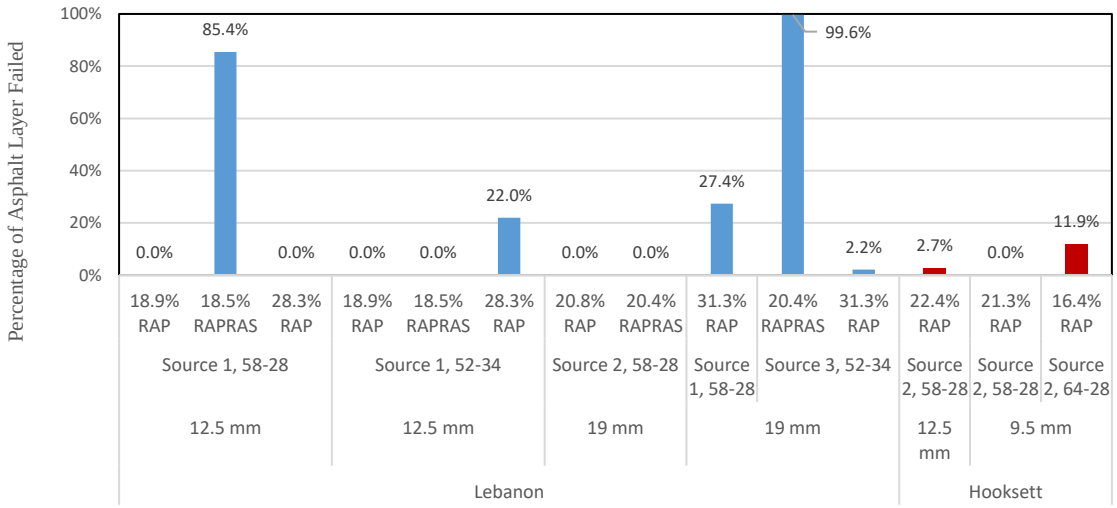

Figure 4-16. Percentage of Failure Points in Pavement Cross Section at the End of 20-year LVECD Analysis

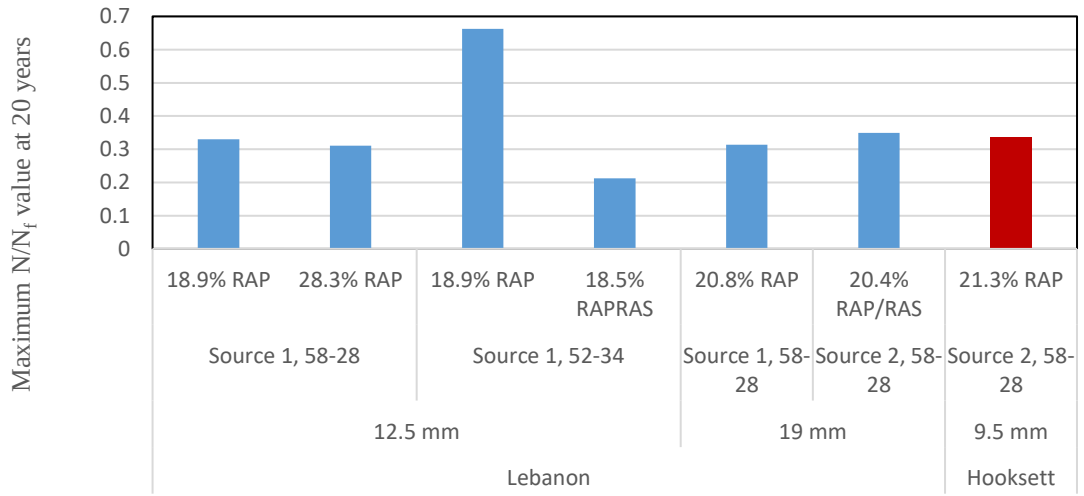

Figure 4-17. Maximum N/N_f Value in Pavement Cross Section at the End of 20 year LVECD Analysis

4.5 Discussion

In this section, the overall rankings and comparisons of properties measured from plant produced binders and mixtures are presented. The purpose of this comparison is to evaluate

how different binder and mixture parameters rank materials and under what circumstances testing of binders is a reasonable representation of the mixture test results. It should be noted that the aging condition of mixtures and extracted and recovered binders were different. The mixtures were compacted immediately after production at the plant without reheating and are therefore in a short-term aged condition. Binder testing was conducted on extracted and recovered binders that were subjected to 20 hr PAV, and are therefore in a long-term aged condition.

4.5.1 Comparison of Binder Parameters

Table 4-2 shows the value of the parameters and the ranking for different binders extracted and recovered from the mixtures. Ranks represent the best (value of 1) to worst with respect to cracking. The values are color coded for those parameters that have defined limits; **green** indicates the material passes, red indicates failure and *yellow* indicates intermediate values. Generally, the binder parameters have good agreement with each other. The Pearson correlation factor was used to investigate the correlation between all binder parameters. This parameter shows the strength of linear relationship between each pair of index parameters; a correlation factor of 1 equals to a perfect direct linear relationship and a correlation factor of -1 indicates a perfect inverse linear relationship. A value of zero indicates no relationship between two variables. The Pearson correlation factors for the parameter values and the rankings are presented in Tables 4-3 and 4-4, respectively. Values above an absolute value of **0.7** are shaded **green**, those between *0.4* and *0.7* are shaded *yellow* and those below 0.4 are shaded red. Some of the parameters are inherently unrelated to each other, but generally, R value, G-R parameter, ΔT_{cr}, and the continuous PG temperatures show a very good correlation. Similar results are obtained with the parameter rankings and the actual parameter values.

4.5.2 Comparison of Mixture Parameters

Table 4-5 shows the mixture parameter values and the relative ranking of the different mixtures. Tables 4-6 and 4-7 show the Pearson correlation factors between the mixture parameter values and ranking, respectively. The strength of the correlations is color coded similarly to the binder parameters. Generally, the relationships between mixture parameters are not as strong as those observed between the binder parameters. The results of LVECD analysis does not agree with the N_f @ G^R=100 parameter obtained from SVECD fatigue testing, especially for RAP/RAS mixtures. The difference between fatigue and DCT testing results can be explained due to the different cracking mechanism. A higher correlation factor for mix-based G-R with dynamic modulus and phase angle values is not surprising, since this parameter is based on Black space diagram. The color codes for values and ranking are generally very close, with several exceptions. For example, the Pearson correlation factor between the fracture energy and G_f/m values are higher than the correlation factor between their rankings. The existence of very close or very different data in each parameter can however make the rankings comparison misleading.

Table 4-2. Binder Parameter Rankings for Different Mixtures

Mixture		G-R		Delta Tcr		High PG Temp.		Low PG Temp.		R value	
		Mpa	rank	℃	rank	℃	rank	℃	rank	value	rank
Lebanon	PG 58-28, 12.5, 28.3% RAP	0.16	3	-3.0	3	70.9	6	-26.5	2	2.78	2
	PG 58-28, 12.5, 18.5% RAP/RAS	0.40	8	-6.3	11	77.5	13	-22.0	10	3.26	7
	PG 58-28, 12.5, 18.9% RAP	0.12	2	-4.3	8	66.9	2	-26.9	1	3.11	5
	PG 52-34, 12.5, 28.3% RAP	0.12	1	-4.1	6	66.1	1	-26.4	3	3.00	3
	PG 52-34, 12.5, 18.5% RAP/RAS	0.28	5	-6.5	12	71.5	7	-24.3	8	3.38	8
	PG 52-34, 12.5, 18.9% RAP	0.32	6	-4.2	7	70.2	3	-24.9	5	3.15	6
	PG 58-28, 19, 31.3% RAP	0.18	4	-2.2	2	70.4	4	-25.3	4	2.58	1
	PG 58-28, 19, 20.4% RAP/RAS	0.58	9	-5.4	10	77.3	12	-22.2	9	3.08	4
	PG 58-28, 19, 20.8% RAP			5.2	9	72.7	10	-24.8	7		
	PG 52-34, 19, 31.3% RAP	0.40	7	-7.5	13	75.7	11	-24.8	6	3.79	9
	PG 52-34, 19, 20.4% RAP/RAS	0.72	10	-10.8	14	80.8	14	-21.0	13	4.26	10
Hooksett	PG 58-28, 12.5, 22.4% RAP			-3.9	5	72.2	8	-21.4	12		
	PG 58-28, 9.5, 21.3% RAP			-3.3	4	70.4	5	-20.5	14		
	PG 64-28, 9.5, 16.4% RAP			-1.2	1	72.6	9	-21.9	11		

Mixture		G* (@ 0°C)		G* (@25°C)		Phase Angle (@0 °C)		Phase Angle (25 °C)	
		Pa	rank	Pa	rank	Degree	rank	Degree	rank
Lebanon	PG 58-28, 12.5, 28.3% RAP	1.2E+08	8	5.2E+06	6	25.2	3	46.4	1
	PG 58-28, 12.5, 18.5% RAP/RAS	1.1E+08	7	7.0E+06	8	23.7	8	41.5	8
	PG 58-28, 12.5, 18.9% RAP	9.2E+07	5	3.8E+06	1	25.8	2	45.7	4
	PG 52-34, 12.5, 28.3% RAP	9.2E+07	4	3.9E+06	2	25.9	1	46.2	3
	PG 52-34, 12.5, 18.5% RAP/RAS	8.7E+07	3	4.9E+06	5	24.5	5	42.0	6
	PG 52-34, 12.5, 18.9% RAP	9.7E+07	6	4.4E+06	3	25.2	4	44.1	5
	PG 58-28, 19, 31.3% RAP	1.5E+08	9	7.0E+06	9	23.9	7	46.3	2
	PG 58-28, 19, 20.4% RAP/RAS	1.5E+08	10	8.3E+06	10	22.4	10	41.9	7
	PG 58-28, 19, 20.8% RAP								
	PG 52-34, 19, 31.3% RAP	8.6E+07	2	4.9E+06	4	24.1	6	40.1	9
	PG 52-34, 19, 20.4% RAP/RAS	8.4E+07	1	5.5E+06	7	23.2	9	37.1	10
Hooksett	PG 58-28, 12.5, 22.4% RAP								
	PG 58-28, 9.5, 21.3% RAP								
	PG 64-28, 9.5, 16.4% RAP								

Table 4-3. Correlation between Binder Parameter Values

	G-R	ΔT_{cr}	High PG Temp	Low PG Temp	R value	G* (0°C)	G* (25°C)	Phase Binder (0°C)	Phase Binder (25°C)
G-R	1.00	**-0.81**	**0.93**	**0.92**	**0.73**	0.00	*0.48*	**-0.84**	**-0.90**
ΔT_{cr}	**-0.81**	1.00	**-0.76**	**-0.73**	**-0.98**	*0.54*	-0.01	*0.49*	**0.96**
High PG Temp.	**0.93**	**-0.76**	1.00	**0.92**	0.66	0.07	*0.59*	**-0.88**	**-0.88**
Low PG Temp.	**0.92**	**-0.73**	**0.92**	1.00	0.60	0.08	*0.62*	**-0.86**	**-0.84**
R value	**0.73**	**-0.98**	*0.66*	*0.60*	1.00	-0.65	-0.16	-0.36	**-0.92**
G* (0°C)	0.00	*0.54*	0.07	0.08	*-0.65*	1.00	**0.80**	*-0.45*	0.35
G* (25°C)	*0.48*	-0.01	*0.59*	*0.62*	-0.16	**0.80**	1.00	**-0.85**	-0.23
Phase Binder (0°C)	**-0.84**	*0.49*	**-0.88**	**-0.86**	-0.36	*-0.45*	**-0.85**	1.00	*0.68*
Phase Binder (25°C)	**-0.90**	**0.96**	**-0.88**	**-0.84**	**-0.92**	0.35	-0.23	*0.68*	1.00

Table 4-4. Correlation between Binder Parameter Rankings

	G-R	ΔT_{cr}	High PG Temp	Low PG Temp	R value	G* (0°C)	G* (25°C)	Phase Binder (0°C)	Phase Binder (25°C)
G-R	1.00	**0.70**	**0.90**	**0.92**	*0.62*	-0.09	*0.61*	**0.90**	**0.84**
ΔT_{cr}	**0.70**	1.00	**0.71**	**0.73**	**0.95**	*-0.67*	0.04	*0.48*	**0.94**
High PG Temp.	**0.90**	**0.71**	1.00	**0.88**	*0.59*	-0.12	*0.68*	**0.87**	**0.77**
Low PG Temp.	**0.92**	**0.73**	**0.88**	1.00	*0.66*	-0.21	*0.59*	**0.84**	**0.84**
R value	*0.62*	**0.95**	*0.59*	*0.66*	1.00	**-0.77**	-0.13	0.33	**0.89**
G* (0°C)	-0.09	*-0.67*	-0.12	-0.21	**-0.77**	1.00	*0.53*	0.18	*-0.52*
G* (25°C)	*0.61*	0.04	*0.68*	*0.59*	-0.13	*0.53*	1.00	**0.85**	0.20
Phase Binder (0°C)	**0.90**	*0.48*	**0.87**	**0.84**	0.33	0.18	**0.85**	1.00	*0.65*
Phase Binder (25°C)	**0.84**	**0.94**	**0.77**	**0.84**	**0.89**	*-0.52*	0.20	*0.65*	1.00

Table 4-5. Mixture Parameter Rankings for Different Mixtures

Mixture		N_f@G^R=100		Fracture Energy		G_f/m		LVECD		Mix Based G-R	
		cycles	rank	J/m2	rank	.mm/ kN.m	rank	Failure Points	rank	MPa	rank
Lebanon	PG 58-28, 12.5, 28.3% RAP	7848	9	650.9	4	211.9	3	0% (0.31)	2	7.40E+02	5
	PG 58-28, 12.5, 18.5% RAP/RAS	25838	1					85%	13	8.29E+02	7
	PG 58-28, 12.5, 18.9% RAP	8926	6					0% (0.33)	4	5.74E+02	3
	PG 52-34, 12.5, 28.3% RAP	8116	7					22%	11	4.86E+02	1
	PG 52-34, 12.5, 18.5% RAP/RAS	11881	4					0%(0.21)	1	5.96E+02	4
	PG 52-34, 12.5, 18.9% RAP	6637	12	703.2	2	231.3	1	0%(0.67)	7	5.08E+02	2
	PG 58-28, 19, 31.3% RAP	7899	8	643.2	5	197.2	4	27.40%	12	9.49E+02	9
	PG 58-28, 19, 20.4% RAP/RAS	7063	11	631.2	6	188.8	6	0% (0.35)	6	8.36E+02	8
	PG 58-28, 19, 20.8% RAP	6136	13					0% (0.31)	3	8.00E+02	6
	PG 52-34, 19, 31.3% RAP	14595	3	599.6	9	212.5	2	2.20%	8	1.01E+03	10
	PG 52-34, 19, 20.4% RAP/RAS	7324	10	608.2	7	126.0	9	99%	14	1.42E+03	12
Hooksett	PG 58-28, 12.5, 22.4% RAP	9973	5	604.4	8	142.9	8	2.70%	9	2.03E+03	13
	PG 58-28, 9.5, 21.3% RAP	15150	2	721.4	1	188.5	5	0% (0.33)	5	2.83E+03	14
	PG 64-28, 9.5, 16.4% RAP	4180	14	692.4	3	179.0	7	11.80%	10	1.15E+03	11

Mixture		Gamma		E*(@ 4.4°C)		E* (@ 21°C)		Phase Angle (@ 4.4°C)		Phase Angle (@21°C)	
		value	rank	MPa	rank	MPa	rank	Degree	rank	Degree	rank
Lebanon	PG 58-28, 12.5, 28.3% RAP	-0.52	6	14176	11	3669	8	14.7	11	28.1	9
	PG 58-28, 12.5, 18.5% RAP/RAS	-0.70	1	12220	8	3614	7	15.1	9	32.4	4
	PG 58-28, 12.5, 18.9% RAP	-0.52	7	11272	4	2290	1	18.7	6	35.4	1
	PG 52-34, 12.5, 28.3% RAP	-0.59	3	12170	7	2832	5	20.8	1	33.6	3
	PG 52-34, 12.5, 18.5% RAP/RAS	-0.57	5	9884	2	2329	2	19.3	4	30.5	6
	PG 52-34, 12.5, 18.9% RAP	-0.47	11	12358	9	2523	3	19.8	2	35.4	2
	PG 58-28, 19, 31.3% RAP	-0.57	4	13788	10	4177	11	14.8	10	28.3	8
	PG 58-28, 19, 20.4% RAP/RAS	-0.60	2	12015	6	4329	12	16.5	7	26.7	10
	PG 58-28, 19, 20.8% RAP	-0.51	8	14539	12	3967	9	15.2	8	28.7	7
	PG 52-34, 19, 31.3% RAP	-0.48	10	11526	5	3190	6	19.1	5	31.9	5
	PG 52-34, 19, 20.4% RAP/RAS	-0.35	14	9302	1	2739	4	19.5	3	25.9	11
Hooksett	PG 58-28, 12.5, 22.4% RAP	-0.39	12	16103	14	5155	14	10.8	13	22.6	13
	PG 58-28, 9.5, 21.3% RAP	-0.36	13	14968	13	5082	13	10.5	14	20.5	14
	PG 64-28, 9.5, 16.4% RAP	-0.51	9	10945	3	4025	10	11.4	12	22.8	12

Table 4-6. Correlation between Mixture Parameters Values

	N_f @ G^R=100	Fracture Energy	G_f/m	Mix-based G-R	Gamma	E* (4.4°C)	E* (21°C)	Phase angle (4.4°C)	Phase angle (21°C)
N_f @ G^R=100	1.00	-0.08	0.10	0.19	-0.32	0.04	0.07	-0.09	0.13
Fracture Energy	-0.08	1.00	*0.44*	0.27	0.01	0.16	0.10	-0.33	-0.11
G_f/m	0.10	*0.44*	1.00	-0.37	*-0.56*	0.13	-0.26	0.24	*0.65*
Mix-based G-R	0.19	0.27	-0.37	1.00	*0.68*	*0.46*	**0.71**	**-0.70**	**-0.81**
Gamma	-0.32	0.01	*-0.56*	*0.68*	1.00	0.18	0.21	-0.23	*-0.51*
E* (4.4°C)	0.04	0.16	0.13	*0.46*	0.18	1.00	**0.76**	*-0.66*	-0.37
E* (21°C)	0.07	0.10	-0.26	**0.71**	0.21	**0.76**	1.00	**-0.89**	**-0.80**
Phase angle (4.4°C)	-0.09	-0.33	0.24	**-0.70**	-0.23	*-0.66*	**-0.89**	1.00	**0.80**
Phase angle (21°C)	0.13	-0.11	*0.65*	**-0.81**	*-0.51*	-0.37	**-0.80**	**0.80**	1.00

Table 4-7. Correlation between Mixture Parameters Ranking

	N_f @ G^R=100	Fracture Energy	Gf/m	Mix-based G-R	Gamma	LVECD	E* (4.4°C)	E* (21°C)	Phase angle (4.4°C)	Phase angle (21°C)
N_f @ G^R=100	1.00	-0.25	0.10	-0.16	0.10	-0.03	-0.12	0.03	-0.13	0.10
Fracture Energy	-0.25	1.00	0.27	-0.25	-0.02	*0.40*	-0.22	0.02	-0.25	-0.13
Gf/m	0.10	0.27	1.00	0.10	0.32	*0.50*	-0.17	*0.42*	0.33	**0.77**
Mix-based G-R	-0.16	-0.25	0.10	1.00	*0.53*	0.32	0.17	*0.68*	*0.64*	**0.85**
Gamma	0.10	-0.02	0.32	*0.53*	1.00	0.01	0.09	0.07	0.13	*0.42*
LVECD	-0.03	*0.40*	*0.50*	0.32	0.01	1.00	-0.16	0.12	-0.09	0.08
E* (4.4°C)	-0.12	-0.22	-0.17	0.17	0.09	-0.16	1.00	*0.64*	*0.56*	*0.26*
E* (21.1°C)	0.03	0.02	*0.42*	*0.68*	0.07	0.12	*0.64*	1.00	**0.79**	**0.77**
Phase angle (4.4°C)	-0.13	-0.25	0.33	*0.64*	0.13	-0.09	*0.56*	**0.79**	1.00	*0.69*
Phase angle (21°C)	0.10	-0.13	**0.77**	**0.85**	*0.42*	0.08	0.26	**0.77**	*0.69*	1.00

4.5.3 Comparison of Mixture and Binder Parameters

The rankings of the different binder and mixture parameters are examined to evaluate the relative expected cracking performance. Ranking of similar parameters in Tables 4-2 and 4-5 are compared. The Pearson correlation factors are presented in Table 8 for the corresponding mixture and binder parameters. The stiffness parameters, mixture dynamic modulus and binder shear

modulus follow a similar trend at both low and intermediate temperatures. However, phase angle values do not show the similar ranking for relaxation capability of binder and mixtures.

There is a very good correlation between mix-based Glover-Rowe parameter and the binder Glover-Rowe parameter. For thermal cracking, the ΔT_{cr} and DCT values can be compared. The rankings for the Hooksett surface layer and Lebanon binder layer materials (Tables 4-2 and 4-5) are similar, but the overall correlation with all mixtures is not strong (Table 4-8). In terms of fatigue cracking, the binder parameter (ΔT_{cr}) does not rank the materials in the same order as any of the mixture parameters. The difference between aging condition of the mixtures and binders might be a reason for lack of strong correlation between the different parameters. Another important point that might be the source of difference between binder and mixture indices is the difference in the testing mode. While the binder testing methods are usually conducted in the linear range, the mixtures testing like SVECD fatigue and DCT testing go into nonlinear range and failure.

Table 4-8. Correlation Factors between Mixture and Binder Parameters

Category	Comparison	Pearson Correlation Coefficient	
		Parameter Values	Parameter Rankings
Stiffness	G* at 0°C vs E* at 4.4°C	*0.64*	*0.59*
	G* at 25°C vs E* at 21.1°C	**0.85**	**0.78**
Relaxation	Phase angle (0°C binder vs 4.4°C mixture)	0.36	*0.58*
	Phase angle (25°C binder vs 21.1°C mixture)	0.38	0.22
Aging	G-R vs mixed-based G-R	**0.74**	**0.70**
	R value vs. Gamma	*0.59*	*0.47*
Low Temp. Cracking	ΔT_{cr} vs DCT G_f/m	*0.41*	0.07
Fatigue Cracking	G-R vs N_f @ G^R=100	0.08	0.16
	G-R vs LVECD	-	0.36
	ΔT_{cr} vs N_f @ G^R=100	-0.34	-0.26
	ΔT_{cr} vs LVECD	-	0.12

4.6 Summary and Conclusion

The main objective of this research was to compare different binder and mixture parameters that

are used to evaluate cracking potential of asphalt mixtures. To this aim, PG grading and 4 mm DSR testing on virgin and extracted and recovered binders was conducted; mixture testing included complex modulus, SVECD fatigue, and DCT testing. Tests were conducted on 14 different mixtures produced in drum plants. The following conclusions were drawn from the results of testing and analysis:

- There were very good to good correlations between high and low PG temperatures, Glover-Rowe parameter, R value, and ΔT_{cr} binder index parameters. The strongest correlation is between R value and ΔT_{cr} with a Pearson correlation factor of more than 0.98.
- Different mixture indices including stiffness, relaxation, fatigue and low temperature cracking parameters were considered; for the mixtures evaluated in this project, the mixture factors did not show strong correlation with each other.
- Binder and mixture stiffness are strongly correlated, as expected.
- Cracking parameters for binders in the long-term aging condition and mixtures in the short-term aging condition were not strongly correlated; either for fatigue or low temperature cracking. This indicates that short-term cracking behavior of mixtures may not be accurately predicted only by rheological parameters of the binder.

The following extension to the work presented in this study are needed to verify the conclusions and to advance the knowledge on mixture and binder correlations:

- This study provides a wide range of binder and mixture testing on different mixtures, but all the mixtures are from a single region and use unmodified binders. A larger data base is needed to to more completely understand the relationships between mixture and binder properties.

- The actual field cracking performance of mixtures needs to be incorporated in the analysis. The mixtures in this study were placed in the field in 2013 and the performance will be tracked over time.
- The mixtures used in this paper were in short-term aged condition, while the binder testing was conducted on long-term aged binders. Testing on long-term aged mixtures is needed to conduct a better comparison; this work is currently underway in a new project.
- Pearson correlation factor only assess the linear correlations, while some of the binder and mixture parameters may be more strongly correlated with nonlinear functions. Additional statistical analysis may help to identify stronger mixture and binder relationships.

Chapter 5

FATIGUE AND THERMAL CRACKING ANALYSIS OF ASPHALT MIXTURES USING VISCOELASTIC CONTINUUM DAMAGEAND COHESIVE ZONE FRACTURE MODELS

5.1 Introduction

Cracking is one of the major distress modes for asphalt pavements and is categorized in two main groups: load associated (mainly fatigue cracking) and non-load associated (thermal) cracking. Fatigue cracking occurs when tensile stresses due to repetitive traffic loading exceed the tensile strength of the material creating microcracks that grow and coalesce into macrocracks that lower pavement smoothness and integrity. Fatigue cracks can initiate at the bottom of the pavement layer (bottom up) or near the pavement surface (top down). Thermal cracking, common in cold climates, occurs when the thermal stress that builds up during cooling events in the pavement exceeds the tensile strength of the asphalt. Cracked pavements allow water to infiltrate to underlying pavement layers, further weakening the pavement and leading to a rougher ride and shorter service life.

Many researchers have been working on the prediction of fatigue and thermal cracking of asphalt pavements using laboratory testing and numerical modelling. These efforts have made many advancements in both testing and modeling to predict the cracking performance of pavements. The Simplified Viscoelastic Continuum Damage (SVECD) approach using uniaxial tensile fatigue and Disk-Shaped Compact Tension (DCT) testing are two experimental methods which have drawn a

lot of attention in recent years for evaluation of fatigue and thermal cracking, respectively. Both methods use energy-based approaches. The SVECD approach is based on three principles: elastic-viscoelastic correspondence principle, continuum damage mechanics, and time-temperature superposition with growing damage (Cao et al., 2016). The DCT test for asphalt concrete was proposed by Wagoner et al. (2005). This procedure has been specified as ASTM D7313 and was extensively evaluated through multiple studies (Marasteanu et al. 2007, Marasteanu et al. 2012, Dave et al. 2016a). In addition to field validation by Marasteanu et al. (2012), Dave et al. (2016a) demonstrated suitability of DCT fracture energy in distinguishing asphalt pavement transverse cracking performance of field sections.

In general, the asphalt industry is moving towards use of performance based specifications and use of performance-based design approaches. Use of prediction models are essential in predicting the performance of asphalt mixtures during, and at the end of service life. In the present research, energy based fully mechanistic performance prediction models were employed using laboratory fatigue and fracture tests. For fatigue pavement performance, SVECD results were used in the layered viscoelastic pavement analysis for critical distresses (LVECD) framework (Eslaminia et al. 2012). The IlliTC thermal cracking prediction system (Dave et al. 2013) was used for thermal cracking predictions; this system utilizes cohesive zone fracture based analysis of thermal cracking performance prediction. Since fracture properties were only available for limited number of mixtures and viscoelastic characterization was available for all mixtures, SHRP TCModel (Lytton et al., 1993) was also employed for thermal cracking performance prediction. This model is included in the current AASHTOWare PavementME system for thermal cracking prediction.

The objective of this paper is to evaluate fatigue and thermal cracking performance of nine asphalt mixtures representing different aggregate sources, aggregate gradation and sizes, recycled asphalt

amounts, and asphalt binder grades and sources using energy based models for fatigue (continuum damage) and thermal (cohesive zone) cracking. A current state of practice approach for thermal cracking simulation was also evaluated through use of the SHRP TCModel. The purpose of such study is to not only determine if mixture parameters consistently affect lab measured performance prediction parameters but also to determine if any correlations are seen between predicted fatigue and thermal cracking performance. Laboratory evaluation was conducted for viscoelastic characterization as well as for measurement of necessary properties that are used in fatigue and fracture models. Brief descriptions of laboratory tests, performance models and theories employed in those models are presented in the next section.

5.2 Methodology

5.2.1 Brief Description of Laboratory Tests

Viscoelastic Characterization

Tests on both binder and mixtures were conducted for viscoelastic characterization. The resistance of binders to low temperature cracking was evaluated by bending beam rheometer (BBR) testing following AASHTO T313. Creep stiffness (S(t)) and the rate of change of creep stiffness (m) were obtained. Mixture complex modulus testing, following AASHTO TP-79, was performed to determine dynamic modulus and phase angle for each mixture. Testing was performed on three replicate specimens at three temperatures and six frequencies to develop master curves.

SVECD Fatigue Test

Uniaxial fatigue testing was conducted following the AASHTO TP 107 procedure. Damage analysis for each mixture was performed and damage characteristic curves (DCC) were obtained.

Finally, to compare fatigue cracking resistance of different mixtures, relationships between energy based fatigue failure criterion (G^R) and number of load cycles were developed.

Disk-shaped Compact Tension (DCT) Fracture Test

Fracture energy (G_f) of asphalt mixtures is a measure of the amount of energy needed to produce a unit fractured surface. Following the ASTM D7313 procedure, the tests were conducted to obtain a constant crack mouth opening displacement (CMOD) rate of 0.166 mm/s. Since the application of this test in the present study is for assessment of thermal cracking performance of mixtures, DCT tests were conducted at -18ºC. This temperature was selected as per the recommendations by Marasteanu et al. (2012).

Due to limited amount of plant produced specimens, DCT fracture energy testing was only possible on five of the nine mixtures discussed here (the mixtures tested using DCT are indicated in Table 5-1).

5.2.2 Fatigue Cracking Prediction

Layered Viscoelastic Pavement Design for Critical Distresses (LVECD) is a program developed by North Carolina State University to calculate responses and predict the fatigue and rutting behaviour of asphalt pavements (Eslamnia et al. 2012). To assess the fatigue behaviour, this three-dimensional finite element based software employs simplified viscoelastic continuum damage (SVECD) approach. A damage characteristic curve (DCC) from SVECD is used in this model. DCC can be used to assess the mixture's response to any combination of uniaxial loading history and temperature, since it is developed by removing the bulk viscoelastic response of material from the constitutive response. (Chehab, et al. 2003; Keshavarzi and Kim, 2016)

Failure criterion, G^R, is an energy-based parameter and important component of damage modelling, which can be calculated from Equation 5.1. This equation is suggested by Saburi et al 2015, Where $(\varepsilon_{0,ta}^R)_i$ is the pseudo strain amplitude at cycle i, F_i is the pseudo stiffness at cycle i, and N_f is total number of cycles to failure.

$$G^R = \frac{\frac{1}{2}\int_0^{N_f}\left(\varepsilon_{0,ta}^R\right)_i^2(1-F_i)}{N_f^2} \quad 5.1$$

The number of cycles to failure at G^R=100 is a parameter suggested by Norouzi et al. (2016) to compare the fatigue behavior of different mixtures. This parameter is used in this research to rank the fatigue cracking characteristics of the mixtures based on the results SVECD fatigue testing.

5.2.3 Thermal Cracking Prediction

In the present study, two thermal cracking performance prediction models were used. The first model, SHRP Thermal Cracking Model (TCModel), was used for evaluation of all nine mixtures (Lytton et al., 1993). TCModel utilizes climatic data from the last 20 years and with a one dimensional thermo-viscoelastic stress calculation scheme to determine the thermally induced stresses as function of pavement depth and time. Using the Paris law based crack propagation approach, TCModel determines the depth of crack and couples that with probabilistic crack distribution model to predict extent of field cracking. Primary material inputs for TCModel are viscoelastic characterization, coefficient of thermal expansion and contraction, and tensile strength. Using the complex modulus master-curves and time-temperature shift factors, time dependent viscoelastic properties (relaxation modulus and creep compliance) were determined for the nine mixtures. Since tensile strength measurements were not conducted as part of this study, tensile strengths were estimated using the peak load from the DCT test (Marasteanu et al., 2012). For the four mixtures that were not evaluated using DCT fracture test, a tensile strength value

representative of similar mixtures was used (same nominal maximum aggregate size, binder grade and approximate recycled asphalt amount). Based on field geographical region, climatic data representative of the Southern-central portion of New Hampshire was used in the analysis of asphalt mixtures.

Limitations of TCModel have been discussed by Dave et al. (2013). The main short comings are use of one-dimensional thermo-viscoelastic stress evaluation approach as opposed to treating pavement as two- or three-dimensional structure and use of Paris law based cracking model that is only applicable to purely brittle materials. To alleviate these short-comings, the IlliTC thermal cracking prediction system has been proposed (Dave et al., 2013). The IlliTC system utilizes two dimensional thermo-viscoelastic finite element analysis with a cohesive zone fracture model to simulate quasi-brittle cracking in asphalt concrete. The suitability of IlliTC for thermal cracking performance prediction has been independently shown in two studies (Dave et al., 2013; Dave et al., 2015). The cohesive zone fracture model in IlliTC uses tensile strength and fracture energy to simulate quasi-brittle and ductile crack propagation. A number of researchers have shown that cohesive zone fracture approach is well suited for simulation of discrete cracking in asphalt mixtures (such as, de Souza et al., 2004; Baek et al., 2010; Dave and Buttlar, 2010 and Kim et al., 2013).

5.3 Materials

This study includes modelling of 9 plant-mixed, plant-compacted mixtures fabricated at two drum plants, as shown in Table 5-1. Mixtures include three nominal maximum aggregate sizes (NMAS) and three binder sources. The average air void content of the fatigue and DCT specimens are also presented in Table 5-1, note that only five mixtures were tested using DCT due to limited specimen

availability. The total binder replacement is the ratio of the percentage of recycled binder divided by the percentage of total binder (virgin and recycled). The mixtures were compacted at the plant and are thus considered to be in the short-term aged condition. The RAP binder of mixtures produced in plant 1 has a continuous grade of 81.3-19.3˚C. The RAS material was primarily from tear-off shingles which could not be graded in the laboratory.

Table 5-1. Mixture Types and Properties

Plant	Binder PG Grade	NMAS (mm)	%AC	%Total Binder Replacement	% RAP Binder	% RAS Binder	Average Air Void (%)	
							Fatigue	DCT
Lebanon (2013)	58-28 Source 1	12.5	5.3	28.3	28.3	0	7.4	8.4
				18.5	7.4	11.1	6.8	N.A.
				18.9	18.9	0	7.7	N.A.
	52-34 Source 1	12.5	5.3	28.3	28.3	0	6.9	N.A.
				18.5	7.4	11.1	6.8	N.A.
				18.9	18.9	0	6.3	7.6
Hooksett (2014)	58-28 Source 2	9.5	6.1	21.3	21.3	0	5.8	6.8
		12.5	5.8	22.4	21.3	0	5.3	7.0
	64-28 Source 2	9.5	6.1	16.4	16.4	0	5.8	7.2

5.4 Experimental Results

5.4.1 Viscoelastic Characterization

Figure 5-1 shows the low PG temperature of extracted and recovered binders. Generally, the binders extracted and recovered from the mixtures produced in plant 1 have colder low PG temperature than mixtures of plant 2. The low temperature PG grade of extracted and recovered binders from RAP/RAS mixtures are warmer than mixtures with only RAP. Figure 5-2 shows the ΔT_{cr} values for the binders extracted and recovered from the mixtures evaluated in this study. ΔT_{cr}, is an indicator of crack susceptibility of the binder and is defined as the difference between the temperature at which the material has a creep stiffness (S-value) of 300 MPa and the temperature

at which the log-log slope of creep curve (m-value) is 0.300. The cracking warning (Anderson, 2011) and cracking limit (Rowe, 2011) lines are drawn in this figure as well. Lower ΔT_{cr} values indicate a higher susceptibility to cracking. The results show that binders extracted and recovered from the mixtures produced in plant 1 have lower ΔT_{cr} than the mixtures of plant 2 (c.f. Figure 5-2), indicating that mixtures from plant 1 might be more susceptible to cracking. For plant 1, mixtures with RAP/RAS have lower ΔT_{cr}, followed by 18.9% RAP and 28.3% RAP, for both binder grades. Generally, PG 52-34 binders extracted from mixtures produced in plant 1 have lower ΔT_{cr} as compared with the PG 58-28 binders extracted from the same mixtures.

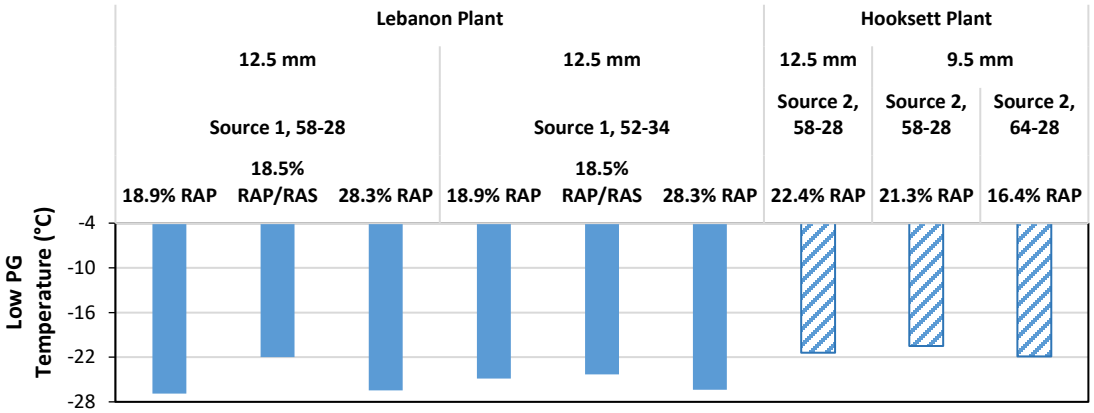

Figure 5-1. The Low PG Temperature for Extracted and Recovered Binders

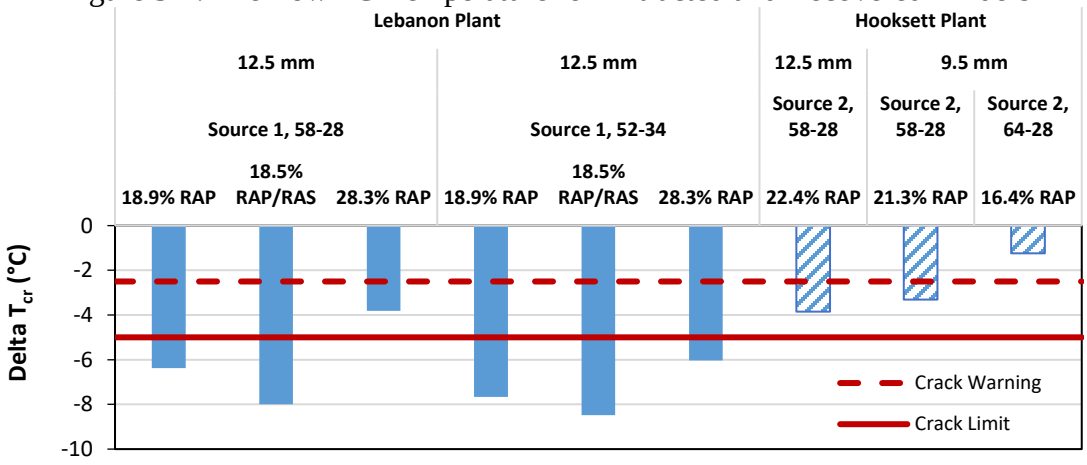

Figure 5-2. Delta T_{cr} Values for Extracted and Recovered Binders

The dynamic modulus mastercurves presented in Figure 5-3 are the average of three replicate specimens for each mixture. All of the mixtures produced from Plant 2 are stiffer than those produced from Plant 1, regardless of binder grade or recycled material content. The Plant 1 mixtures follow the expected trends with respect to binder grade and recycle content and type.

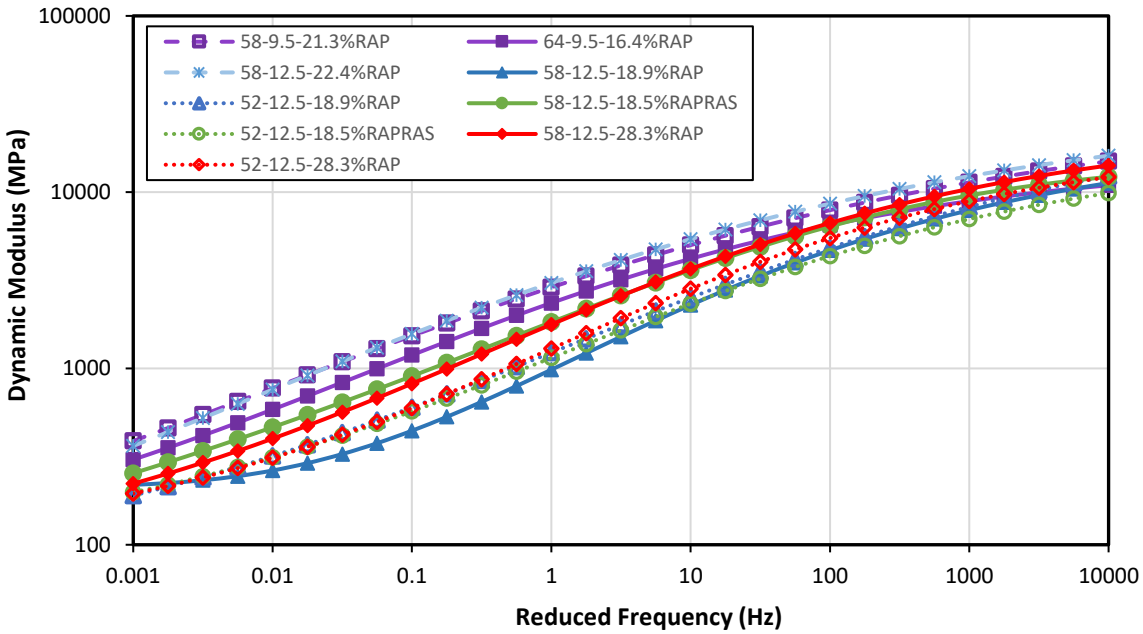

Figure 5-3. Dynamic Modulus Master Curves for Different Mixtures

To capture the stiffness and relaxation capability of the mixtures together, Black space diagram is presented in Figure 5-4. The combination of higher stiffness and lower phase angle can indicate that a mixture may be more susceptible to cracking. Generally, the stiffer mixtures in Figure 5-3 show lower phase angle and more elastic behavior in Figure 5-4. The mixtures from plant 2 have lower phase angle (less relaxation capability) especially at low and intermediate temperatures, while the mixtures produced in plant 1 with PG 52-34 show higher phase angle values.

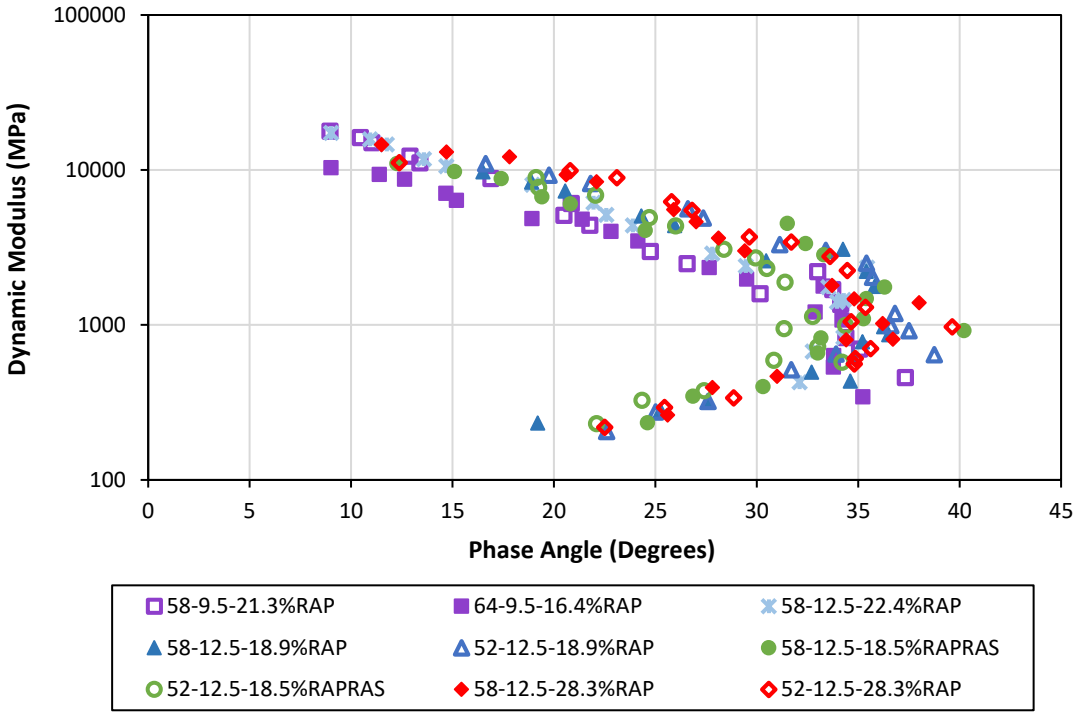

Figure 5-4. Black Space Diagrams for Different Mixtures

5.4.2 SVECD Fatigue Testing Results

Figure 5-5 compares the fatigue failure criterion (G^R) versus the number of cycles (N_f) of mixtures. Generally, the higher G^R values at the same number of cycles (N_f) indicates better fatigue behavior. The G^R-N_f slope of all of the mixtures except PG 58-28, 12.5 mm, 18.5% RAP/RAS are very similar. The lowest G^R values are observed in the mixture with PG 64-28 binder which is the stiffest among the other binders.

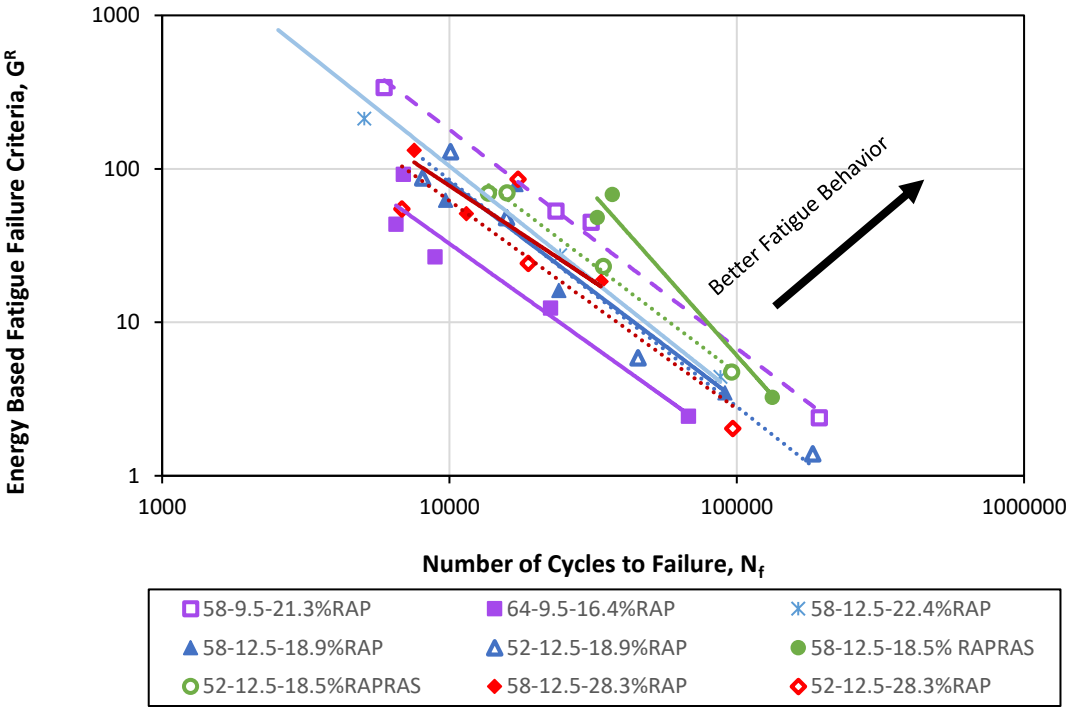

Figure 5-5. Fatigue Failure Criteria (GR – Nf) Plots for Different Mixtures

5.4.3 Fracture Testing Results

The results presented in Figure 5-6 show the average fracture energy of specimens measured from the DCT test. Error bars on the plot indicate one standard deviation interval of three replicates. As can be seen, the variability of test results is limited to 10%, except for PG 58-28, 9.5 mm, 21.3% RAP. Overall, all mixtures exhibit high fracture energy; current low temperature cracking specifications in use by Minnesota Department of Transportation recommend use of a minimum of 400 J/m^2 (Van Deusen et al. 2015). Only the PG 58-28, 12.5 mm, 22.4% RAP mixture has a value that is statistically lower than the other five. Another observation that can be made from the results is that in this study the PG 52-34 mixtures did not show appreciably higher fracture energy as compared to mixtures made with PG XX -28 binder grade. Similarly, in this group of five

mixtures the amount of recycled asphalt also did not show considerably different fracture energies. Both of these aspects, inconsistent effects of using -34 binder low temperature grade as compared to -28 low temperature binder grade as well as the effect of recycled asphalt content were also evident in the fatigue test results. These aspects reinforce need for performance testing based specification for asphalt mixtures. Furthermore, for predicting thermal cracking pavement performance it is necessary to couple laboratory measured properties with pavement structural response. In the present work this was done by use of TCModel and IlliTC thermal cracking prediction systems.

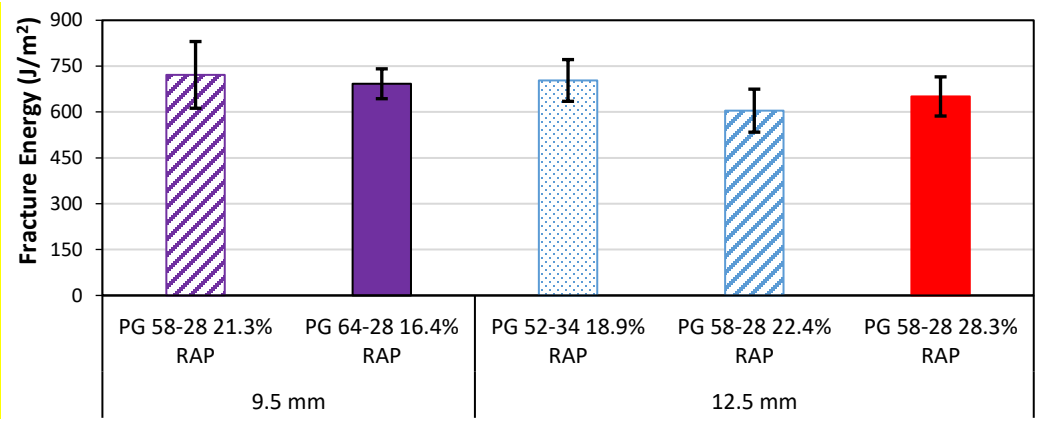

Figure 5-6. Fracture Energy (DCT testing) for Different Mixtures

Another parameter to evaluate mixtures behaviour against thermal cracking is Fracture Strain Tolerance (FST) suggested by Zhu et al. (2017). FST is calculated by normalizing the fracture energy of mixture with the fracture strength (G_f/S_f). This parameter better describes the fracture process in asphalt mixtures as it combines both energy as well as the strain capacity of the mixture; results for various mixtures are shown in Figure 5-7. The general trend for 12.5 mm and 9.5 mm mixtures is similar to fracture energy. The 12.5 mm 22.4% RAP mixture shows the worst performance and PG 52-34 18.9% RAP mixtures the best. However, it should be noted that the range of FST values amongst mixtures is small.

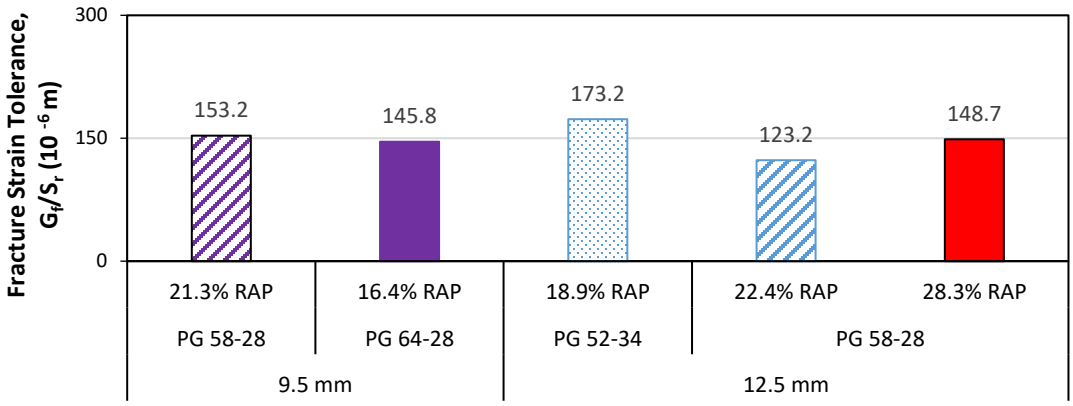

Figure 5-7. Fracture Strain Tolerance, FST (DCT testing) for Different Mixtures

5.5 Performance Prediction Results

5.5.1 Fatigue Performance Prediction

The mixtures produced in plant 1 were placed in the field during the 2013 construction season. Figure 5-8 shows the cross section of the pavement that is used in the LVECD program to simulate the fatigue performance of mixtures in the field. The mixtures studied herein are considered as surface layer on top of a 19mm binder layer (PG 58-28, 31.3% RAP). In addition to the measured mixture properties, parameters shown in Figure 8 were used for simulations.

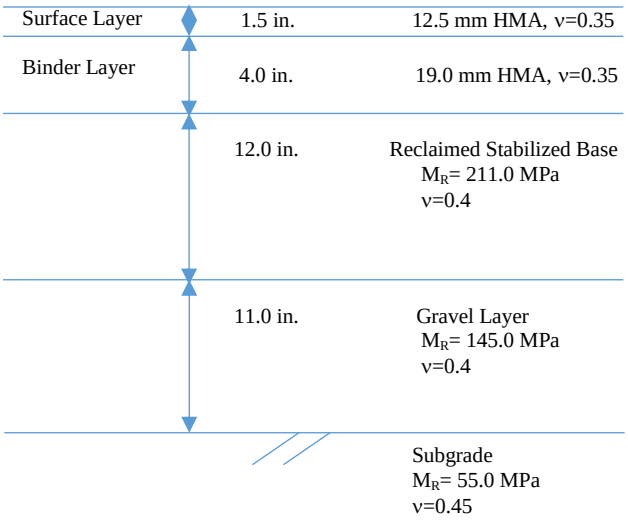

Simulation Parameters:

Design life: 20 years (from 1 Nov. 2013)

Vehicle speed: 96.5 km/h (60 mph)

Tire load: single axle, 40 kN (8992 lbf)

Tire pressure: 759 kPa (110.1 psi)

Tire imprint shape: rectangular

Average annual daily truck traffic: 1800 vehicles per day

Growth rate: Linear at 2.8% per year

Figure 5-8. Pavement Cross Section and Simulation Parameters

LVECD model predicts pavement responses and damage evolution (fatigue and rutting) in both spatial distribution and time history modes. One of the most useful outputs of this program is damage factor which is calculated on the basis of cumulative damage model and Miner's rule. The damage factor (Equation 5-2) varies in magnitude from 0 (no damage) to 1 (completely damaged element).

$$Damage\ Factor = \sum_{i=1}^{T} \frac{N_i}{N_{fi}} \quad 5.2$$

Where T: total number of periods, N_i: traffic for period i, and N_{fi}: the allowable failure repetitions under the conditions that prevail in period i (Sabouri et al. 2015). In spatial distribution mode, the damage factor (N/N_f) is shown in contour format for a specific time. The progression of damage in pavement cross section can be tracked by changing the time periods.

Figure 5-9 presents comparisons of damage contour plots for the different mixtures at the end of 5, 10, and 20 years. Based on the results, users can predict how fatigue cracking initiates and propagates in pavement (bottom-up, or top-down) and assess the propagation rate. (Mensching et al. 2016)

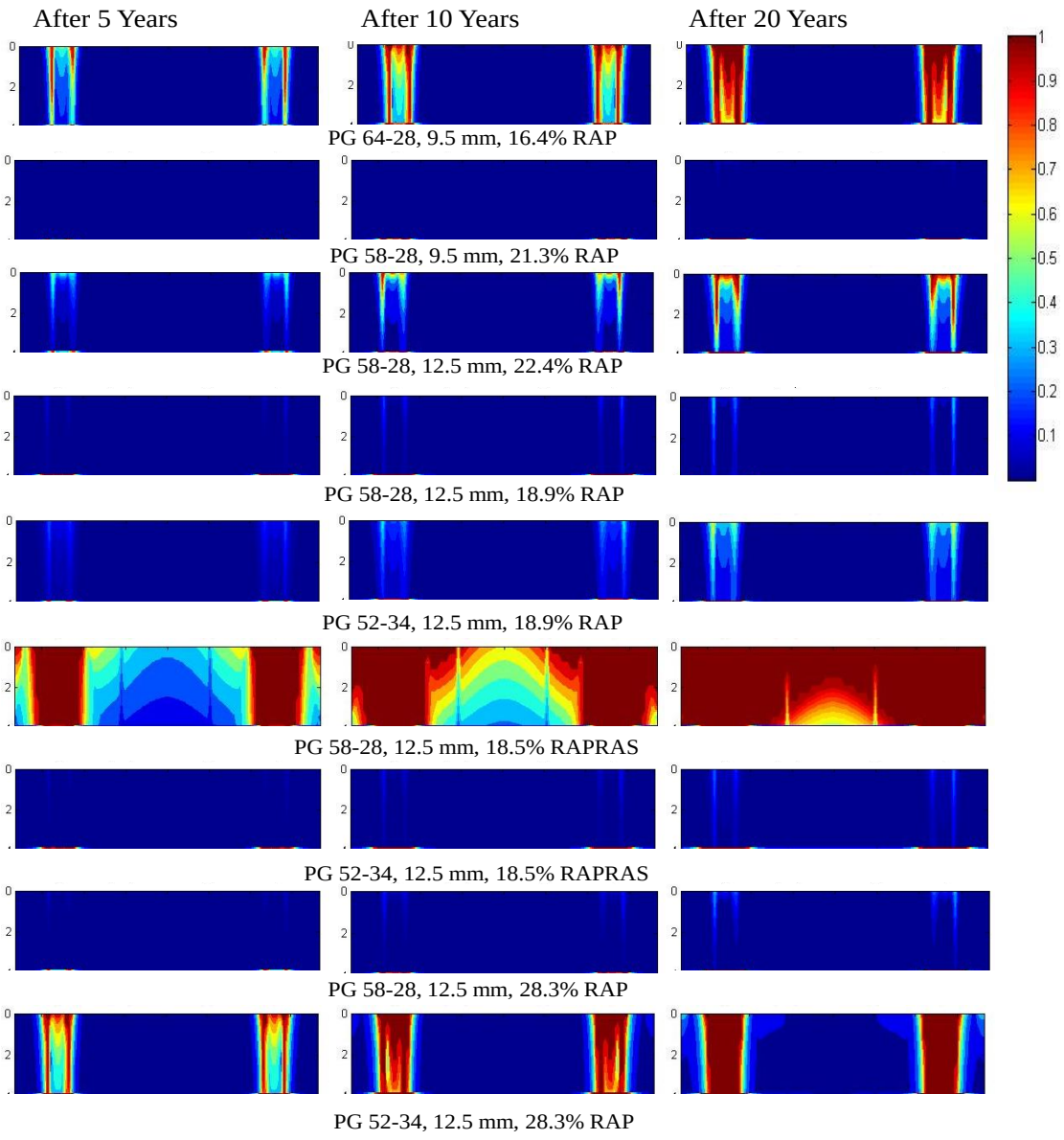

Figure 5-9. Set of Damage Contours for Different Mixtures after 5, 10, and 20 years

The first three contours of Figure 5-9 show the damage factor distribution of mixtures from plant 2, while the others are the mixtures from plant 1. To compare two 9.5 mm mixtures, more damage is observed for mixture with stiffer binder (PG 62-28, 9.5 mm, 16.4% RAP) than PG 58-28, 9.5 mm, 21.3% RAP, despite the lower RAP content. More fatigue cracking distribution is shown for 12.5 mm mixture from plant 2 than 9.5 mm mixture with the same binder.

PG 58-28, 12.5 mm, 18.5% RAP/RAS has the worst performance among mixtures produced in plant 1, while the similar mixture with the PG 52-34 does not show serious cracking. Surprisingly, this trend is reversed for 12.5 mm, 28.3% RAP so that more damage distribution appears for the mixture with softer binder (PG 52-34).

In the LVECD analysis, an element of the pavement cross section is considered to be completely failed when the N/N_f ratio equals 1.0 (indicated by the red color in Figure 5-9). Figure 5-10(a) shows the percentage of the cross section that has failed over the service life of the pavement containing each mixture. The percentage is calculated by summing all of the failed elements and dividing by the total number of points in the cross section. The PG 58-28, 12.5 mm mixture with 18.5% RAP/RAS shows the highest percentages of failure and a sudden increase in the damage at 20 months, reaching 20% failure in the next year before the damage rate decreases for the remaining service life. The PG 52-34, 12.5 mm mixture with 28.3% RAP shows the next highest amount of damage followed by the PG 64-28, 9.5 mm mixture with16.4% RAP, and then the PG 58-28, 12.5 mm mixture with 22.4% RAP.

Five of the mixtures do not show any failure points, indicating that fatigue cracking would not be a primary concern in this pavement structure with these mixtures. To evaluate potential differences in the fatigue behaviour of these mixtures, the maximum damage factor value at the end of the 20-year analysis is shown in Figure 5-10(b) for these mixtures. The PG 52-34, 12.5 mm, 18.9% RAP mixture has the highest damage factor, while the same mixture with PG 58-28 binder has the lowest value.

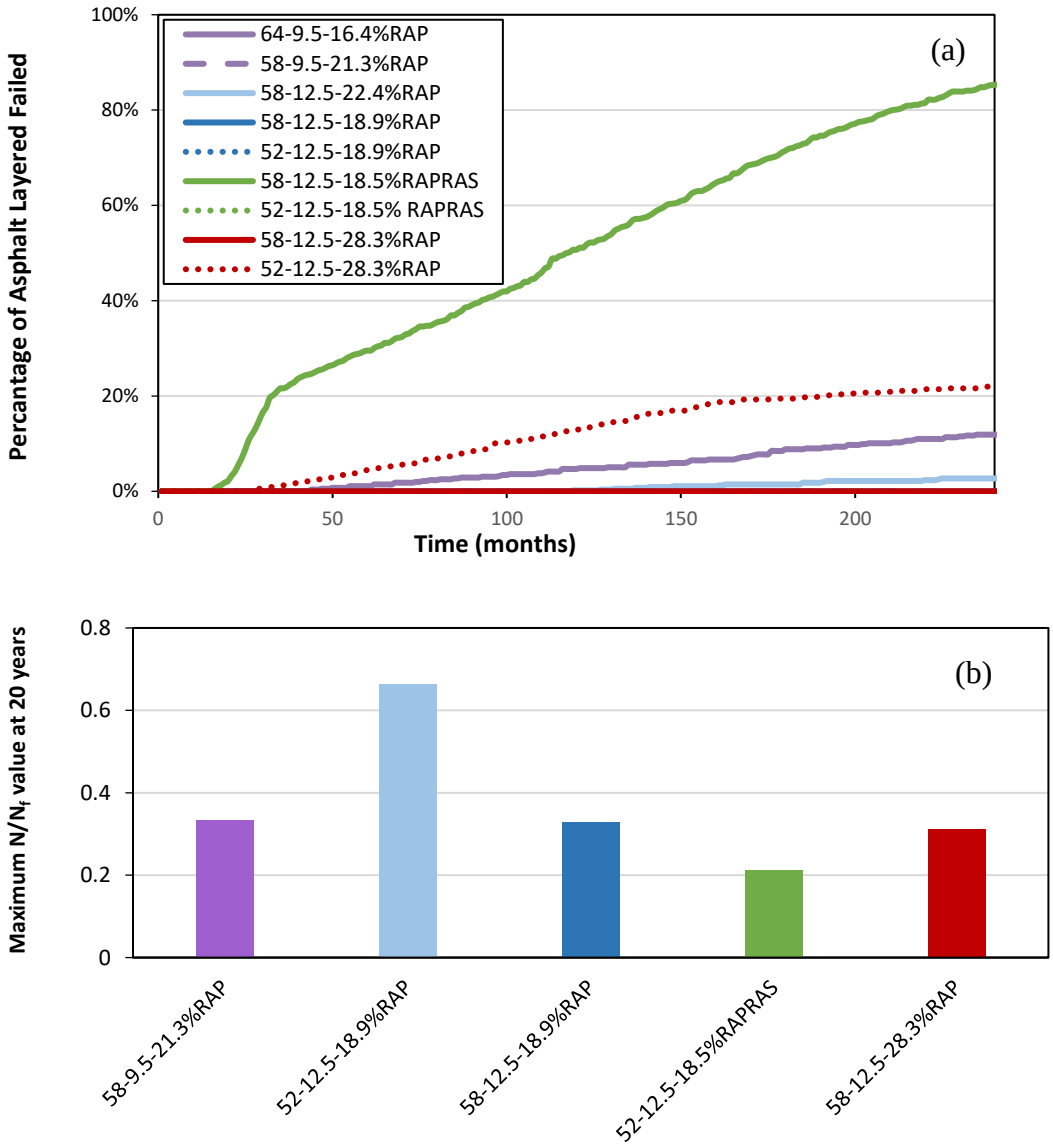

Figure 5-10. Pavement Performance from LVECD Analysis; (a) Percentage of asphalt layer failed; (b) Maximum damage level for mixtures without completely failed elements

5.5.2 Thermal Cracking Performance Predictions

Results from TCModel and IlliTC simulations for prediction of thermal cracking performance for the nine mixtures evaluated in this study are presented in this section. The input values used for thermal cracking modeling are provided in Appendix. Predicted thermal cracking amounts from TCModel for 20-year duration are plotted in Figure 5-11. It can be observed from the figure that

only three mixtures exhibit thermal cracking concern. The thermal cracking predictions from TCModel seem to be linked most closely to the viscoelastic characteristics of the asphalt mixtures. This is not entirely unexpected, TCModel uses thermo-viscoelastic stress calculation as the mechanistic component of the thermal cracking analysis. The reason for PG 58-28, 12.5 mm, 28.3% RAP mixture to be predicted with worst thermal cracking performance can be attributed to a combination of following factors:

- Tensile strength of 4.3 MPa as compared to the average strength of 4.7 MPa for all other mixtures with PG XX-28 binder
- Relatively non relaxant behaviour (lower phase angle) and greater stiffness at shorter loading times and low temperatures as compared to other mixtures (as seen in Figures 5-3 and 5-4).
- While there are other mixtures with even flatter master-curve shapes (such as, PG 58-28, 9.5 mm, 21.3% RAP), it should also be noted that the average time-temperature shift factor for the worst performing mixture is approximately $10^{2.22}$/10 ºC versus $10^{1.17}$/10 ºC for PG 58-28, 9.5 mm, 21.3% RAP mixture. Thus, the poor performing mixture has substantially higher temperature susceptibility, which has led to inferior thermal cracking performance.

The other two mixtures (PG 58-28, 9.5 mm, 21.3% RAP and PG 64-28, 9.5 mm, 16.4% RAP) that exhibit thermal cracking also have relatively high stiffness values compared to the other mixtures.

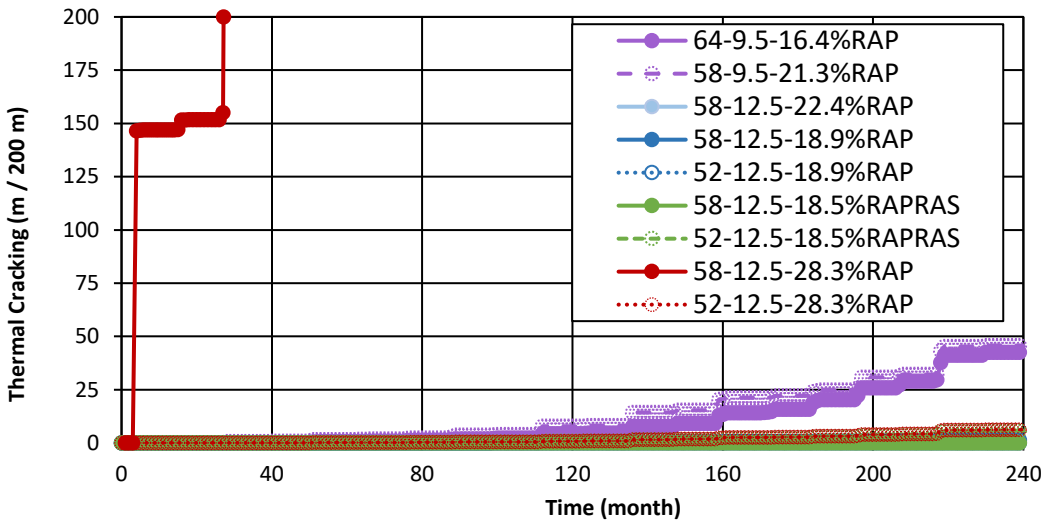

Figure 5-11. Thermal Cracking Performance from TCModel

IlliTC thermal cracking prediction system utilizes a two step analysis approach for maintaining practical analysis times for various cases. The system is designed to use critical cracking conditions approach; whereby thermo-viscoelastic stress analysis identifies the time period when thermal stresses exceed 80% of mixture tensile strength. These critical conditions are evaluated using finite element analysis with cohesive zone fracture model. IlliTC simulations were conducted for the five mixtures evaluated using the DCT test in the laboratory and the results are presented in Table 5-2. The results show that only three mixtures have potential for thermal cracking, this is consistent with the TCModel results. This finding is not entirely unexpected, since both IlliTC and TCModel utilize thermo-viscoelastic stress calculations. Out of those three mixtures, only the PG 58-28, 12.5 mm, 28.3% RAP mixture showed high risk for thermal cracking. While simulations did not predict formation of thermal cracks for the other two mixtures, both mixtures did begin to undergo softening near the top of asphalt layer. In general, mixtures with high fracture energies, such as all five of the analyzed mixtures, are well resistant to thermal cracking distress, these results demonstrate need for performance predictions using simulation models. Simulation models such

as IlliTC allow for combining the bulk viscoelastic behaviour of material with the non-linear fracture response in the context of the pavement structure.

Table 5-2. IlliTC Thermal Cracking Performance Predictions

Mix	DCT Fracture Energy (J/m^2)	Critical Cracking Condition Identified	Thickness of Asphalt Layer Cracked / Softened (%)	Predicted Thermal Cracking Amount at 5 Years (m/200 m)
58-12.5-28.3%	650.9	Yes	100% Cracked	200
58-9.5-21.3%	721.4	Yes	30% Softened (Damaged)	None
52-12.5-18.9%	703.2	No		
58-12.5-22.4%	604.4	No		
64-9.5-16.4%	692.4	Yes	17% Softened (Damaged)	None

5.6 Discussion

The results of fatigue and thermal cracking laboratory testing and pavement evaluation are summarized in Table 5-3. The table is color-coded for each parameter to categorize the values in three groups as relatively good (green), intermediate (yellow), and poor (red) behavior against cracking. The mixtures are sorted from the best to worst according to the LVECD results. The mixtures with no failure points are considered as good (green) mixtures, three mixtures with about 20% failure or less after 20 years service life are categorized as intermediate (yellow) mixtures, and the performance of mixture with more than 80% failure is designated as poor (red). Although the comparison of fatigue and thermal cracking performance shows good agreement for some of the mixtures, it does not show a similar performance for the others. This is not surprising because of differences in traffic load and thermally induced cracking mechanisms. This demonstrates that for different cracking distress mechanisms use of the same laboratory measured performance prediction parameter or model may not be suitable.

The dynamic modulus ranking from 1 (softest) to 9 (stiffest) indicates the value of dynamic modulus at the frequency of 10 Hz and temperature of X. Despite the high (more negative) ΔT_{cr}

values, the softest mixtures (dynamic modulus rank 1 to 3) have very good performance for both fatigue and thermal cracking, while the PG 64-28, 9.5 mm, 16.4% RAP mixture with a very low ΔT_{cr} and higher dynamic modulus value shows some levels of both types of cracking. The largest difference between fatigue and thermal cracking evaluation is observed in three mixtures: PG 58-28, 12.5 mm, 28.3%RAP, PG 58-28, 12.5 mm, 18.5% RAP/RAS, and PG 52-34, 12.5 mm, 28.3% RAP. A hypothesis is that the fatigue cyclic degradation and the single critical event for low temperature cracking might be more different for the mixtures with greater amounts of aged binder (higher RAP content or with presence of RAS). This is a preliminary hypothesis and needs to be further explored in future studies.

To compare the number of cycles at G^R=100 with the LVECD fatigue prediction, there is not any failure point or significant predicted fatigue cracking for first five mixtures, while the number of cycles to failure for these mixtures varies from 6600 to 15000 cycles. PG 58-28, 12.5 mm, 18.5% RAP/RAS mixtures with highest number of cycles to failure show the worst predicted fatigue performance.

In summary, results presented in this work demonstrate that it is not possible to entirely rely on PG binder grade, recycled binder amounts, maximum aggregate size or only using single mixture or binder index property to entirely control fatigue and thermal cracking performance. Use of energy based cracking tests and pavement cracking simulation models are necessary to combine all the complexities of material behavior in both linear and non-linear response ranges with pavement structure. Use of simulation models allow for representation of loading and boundary conditions that pavements undergo in field that cannot be easily replicated in laboratory tests.

Table 5-3. Comparison of Fatigue and Thermal Cracking Test and Model Predictions

Mix	**Laboratory Testing**					**LVECD Model Prediction**		**TC Model Prediction** (% cracking at 20 year)	**IlliTC Prediction** (amount of predicted cracking)
	Binder (ΔT_{cr})	Dynamic Modulus Rank*	SVECD Fatigue (N_f @ G^R=100)	DCT		Rank	Level		
				Fracture Energy (J/m^2)	FST (10^{-6} m)				
58-12.5-18.9%RAP	-6.4	1	8926			1	Good	Negligible	
58-12.5-28.3%RAP	-3.8	5	7848	650.9	148.7	2	Good	100	100
52-12.5-18.5%RAP RAS	-8.5	2	11270			3	Good	Negligible	
58-9.5-21.3%RAP	-3.3	8	15150	721.4	153.2	4	Good	45.8	Softening for top 45 mm
52-12.5-18.9%RAP	-7.7	3	6636	703.2	173.2	5	Good	Negligible	No Cracking
58-12.5-22.4%RAP	-3.9	9	9973	604.4	123.2	6	Inter.	Negligible	No Cracking
64-9.5-16.4%RAP	-1.2	7	4180	692.4	145.8	7	Inter.	42.5	Softening for top 25 mm
52-12.5-28.3%RAP	-6.0	4	8115			8	Inter.	Negligible	
58-12.5-18.5%RAP RAS	-8.0	6	22500			9	Poor	Negligible	

* Ranks 1 to 9 show the softest to stiffest mixtures at 10 Hz.

5.7 Summary and Conclusion

The objective of this study was to evaluate fatigue and thermal cracking performance of asphalt mixtures using energy based models for fatigue and thermal cracking. The study included the laboratory testing on extracted and recovered binder and mixture and pavement performance evaluation. The following conclusions can be drawn on basis of the results and discussions presented in this paper:

- DSR and BBR testing on binders and complex modulus testing on mixtures were conducted to characterize the viscoelastic behavior of asphalt mixtures. Generally, the results were as expected in terms of higher stiffness for stiffer binders and more recycled materials for each plant. However, there were significant differences in the stiffness of the mixtures from the two plants. The

viscoelastic characteristics for both binder and mixture have considerable impacts on cracking behavior of mixtures, however their impacts are not consistent for either fatigue or thermal cracking.

- The results of pavement evaluation by LVECD for fatigue cracking, and TCModel and IlliTC for thermal cracking do not follow a consistent trend for all of the mixtures. Due to the difference in the mechanisms of fatigue and thermal cracking, it might be expected to have different cracking performance. This difference is also observed in the results of SVECD and DCT testing.

- The fatigue or thermal cracking performance of asphalt mixtures could not be predicted by using a single index property or binder and mixture parameter.

-Future investigation is planned to include more mixtures to obtain a larger data base and investigate the effect of long term aging on cracking performance. Also, the fatigue and thermal cracking performance of mixtures in the field are being tracked to be compared with the results of pavement performance predictions.

Chapter 6

THE EVALUATION OF VISCOELASTIC, FATIGUE, AND FRACTURE PROPERTIES OF HMA WITH LONG-TERM LABORATORY CONDITIONING

6.1 Introduction

Cracking has always been a challenging issue for asphalt pavements that negatively impacts the ride quality and pavement service life. Typically cracking susceptibility of asphalt mixtures change over the time as asphalt materials age. Asphalt materials undergo aging during production, construction, and over the service life of the pavement. The aging process is the change of binder chemistry due to two primary processes: volatilization and oxidation. Volatilization is the evaporation of lighter fractions (hydrocarbons) resulting in the increase of asphalt specific gravity. Volatilization occurs primarily during the production and construction stages where the binder temperature is very high (about 150° C). The volatilization rate increases dramatically with the increase of temperature (Lavin 2003, Fernandez et al. 2013).

Oxidation occurs due to the chemical reaction of asphalt hydrocarbons with oxygen that over its service life. The interaction of hydrocarbons with hydroatoms like oxygen causes an imbalance in electrochemical forces and the polarity increases in the binder molecules. More polarity results in stronger intermolecular forces, and accordingly, the elastic modulus and viscosity of the asphalt increase. It is well known that the ambient temperature has a significant effect on aging rate. Other

environmental conditions (e.g. pressure and moisture), traffic loading and mix volumetrics also effect the aging process.

Aging causes physical property changes to asphalt mixtures by increasing stiffness and brittleness and decreasing relaxation capability. Consequently, the cracking resistance of aged mixtures is expected to be lower than that of unaged mixtures. Considering the importance of performance-based design methodologies, the evaluation of fatigue and thermal cracking properties of aged asphalt mixtures is desired during mix design stage. To this aim, it is required to simulate the aging of asphalt materials in the laboratory.

Several methods for laboratory conditioning of asphalt mixtures are documented in the literature; three of these were evaluated in this study:

1. The current standard to simulate short and long term aging of asphalt mixtures is AASHTO R30. In this standard practice, the loose mix asphalt is placed in a forced-draft oven for 4 hours ± 5 min at a temperature of 275 ± 5° F (135 ± 3° C) to simulate short term aging, based on the strategic highway research program (SHRP) research by Bell et al. (1994). For long term aging, short term aged mixtures are compacted (following AASHTO T 312) into a specimen that is then conditioned in a forced-draft oven for 5 days (120 ± 0.5 hour) at 85 ± 3°C. Studies have shown that laboratory aging method simulates only 2 to 3 years of asphalt aging in service life. Another shortcoming of this standard is that only one conditioning time and temperature is considered for all locations and climate conditions (Kim et al. 2013).
2. Asphalt Institute procedure proposed by Blankenship et al., 2010 recommends loose mix asphalt conditioning in oven for 24 hours at 135°C. This level of conditioning is expected to simulate 7 to 10 years of aging in the field. The long term aging of loose mix at 135°C

was first suggested by Von Quintus (1988). Braham et al. (2009) also used 24 hr. aging of loose mix at 135°C. They suggested that this level of aging might be slightly conservative for fracture evaluation of asphalt mixtures.

3. The recent findings of the NCHRP 09-54 project on long-term aging of asphalt mixtures for performance evaluation suggests the aging of loose mix asphalt at 95°C for various times depending upon the climatic location of the pavement to be simulated (Elwardany et al., 2016). These findings are based on temperature conditioning of asphalt for both compacted and loose mix with and without pressure. Volumetric, stiffness and fatigue properties of the mixtures were compared. Oven aging on loose mix asphalt was recommended because of the uniformity of aging gradient in the final test specimen. Various researches indicates that a conditioning temperature above 100°C causes serious effects on binder chemistry and differences in the response of the mixtures to damage (Peterson and Harnsberger, 1998; Glaser et al. 2013). Yousefi Rad et al. (2017) recommended the conditioning temperature of 95°C as an optimal temperature for aging of loose mix asphalt. The conditioning time should be adjusted based on climate and depth in the pavement; for example, their results show 8.2 days aging of loose mix at 95°C can match 17 years aging of the top 6 mm of a pavement in Marathon County, WI in terms of binder rheology.

6.2 Mixtures and Materials

This study includes testing on nine different recycled mixtures from New Hampshire and one virgin mixture from Virginia. The mixtures are varied in binder PG grade (PG 52-34, PG 58-28, PG 76-22), nominal maximum aggregate size (NMAS) (9.5, 12.5 and 19 mm), recycled material type, and binder replacement (18% – 32% RAP or RAP/RAS). Table 6-1 shows the combinations

evaluated and the levels of aging conducted for different mixtures. It should be noted that there were not enough materials for some of the mixtures to conduct full factorial of testing and cage conditioning. The cells are shown with three letters of A, C, and N, which are respectively indicators of the mixture-aging combinations for which All testing results (complex modulus, DCT, and SCB testing) are available, the mixture-aging combinations with only Complex modulus data, and the mixture-aging combinations with No data (no material). In the results and discussion section, 18.9% RAP, and 28.3% and 31.3% RAP mixtures are rounded to 20% RAP and 30% RAP, respectively, for presentation purposes. The mixtures which contain the combination of RAP and RAS are simply shown as RAP/RAS mixtures.

Table 6-1. Available Mixtures and Different Aging Levels

Binder PG Grade	NMSA (mm)	%Total Binder Replacement (% RAP/ % RAS)	LTOA			
			5days 85°C compacted	24hr 135°C Loose	12days 95°C Loose	5days 95°C Loose
58-28	12.5	18.9 (18.9/0)	C	A	A	A
	12.5	18.5 (7.4/ 11.1)	N	A	A	A
	12.5	28.3 (28.3/ 0)	C	A	A	A
	19	20.4 (8.2/ 12.2)	N	A	A	A
52-34	12.5	18.9 (18.9/0)	C	A	A	A
	12.5	18.5 (7.4/ 11.1)	N	A	A	A
	12.5	28.3 (28.3/ 0)	C	A	A	A
	19	20.4 (8.2/ 12.2)	N	A	A	N
	19	31.3 (31.3/ 0)	N	A	A	N
76-22	9.5	0	N	A	A	C

6.3 Methodology

6.3.1 Aging

The asphalt materials (both loose mix and compacted specimens) were conditioned in ovens to simulate the aging of asphalt pavements in field. Figure 6-1 shows the steel pans containing loose

mix asphalt and the compacted samples before being placed in oven. The aging of compacted samples was performed following AASHTO R-30. Plant produced material was reheated for 2 hours at the compaction temperature (135°C) and then compacted to a target air void content of in the final test specimen using a Superpave gyratory compactor. Specimens were then cored and trimmed to final test specimen dimensions and wrapped in wire mesh with clamps to prevent any changes in the shape of the specimens during aging.

Figure 6-1. Aging of compacted specimens (right), and loose mix asphalt (left)

Three different conditioning protocols for loose mix asphalt were evaluated in this study:

- 24 hours at 135°C
- 12 days at 95°C, and
- 5 days at 95°C

The 24 hours at 135°C is following the Asphalt Institute procedure. The selection of two other aging levels is based on a study conducted by North Carolina State University (Yousefi Rad et al. 2017). They determine the duration of aging for different mixtures with comparison of stiffness of extracted and recovered binders from two levels of aging, so that the specified G* value (at 64°C and 10 Hz) from 95°C match with the G* of binders from 24 hours at 135°C aging. Based on the

mixtures used in this study, 12 days at 95°C is selected to match with 24 hours at 135°C, and 5 days at 95°C is also considered as intermediate aging level.

The loose mix asphalt was spread in steel pans at an approximate depth of 1 inch. The materials were stirred every other day and the pans were rotated around the oven to obtain a consistent aging condition in materials. The materials were reheated at 135°C for 2 hours before compaction to final test specimens with air void contents of 6 ± 0.5%.

6.3.2 Testing Methods

The complex modulus testing was conducted following AASHTO T 342 to compare the stiffness and relaxation capability of mixtures at different aging levels. An asphalt mixture performance tester (AMPT) machine was used for conducting the complex modulus testing. The raw data were analyzed using Abatech RHEA® software. Dynamic modulus and phase angle master curves were constructed based on the time-temperature superposition principle.

Two common testing methods to characterize the fracture behavior of asphalt materials in laboratory were used in this study: Disc Shaped Compact Tension (DCT) and Semi Circular Bending (SCB) testing. The asphalt mixture materials follow a quasi-brittle behavior under the fracture process. The typical load displacement curve obtained from both tests is shown in Figure 6-2.

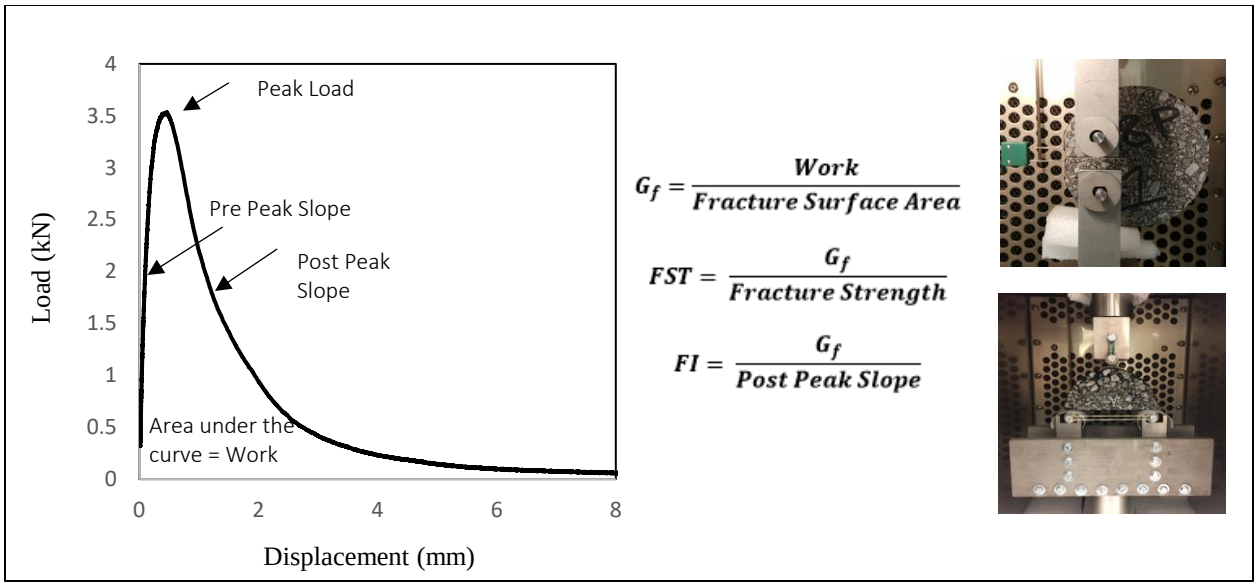

Figure 6-2. Typical Load-Displacement Curve of Fracture Tests

The DCT test (ASTM D 7313) was conducted to compare the thermal cracking behavior of the various mixtures and aging levels. The appropriate low temperature PG grade for New Hampshire mixtures was determined to be -28°C using LTPPBind software. DCT testing was performed at -18° C (10 degrees warmer than low temperature PG grade requirement for the pavement location) for these mixtures and -22° C for virgin mixture. This test was developed to measure the fracture energy of circular notched specimens under a tension load, which provides an oriented crack propagation along the notch. The fracture work is defined as the area under the load versus Crack Mouth Opening Displacement (CMOD) curve. Fracture energy is determined by normalizing the fracture work for specimen thickness and ligament length. The fracture energy is the amount of energy required to develop a unit surface fracture of the asphalt mixture. The fracture strain tolerance (FST), a new parameter suggested by Zhu et al. (2017), is calculated by normalizing the fracture energy of mixture with the fracture strength (G_f/S_f).

The SCB fracture test (AASHTO TP 124) is performed at intermediate temperature (25ºC) and evaluates the resistance of asphalt mixtures to fatigue cracking. The load is applied to a notched

semi circular specimen at a displacement rate of 50 mm/min. The crack propagates along the notch in the middle of the specimen. The measured data are analyzed using the IFIT software developed by Illinois Center of Transportation (ICT), to calculate the fracture energy (G_f) and flexibility index (FI) parameters defined by equations 6.1 & 6.2.

$$G_f = \frac{W_f}{t \times a} \quad 6.1$$

$$FI = \frac{G_f}{m_{Post\ peak}} \quad 6.2$$

where W_f is fracture work, t is the thickness of specimen, and a is ligament length. $m_{Post\ peak}$ is the slope of the post-peak softening curve at an inflection point near the middle of the post-peak region.

6.4 Results and Discussion

6.4.1 Linear Viscoelastic Parameters

The results of dynamic modulus and phase angle master curves for different aging levels are presented as the average of three replicates from a sample mixture (PG 52-34, 12.5 mm, 28.3% RAP) in Figure 6-3. The overall trend is similar for all mixtures evaluated in this study: as the asphalt materials age the stiffness (|E*|) increases while the relaxation capability of mixtures (δ) decreases. Dynamic modulus and phase angle master curves are statistically similar for the 24 hr., 135°C and 12 days, 95°C aging levels. The 5 days at 95°C aging level falls approximately in the middle of short term aged condition and 12 days, 95°C aging. Statistical analysis (t-test) was conducted for dynamic modulus and phase angle results using the measured data obtained from 3 replicates of each mixture. With a significance level of 0.05, there is a significant difference between dynamic modulus and phase angle of STOA mixtures with all levels of long term aging. The results indicate neither dynamic modulus nor phase angle show a statistical difference between

24 hr. (135°C) and 12 days (95°C) aged mixtures. Also, two shorter levels of aging (5 days (95°C) on loose mix and 5 days (85°C) on compacted samples) are not statistically different. It should be mentioned that this comparison was conducted for only 4 available mixtures. To compare 12 days (95°C) and 5 days (95°C) aging levels, there is a significant difference for both |E*| and δ of all mixtures, except two 19 mm, PG 52-34 mixtures.

One interesting observation is that the peak phase angle value moves to the bottom and left (lower frequencies) as materials age, so that for two high levels of aging (24 hr., 135°C and 12 days, 95°C) the peak phase angle was not measured within the standard testing temperatures (4.4, 21.1, and 37.8°C) and frequencies (25, 10, 5, 1, 0.5, and 0.1 Hz). To capture the peak point for these two levels of aging, the complex modulus testing was conducted at an additional frequency (0.01 Hz) at 37.8°C.

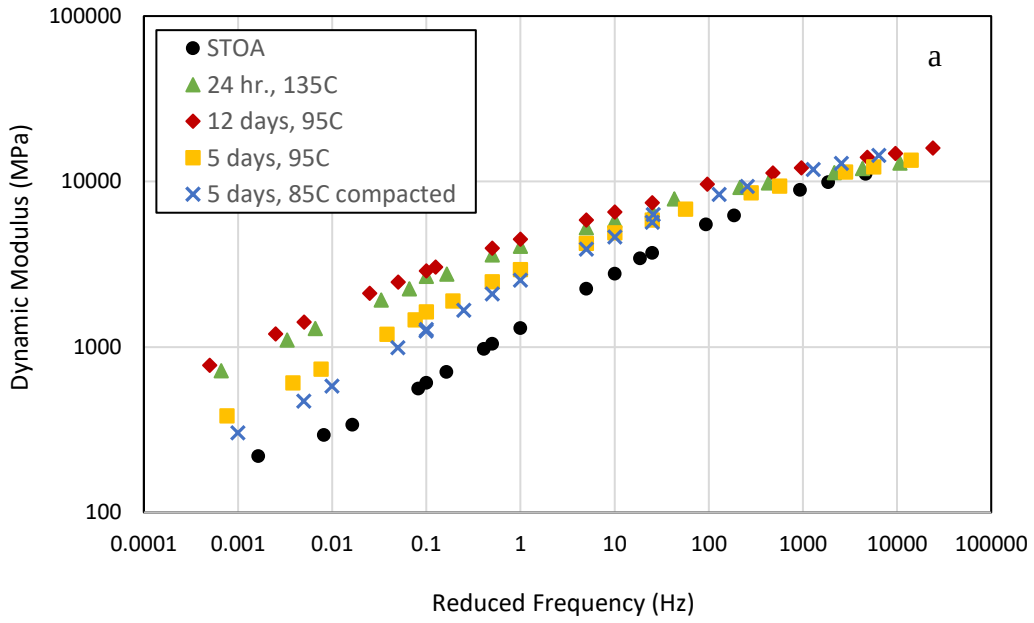

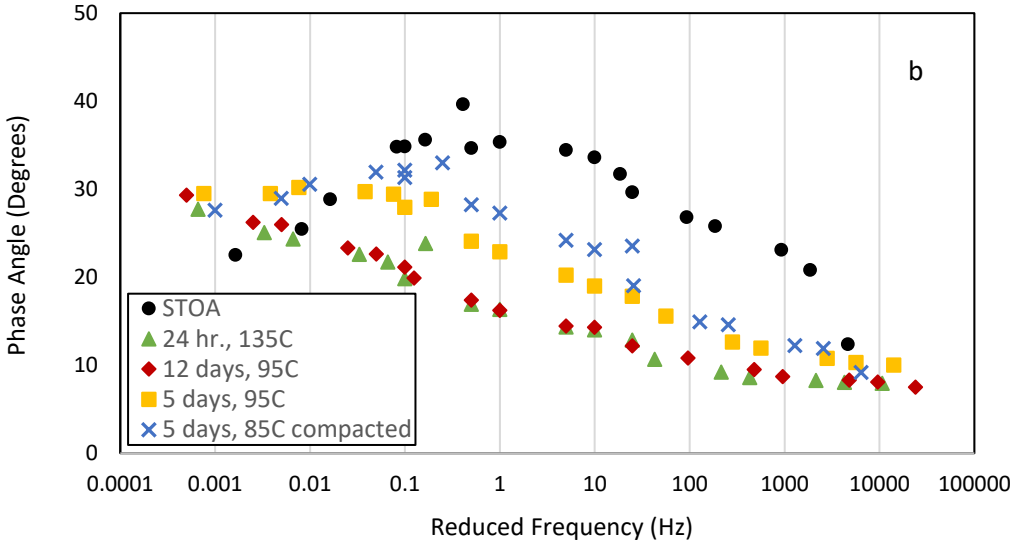

Figure 6-3. a) Dynamic Modulus and b) Phase Angle Master curves for PG 52-34, 12.5 mm, 28.3% RAP Mixture at Different Aging Levels (ref. temperature 21.1°C)

Figure 6-4 compares the average dynamic modulus and average phase angle master curves at different long term aging levels versus to the values measured in the short term aging condition for all of the mixtures evaluated in this study, in the frequency range of 10^{-5} to 10^{5} Hz. All LTOA mixtures have higher dynamic modulus than STOA mixtures. This shows the clear difference between two intermediate aging levels and the two longer term aging levels, and the similarities of the two long term aging levels at the intermediate frequencies. At the very low and high frequencies, the E* of aged mixtures becomes closer to the line of equality, while the difference is more evident at intermediate frequencies. The double and triple lines of $|E^*|_{(STOA)}$ values are drawn in Figure 6-4(a). At the frequencies higher than 10 Hz, the dynamic modulus of long term aged mixtures are lower than twice the $|E^*|_{(STOA)}$, while at the frequencies around 0.01 Hz, the dynamic

modulus of long term aged mixtures might increase to six times of dynamic modulus of short term aged condition.

The phase angle values of all LTOA mixtures are lower that those of STOA mixture at low and intermediate temperature. As shown in Figure 6-3(b), a horizontal shift is observed in phase angle master curves as the aging level increases. At the lower frequencies, the phase angle of STOA mixtures begins to decrease after the inflection point, while the phase angle values of LTOA mixtures are still increasing. At the frequencies lower than the intersection point of STOA and LTOA master curves, the phase angle of STOA mixtures are lower than those of LTOA mixtures (as shown in Figure 6-4b). As the aging level increases, two curves intersect at a lower frequency. Although it changes from one mixture to another, the high levels aged mixtures intersect with STOA mixtures master curves somewhere between 0.001 to 0.001 Hz. This intersection of intermediate aged and short term aged mixtures is between 0.01 to 0.1 Hz. At the frequencies lower than these values, the phase angle of LTOA mixture are higher than phase angle of STOA mixtures.

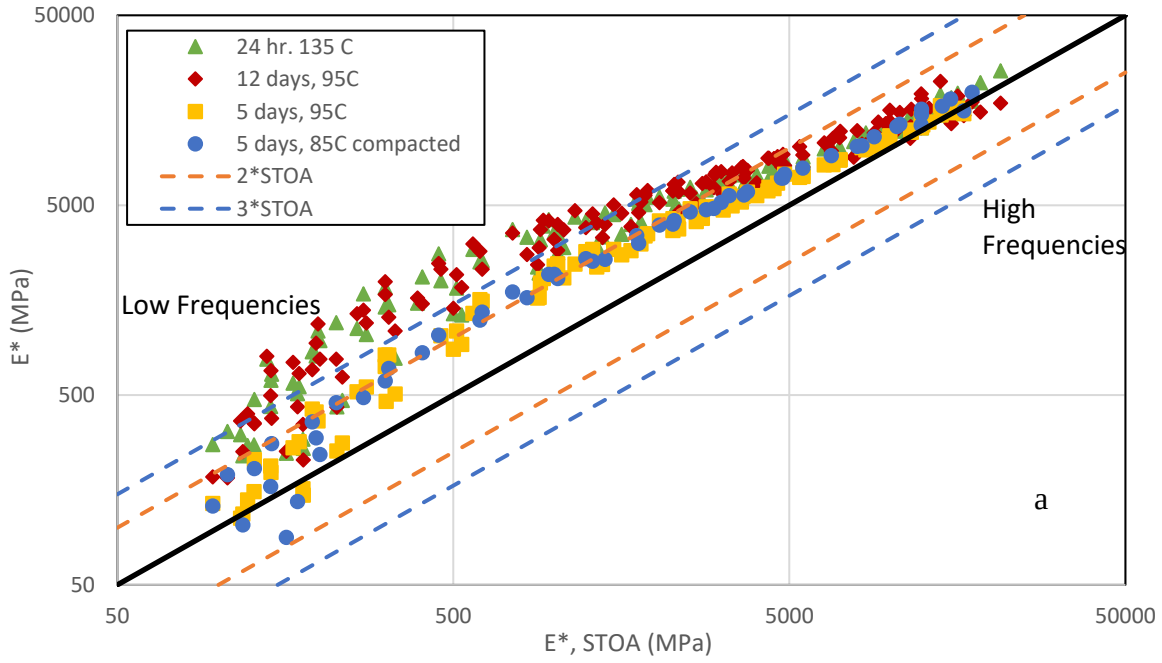

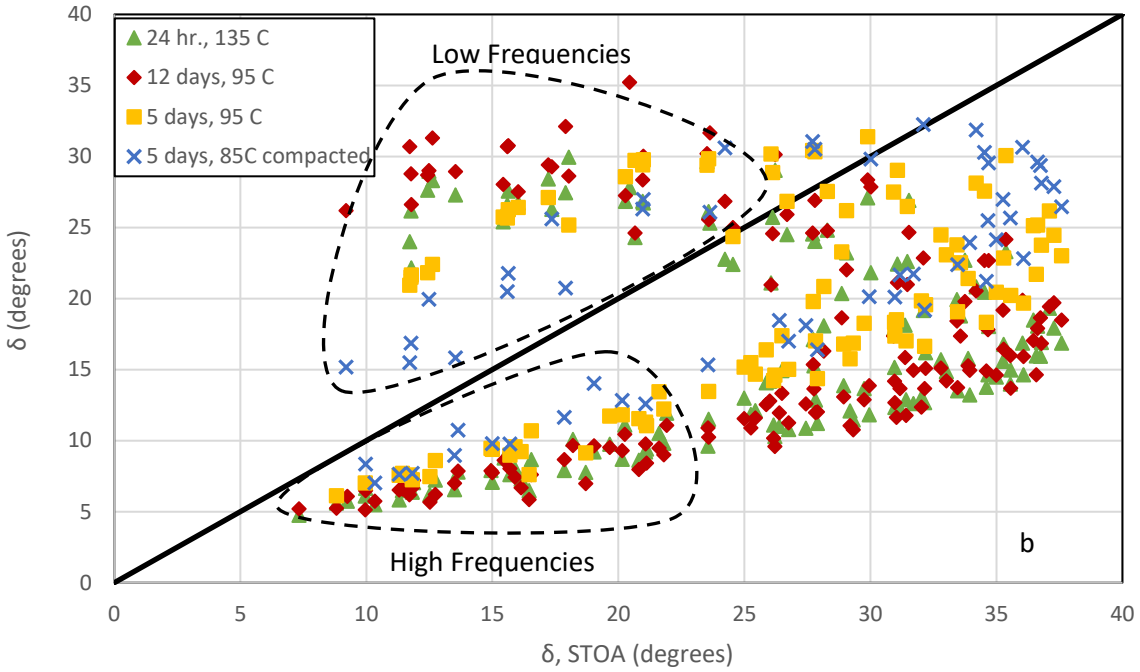

Figure 6-4. LVE Properties a) Dynamic Modulus, b) Phase Angle of LTOA Mixtures versus STOA Mixtures for Different Mixtures

To capture the combination of stiffness and relaxation capability of mixtures in a single plot, Black space diagrams are shown in Figure 6-5. The figure shows how Black space curves move with additional amount of aging. The inflection point moves to the bottom left side as more aging occurs. The observations in Black space diagram can be used to estimate thermal cracking susceptibility of asphalt mixtures. Generally, a mixture with higher stiffness at a constant phase angle is expected to incur greater thermal stress values. If the relaxation capability (phase angle) of this mixture is lower, the mixture relieves the thermal stress at a slower rate, resulting in higher thermal cracking potential. In Figure 6-5, higher phase angle for STOA with decreasing phase angle values are seen for STOA condition as compared to long term aged condition at constant value of stiffness (|E*|). This indicates that even for same level of thermal stress, relaxation capabilities of asphalt mixtures would diminish with increasing aging levels. Thus, aged mixtures would be more prone to cracking at a lower cooling rate than short term aged mixtures.

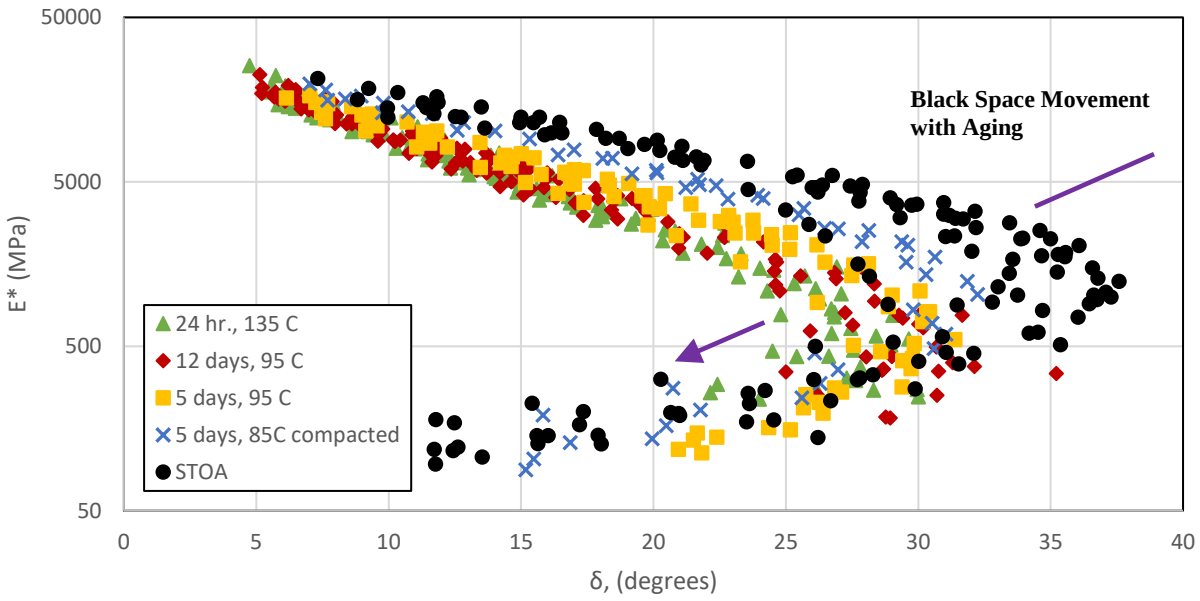

Figure 6-5. Black Space Diagrams of Different Aging Levels

Generally, a standard or generalized sigmoidal model is used to fit the dynamic modulus master curve. In this study, the standard sigmoidal model (Equation 6.3) is employed:

$$\log|E^*| = \delta + \frac{\alpha}{1+e^{\beta+\gamma\log(\omega)}} \qquad 6.3$$

where $|E^*|$ is dynamic modulus, ω is frequency, and δ, α, β, and γ are the fit coefficients that describe the shape of dynamic modulus master curve. As the asphalt materials age, the shape of master curve changes, resulting in a variation in fit coefficients. Accordingly, these coefficients can be the indicators of aging level. The α and δ parameters are related to the equilibrium modulus (lower asymptote) and glassy modulus (upper asymptote) of master curve, respectively. The γ value controls the width of relaxation spectra, and the frequency of the inflection point can be calculated from $10^{-\beta/\gamma}$. As the asphalt material ages, the $|E^*|$ master curve tends to flatten and the inflection point is shifts to lower frequencies (Mensching et al., 2016).

The inflection point parameter ($-\beta/\gamma$) versus relaxation spectra width parameter (γ) plot for mixtures (Figure 6) is similar in concept to a crossover frequency versus R value plot for binders.

The $-\beta/\gamma$ parameter decreases and γ increases, moving points further towards the lower right as more aging occurs. The parameter of $-\beta/\gamma$ for all the short term aged mixtures (except virgin mix) is about zero. This parameter for 5 days (85°C) compacted and 5 days (95°C) aged mixtures also varies between -1.1 to -1.5, and -2 to -2.9, respectively, while the variation of $-\beta/\gamma$ for two highly aged levels (24 hr. and 12 days) mixtures is greater. There is a gap between $-\beta/\gamma$ values of 24 hr. (135°C) aged mixtures which splits the mixtures into two groups. All the PG 52-34, 24 hr. (135°C) aged mixtures have higher $-\beta/\gamma$ than PG 58-28 mixtures, indicating less aging for these mixtures. As a hypothesis, the severe conditioning of 135°C in a short duration (24 hr.) might have different effects on different binder grades. It should be noted that the results of binder testing on extracted and recovered binders from short term aged mixtures showed elevated zinc levels in two 19 mm mixtures with PG 52-34 binder, indicating that re-refined engine oil bottoms (REOB) may have been used in the production of the virgin binder. One of the concerns about using REOB in asphalt mixtures is that it might increase the aging of binder (Mogawer et al. 2017).

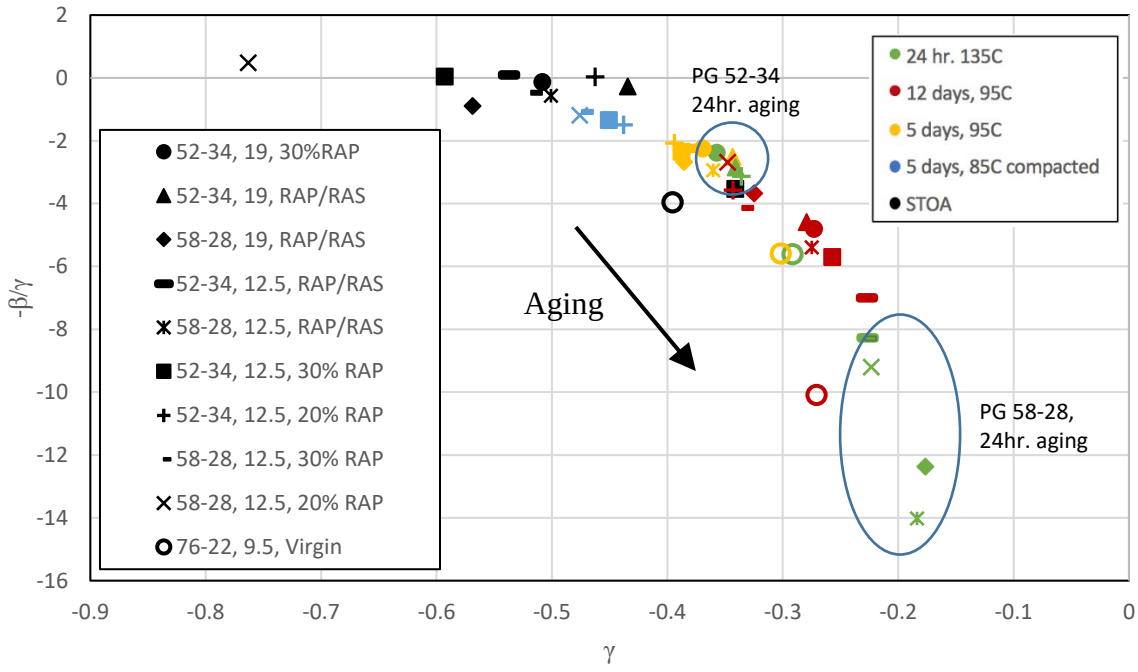

Figure 6-6. Crossover frequency vs. relaxation spectra width parameter in sigmoid model (ref. temperature 21.1ºC)

A Lorentzian equation (Equation 6.4) has been shown to accurately model the phase angle master curve (Nemati and Dave, 2017) and is used in this study.

$$\delta = \frac{a.b^2}{[(\log(\omega)-c)^2+b^2]} \qquad 6.4$$

where δ is phase angle (degree), ω is frequency (Hz), and a, b, and c are the fit coefficients as follows: “a” shows the peak value, b controls the width of transition, and c is related to the horizontal position of the peak point. As the testing results show (Figure 6-3), the phase angle master curves shift vertically and horizontally with different aging conditions. Therefore, the variation of vertical position of peak (a) and the parameter related to horizontal position of peak (c) with aging were selected for evaluation in this study. The parameters are called vertical peak and horizontal peak instead of “a” and “c” in this paper. Figure 6-7 shows how both vertical and

horizontal peak values decrease with increased aging level, moving the points towards the bottom left of the plot. The plot can be an indicator of the relaxation capability of asphalt mixtures. The mixtures with higher horizontal and vertical peak values are expected to have higher relaxation capability and better fatigue and fracture behavior. Similar to what was observed with the dynamic modulus coefficients, for 24 hr., (135°C) aging, PG 52-34 mixtures (except PG 52-34, 12.5 mm, RAP/RAS) are separate from PG 58-28 mixtures with a higher horizontal peak value, shown with two circles in Figure 6-7. The mixtures containing REOB (two PG 52-34, 19 mm mixtures) show lower vertical peak (a) values in all levels of aging. However, the decrease of horizontal peak (c) for these mixtures has been less than the other mixtures.

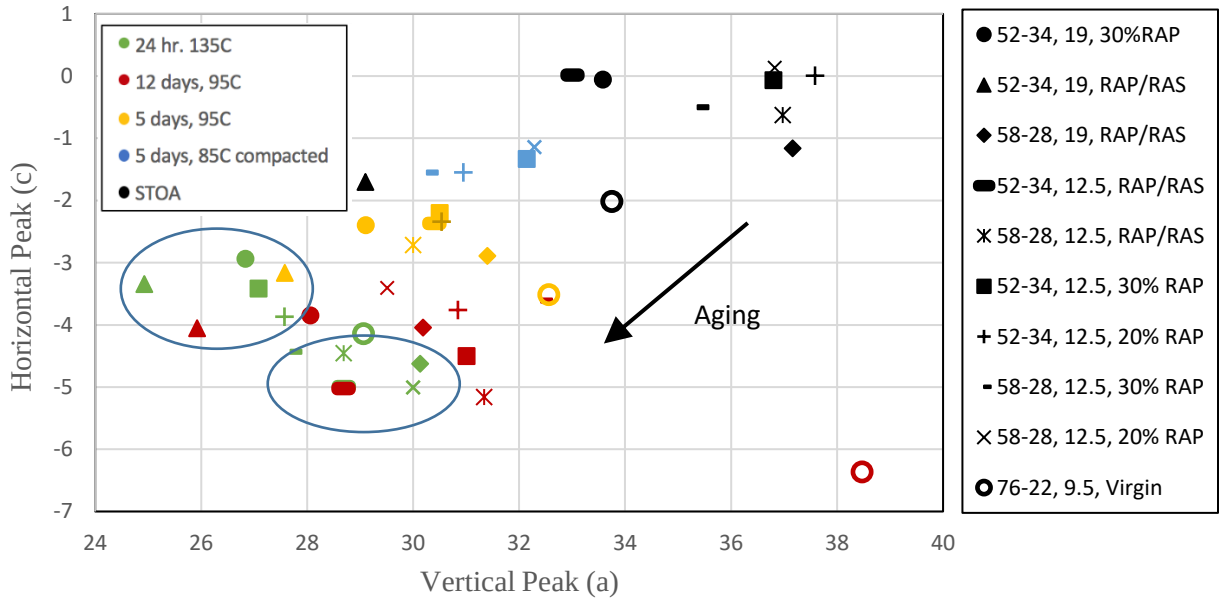

Figure 6-7. Variation of Phase Angle Master Curve Parameters with Aging (ref. temperature 21.1°C)

Mensching et al. (2016) developed a parameter to evaluate the cracking performance of asphalt mixture in the format of the binder Glover-Rowe parameter ($\frac{|E^*| \cos \delta^2}{\sin \delta}$). In this study, the parameter is calculated at the temperature-frequency combination of 15°C - 0.005 rad/s to be consistent with

the binder Glover-Rowe parameter. Figure 6-8a shows the mixture G-R values for different mixtures and aging levels. As expected, the mixture G-R parameter increases as the level of aging changes from short term to two intermediate and then to two high aging levels. There is a jump when aging level increase from 5 days to 12 days at the same temperature. There is not a consistent trend between the 24 hr. (135°C) and 12 days (95°C) aged mixtures. The ratio of mixture based G-R parameter in LTOA condition to the STOA condition is presented in Figure 6-8b. The intermediate aging levels (5 days) increase the mixture G-R parameter from 1 to 3 times, but this ratio is from 3 to more than 7 for two high aging levels. This ratio is smaller for 19 mm, PG 52-34 mixtures (mixtures with REOB) that is in a good agreement with the variation of horizontal peak in Figure 6-5. The parameter has the greatest change for 12.5 mm, RAP/RAS mixtures after 24 hr. (135°C) and 12 days (95°C) aging.

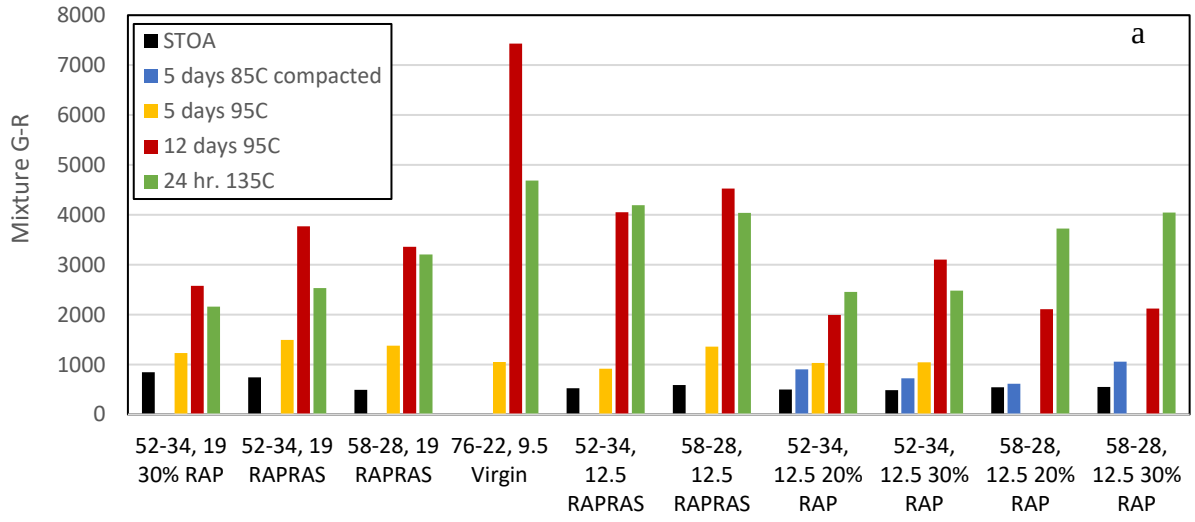

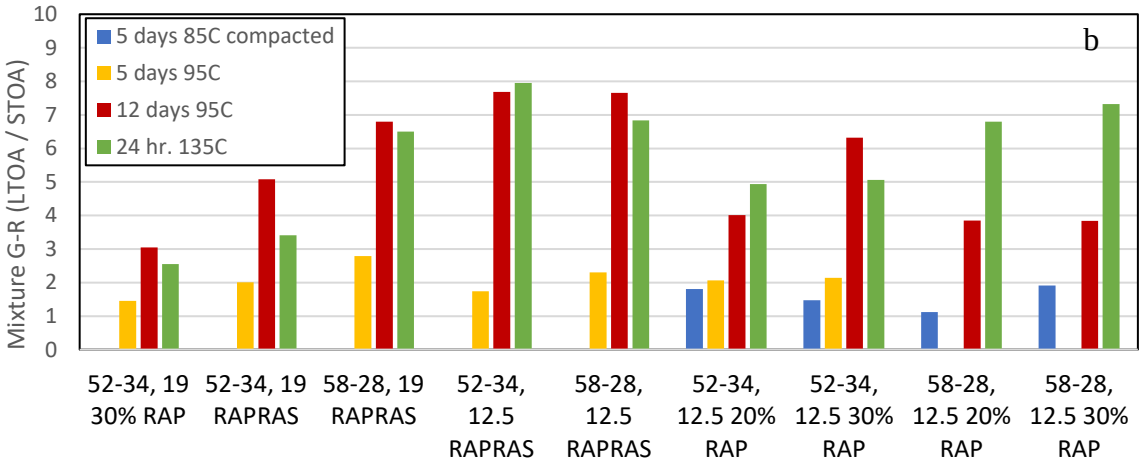

Figure 6-8. a) Mixture G-R values, b) Ratio of (Mixture G-R_{LTOA} / Mixture G-R_{STOA}) (15°C and 0.005 rad/sec)

6.4.2 Fracture Parameters

The results of DCT and SCB fracture testing is presented and discussed in this section. Figure 6-9 shows the average fracture energy and fracture strain tolerance for the various mixtures at different aging levels. The error bars show the standard deviation of 3 replicates tested for each mixture. A threshold value of 400 J/m^2 for fracture energy of DCT has been proposed by previous researchers [Dave and Hoplin, 2015; Van Deusen et al. 2015] for short-term aged mixtures and is shown for visual comparison. Most of the high eged mixtures have the fracture energies less than the limit. There is not a significant difference between the fracture parameters of 5 days aging with the high aging levels for two PG 52-34, 19 mm mixtures (with REOB). This agrees with the mixture G-R and phase angle shape parameters, indicating that the LVE and fracture properties of these mixtures do not increase much with aging. The trend of fracture strain tolerance (FST) is similar to fracture energy for these mixtures. For all the 12.5 mm only RAP mixtures, the trend is that both G_f and FST decrease when aging level changes from 5 days to 12 days, and 24 hour, while for the RAP/RAS mixtures, 24 hour mixtures show better fracture parameters than 12 days aged mixtures.

The reason might be different chemical volatilization process during two levels of aging. The 24 hour aging level seems to be less detrimental to fracture energy than 12 days aging for all RAP/RAS mixtures.

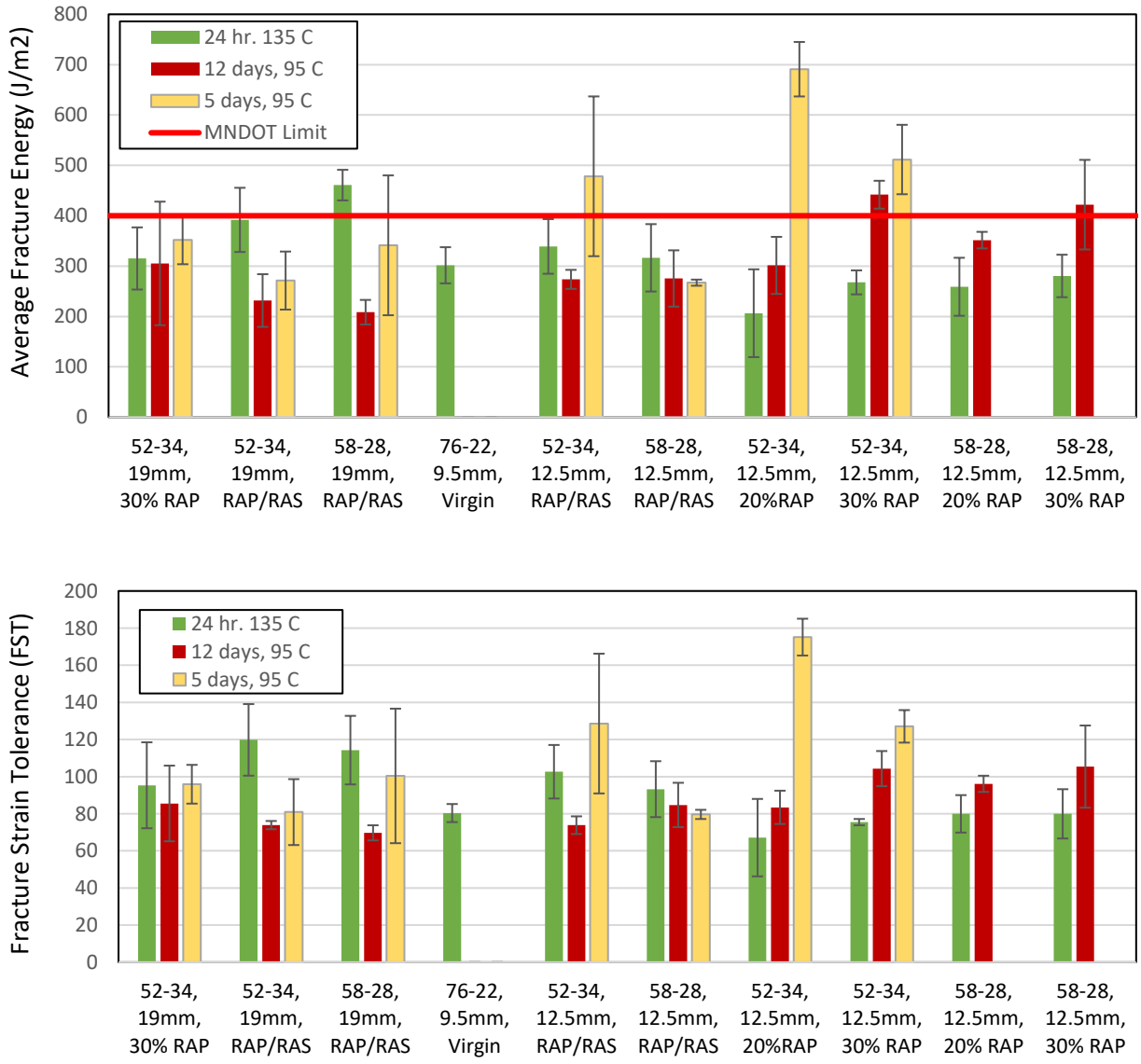

Figure 6-9. Fracture Energy and Fracture Strain Tolerance (DCT Testing)

A potential reason for this behavior of RAP/RAS mixtures might be the greater amount of already aged and oxidized asphalt binder present in these mixtures, which is not as prone to a more severe aging temperature as other mixtures. There is a significant difference between the fracture

properties of 5 days and 24 hour aging for PG 52-34, 12.5mm mixtures, while fracture energy and FST of 5 days aged, PG 58-28, 12.5mm, RAP/RAS mixtures are very close to those of high aged mixtures.

Figure 6-10 shows the fracture energy and flexibility index (FI) parameters which are the average of 3 to 4 replicates for each mixture, with the standard deviation error bars. The testing temperature was 25°C for all mixtures. 24 hr. (135°C) and 12 days (95°C) aged mixtures show comparable fracture energy values, while the difference is greater when the flexibility index is taken into account. The FI values of 5 days aged mixtures are higher than 24 hour and 12 days aged values for all mixtures, with higher differences observed for RAP/RAS mixtures. The flexibility index of PG 52-34 mixtures is generally higher than the similar PG 58-28 mixtures, especially for 5 days aging level. The fracture properties obtained from SCB testing do not show a similar trend with the results of DCT testing. It is not surprising since the loading mode and testing temperature are different in these two fracture tests. Results shown here agree with recent work by Haslett et al. (2017) that showed that a single 25°C test temperature for SCB testing may not as clearly distinguish between mixtures with different low temperature binder grades.

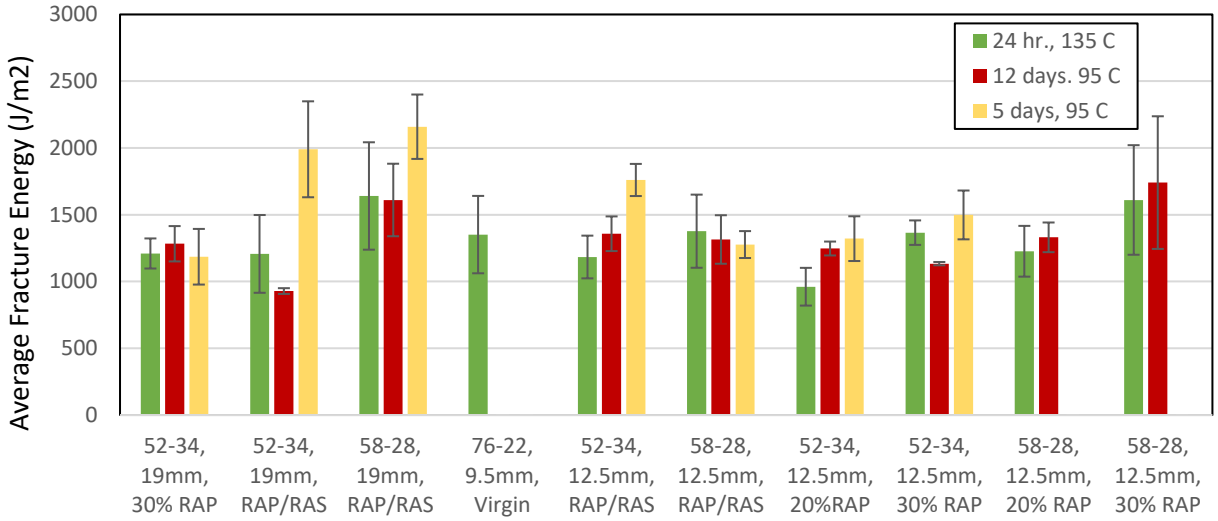

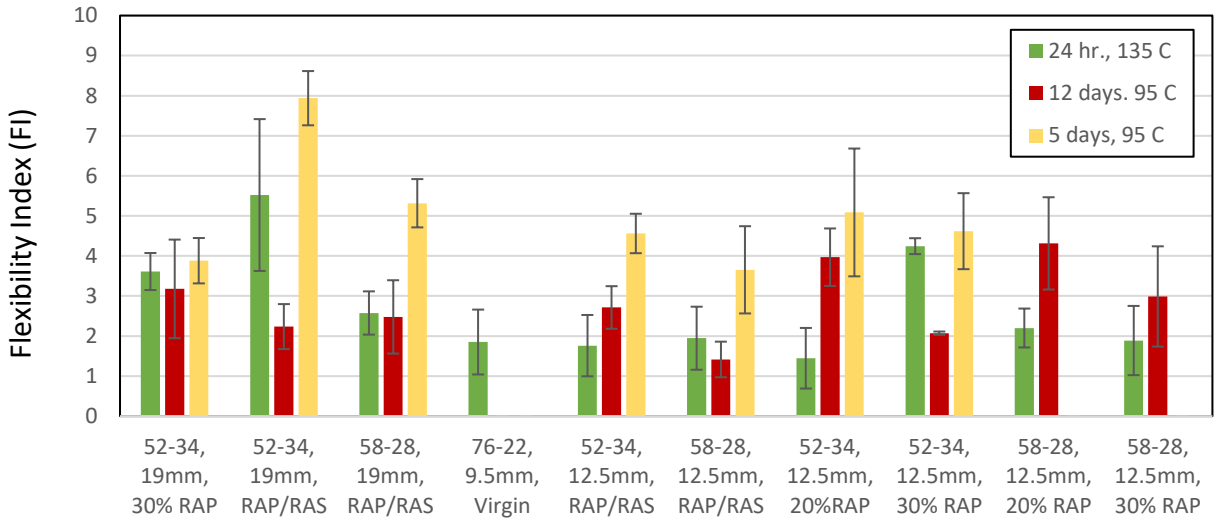

Figure 6-10. Average Fracture Energy and Flexibility Index (SCB Testing)

6.5 Statistical Analysis

The Pearson correlation parameter is used to assess the correlation of different factors discussed in this study. This parameter varies between -1 to +1, indicating a perfect inverse linear to a perfect direct linear relationship, respectively. Zero indicates no relationship. Table 6-2 shows the Pearson correlation factor calculated for different factors. The results show there are good to vey good correlations between vertical peak and horizontal peak values with some other parameters, for example the strong correlation between horizontal peak and mixture based G-R parameter (-0.91). The good correlation of mixture based G-R parameter with dynamic modulus fit parameters ($^{-\beta}/_{\gamma}$ and γ) and phase angle coefficients (specially horizontal peak) is interesting.

Another interesting point is that the phase angle fit parameters ("a" and "c") show good correlations with both DCT fracture parameters, while the correlation between these shape parameters and FI from SCB testing is weak.

The fracture energy values obtained from two testing methods of SCB and DCT do not seem to have a strong correlation (0.43) as well, which is not surprising due to different mechanisms in crack initiation and propagation, and different testing temperatures.

Table 6-2. Pearson Correlation Factor for Different Parameters

	γ	$-\beta/\gamma$	a	c	G_f (SCB)	FI (SCB)	G_f (DCT)	FST (DCT)
$-\beta/\gamma$	-0.83							
a	-0.73	0.47						
c	-0.92	0.80	0.72					
G_f (SCB)	-0.67	0.41	0.71	0.64				
FI (SCB)	-0.29	0.39	-0.13	0.24	0.35			
G_f (DCT)	-0.52	0.46	0.68	0.72	0.43	0.01		
FST (DCT)	-0.67	0.51	0.72	0.79	0.50	0.05	0.95	
Mixture G-R	0.84	-0.83	-0.61	-0.91	-0.58	-0.47	-0.65	-0.67

6.6 Fatigue Cracking Analysis

Figure 6-11 compares the damage characteristic curves of different mixtures (except PG 52-34, 19 mm, 30% RAP and PG 76-22, 9.5 mm, virgin) for different aging levels. Generally, this curve shows the trend of reduction of material integrity as damage is growing in sample through the test. The mixtures that have C-S curves further up and to the right would be expected to have better fatigue properties, since they are able to maintain their integrity better during the test. However, the performance of asphalt mixture in field depends on other factors like pavement structure as well.

Generally, there is not a consistent trend for all the mixtures to show an aging level would work better against fatigue cracking. Although, for some of the mixtures like PG 58-28, 12.5, RAP/RAS and PG 52-34, 19, RAP/RAS, the short term oven aged mixtures show higher integrity throughout the test, the C-S curves of long term oven aged mixtures are higher for the other mixtures. In spite

of similar dynamic modulus and phase angle values for two 24 hr. (135°C) and 12 days (95°C) aging levels from complex modulus testing, the C-S curves of these two levels of aging are not similar for most of the mixtures.

Figure 6-12 presents the fatigue failure criterion (G^R) versus the number of cycles to failure (N_f) of mixtures at different aging levels. Generally, the higher G^R values at the same number of cycles indicates better fatigue behavior. Generally, the fatigue failure criterion does not seem to be very sensitive to aging, since the G^R-N_f diagrams of different aging levels are very close and the distribution of points is scattered. Although, a consistent trend could barely be found between the fatigue life of mixtures with different aging levels, the mixtures aged in 95°C (both 5 and 12 days) seem to behave better than 24 hr. (135°C) mixtures.

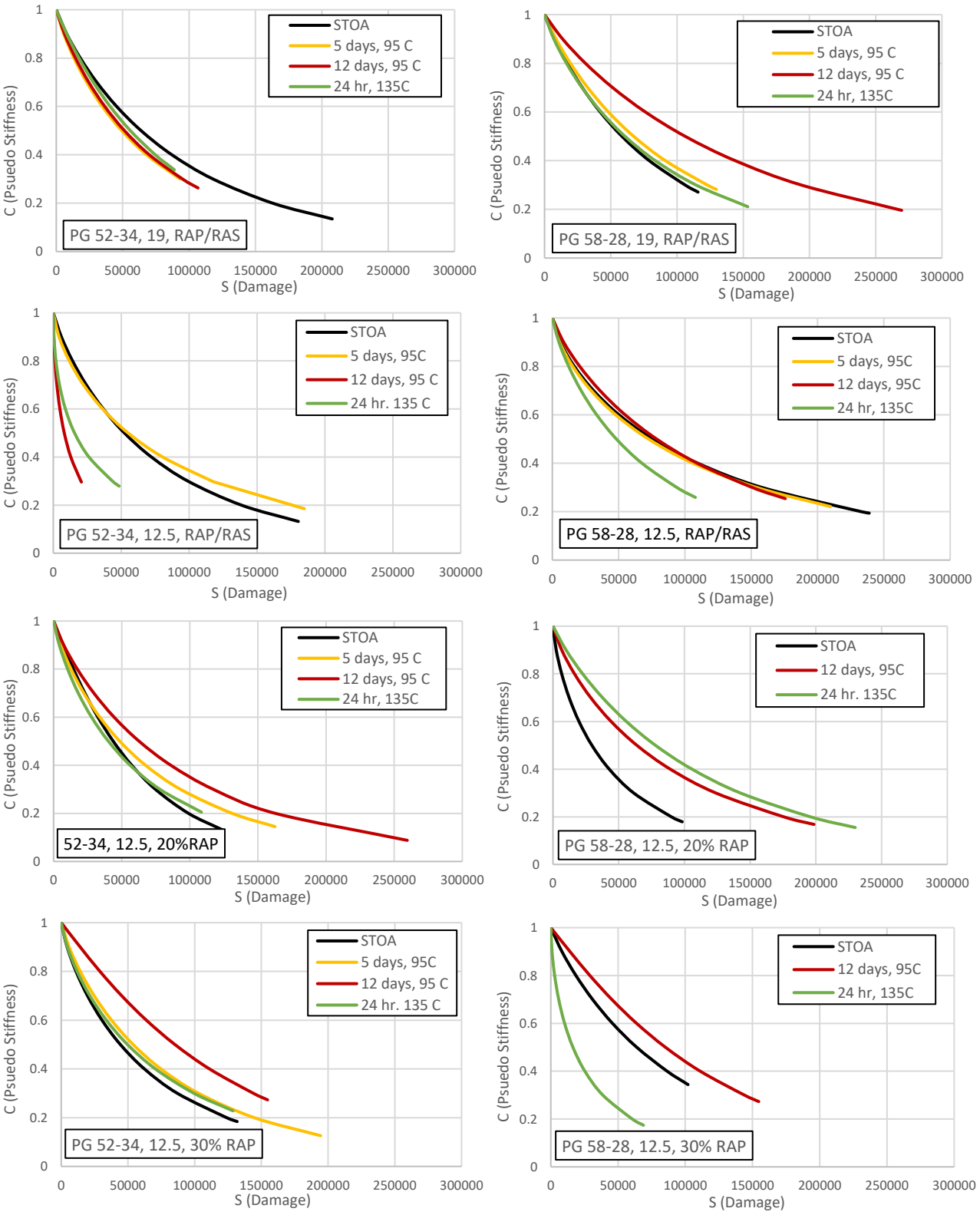

Figure 6-11. Damage Characteristic Curves at Different Aging Levels

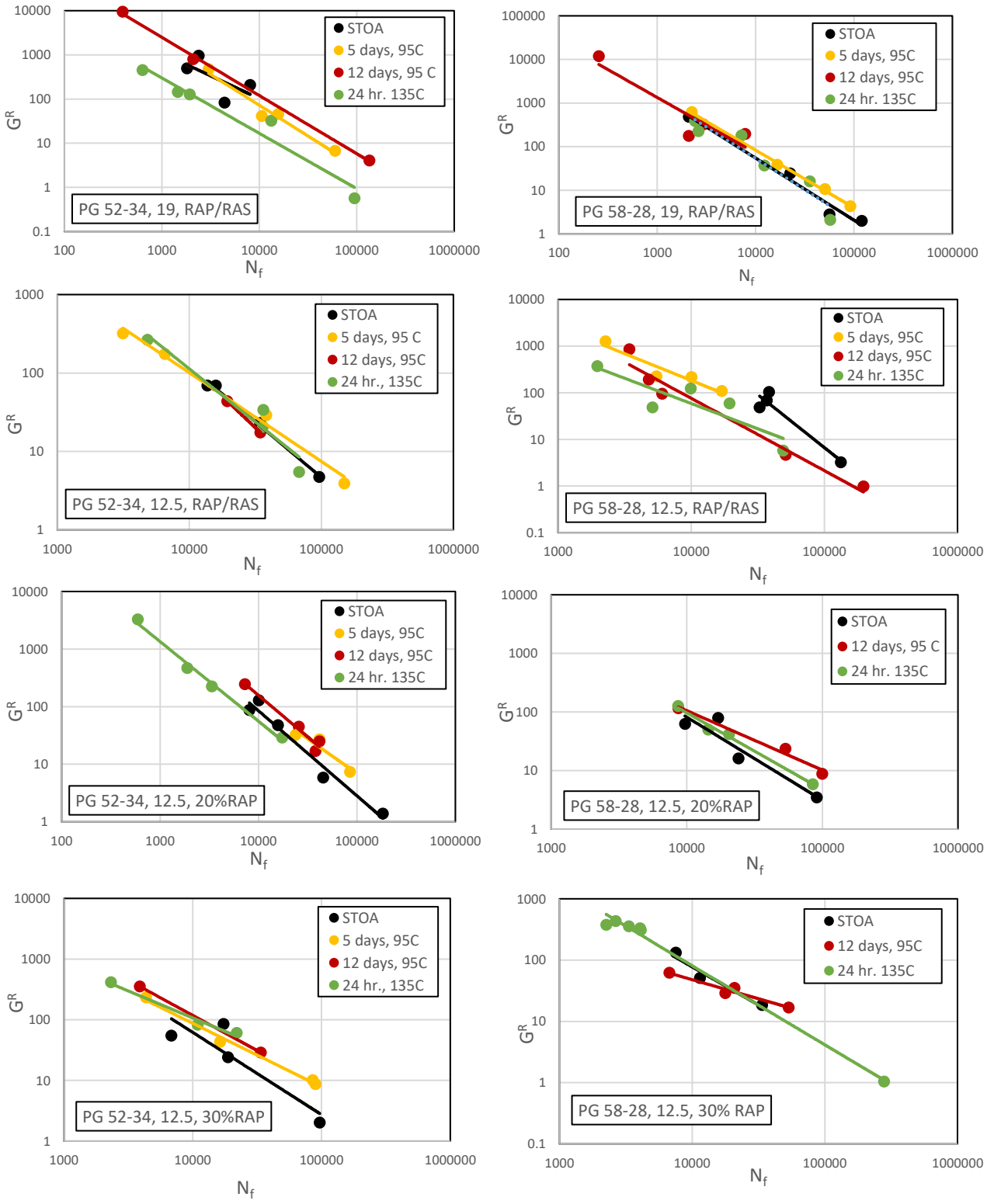

Figure 6-12. Fatigue Failure Criterion vs. Number of Cycles at Different Aging Levels

6.7 Summary and Conclusion

The main objective of this research was to investigate how the mixtures' properties change with different long term aging levels (5 days at 95°C, 12 days at 95°C, and 24 hr. at 135°C) on loose mix and 5 days at 85°C on compacted samples laboratory). This study includes 9 recycled mixtures from NH and one virgin mixture from VA evaluated by complex modulus, DCT, and SCB fracture testing. The following conclusions can be drawn from the results of testing and analysis:

- All levels of long term aging have made a significant difference on linear viscoelastic properties (|E*| and δ) as compared with the properties measure at the STOA level. There was a similar trend in the variation of dynamic modulus and phase angle at different aging levels for the various mixtures. Based on the Black space diagram, the combination of higher dynamic modulus (at constant phase angle) and lower phase angle (at constant dynamic modulus) can be translated to higher thermal stress and higher relaxation capability, respectively.

- For the mixtures available in this study, 24 hour aged mixtures show very similar dynamic modulus and phase angle values with 12 days aged mixtures. Although 24 hour and 12 days aging create the similar effects on LVE properties, the fracture properties of asphalt mixtures obtained from SCB and DCT testing are not similar for these two aging levels.

- The shape parameters from dynamic modulus and phase angle master curves can indicate the relative aging levels and cracking behavior in mixtures. The evolution of characteristic shape parameters can be utilized in future to develop aging models.

- Generally, the fracture properties of asphalt mixtures (fracture energy, flexibility index, and fracture strain tolerance) decrease as the aging level changes from 5 days to higher levels of aging, but there is not an evident trend between the fracture properties of 24 hour and 12 days. For

the RAP/RAS mixtures, the 24 hour aged mixtures show better fracture properties than 12 days aged mixtures, while there is an inverse trend for most of the only RAP mixtures.

- The fatigue properties (C-S and G^R-N_f) of asphalt mixtures at different aging levels do not follow a consistent trend.

- The statistical analysis shows good correlations between dynamic modulus and phase angle shape parameters. The "c" parameter that is related to horizontal location of phase angle master curve in Lorentzian equation correlates very good with mixture based G-R parameter.

- This study supports 12 days at 95°C aging protocol on basis of fracture test results that indicate increased brittleness compared with 5 days aging level. This recommendation is based on the available mixtures from New Hampshire in this study, and it could change for different materials as binder and mixture testing are conducted on the field cored samples.

Future Work

Additional mixture testing and analysis are underway to compare the cracking properties of long term aged and short term aged mixtures. Most of the mixtures were placed in the field during the 2013 construction season and are being monitored. The cracking performance of field aged asphalt mixtures will be evaluated by laboratory testing on field cored samples. Also, additional mixtures from different areas and with a wider range of binder grades and recycled materials are anticipated to be evaluated.

Further analysis is planned to investigate the correlation between the viscoelastic characteristics, damage coefficients, and different cracking mechanisms including fatigue and reflective cracking and their relationship with field performance. Work is being conducted on the development of an aging prediction model for LVE and fracture properties of asphalt mixtures and comparison with

other existing models such as global aging model (Mirza and Witczak, 1995) that is used in Pavement ME.

More investigation on the shape factors of phase angle master curve is anticipated such as the consideration of Booji and Thoone approximation method (1982).

Chapter 7

SUMMARY AND CONCLUSION

Throughout this dissertation, the cracking susceptibility of asphalt mixtures is investigated from some crack-related perspectives. The overall goal of this study is to improve the cracking performance of asphalt pavements and ride quality through a better design and prediction system. The work has been done to identify the impact of different variables such as rheological parameters, fabrication type, and aging level on the behavior of fatigue and thermal cracking.

A short summary of technical chapters is presented below, as well as the most important closing remarks relevant to each chapter, and how these conclusions can lead to improve the cracking performance of asphalt pavements.

Moving towards the performance based design methods, the prediction of asphalt mixture performance in mix design stage is desired. To be able to accurately predict the field performance in laboratory, the understanding of differences between asphalt production in plant and laboratory, and the relationship between their behavior is required. Designing asphalt mixtures based on laboratory results without considering the differences between plant and lab production might result in an over or underestimated design. The fatigue cracking properties of asphalt mixtures produced in 2 plants have been compared with the corresponding lab produced mixtures, using both experimental testing on binders and mixtures, and numerical modeling in chapter 3. Higher

stiffness and lower relaxation capability were observed for most of the lab produced mixtures and also their recovered binders, compared to plant produced mixtures indicating more aging for lab produced mixtures. However, the viscoelastic and fatigue behavior of mixtures seems to be more plant dependent than mixture dependent. In the other words, a similar trend might be observed for different mixtures produced in a specific plant. To keep this in mind, the relative effects of different plants on the properties of asphalt mixtures can assessed, and shift factors or safety factors values can be applied in performance-based design specifications.

Many parameters have been developed in literature to evaluate the cracking behavior of asphalt mixtures and asphalt binders, based on different testing methods and approaches. In chapter 4, various commonly used and recent parameters and criteria for the assessment of both fatigue and thermal cracking are discussed. In the binder side, some viscoelastic characteristics and rheological properties are considered, and the mixtures parameters include viscoelastic characteristics, shape parameters, and fatigue and fracture testing properties. The Pearson correlation factor is used to evaluate the correlation between the parameters in terms of values and ranking. Generally, the binder cracking parameters show better correlation with each other than the mixtures cracking parameters. Asphalt binder is a less complicated material than asphalt mixture, and the criteria and approaches for binder are better established. To compare binder and mixture parameters together, a good correlation can be barely seen. The main reasons for the poor correlation values might be different testing modes (linear mode in binder testing versus nonlinear mode in mixture testing), different mechanisms in fatigue and thermal cracking, and different aging levels of binder and mixture samples. The current binder testing available in specifications are not sufficient to capture the cracking behavior of asphalt mixtures. Inclusion the fatigue and thermal cracking properties of asphalt mixtures in specifications is recommended.

A comparison of fatigue and thermal cracking behavior is conducted in chapter 5 using the experimental testing and numerical modeling. Uniaxial tensile fatigue based on simplified viscoelastic continuum damage (SVECD) approach and disc-shaped compact tension are the experimental testing used in this section. The numerical modeling was done through three approaches: layered viscoelastic pavement analysis for critical distresses (LVECD) software, the thermal cracking model used in Pavement ME, and the IlliTC thermal cracking simulation systems. Neither the results of experimental methods nor numerical modeling rank and evaluate the fatigue and thermal cracking behavior of asphalt mixture similarly. Considering different mechanisms for initiation and propagation of fatigue and thermal cracking, this study indicates that caution should be exercised to use similar criteria and parameters to assess fatigue and thermal cracking in asphalt mixtures.

The last technical chapter investigates the influence of laboratory conditioning of asphalt mixtures on the linear viscoelastic, fatigue, and fracture properties of asphalt, by simulating the long term aging of loose mix asphalt and compacted specimens in ovens at different aging levels. All the current cracking parameters and thresholds are developed for short term aged condition. Asphalt mixtures are required to be evaluated in long term aged condition as well, since the characteristics of different mixtures might change differently, as the asphalt material age. The current aging standard (AASHTO R-30), the Asphalt Institute procedure, and two aging levels based on an active NCHRP project on long term aging were used. The variation of asphalt mixtures properties at different aging levels are investigated. Different aging levels make significant differences on the linear viscoelastic parameters of short term aged mixtures. Although, two aging levels (24 hr. at 135°C and 12 days at 95°C) can make a similar difference on linear viscoelastic properties of asphalt mixtures, the results of SVECD fatigue testing and fracture parameters do not show a

similar trend for these mixtures. The shape factors obtained from the master curves have shown the potential of the prediction of fracture characteristics of asphalt mixtures.

This dissertation makes a good contribution in asphalt industry to improve the cracking evaluation and prediction approaches. Overall, the following conclusion remarks can be drawn from this research:

- The prediction of asphalt pavement cracking performance based on laboratory testing and numerical modeling does not seem to be an accurate way without considering the differences between the production in plant and lab. Findings of this study show different trends for fatigue performance of mixtures produced in plant and lab. More investigation on additional mixtures and from different plants is required to find a correlation between the mixtures behavior produced in design and production stages and apply a shift factor based on plant type and mixtures properties in specifications.
- The evaluation of mixtures with similar stiffness and relaxation capability conditioned in two levels of aging (i.e. 24 hr. at 135°C and 12 days at 95°C), or with different production type (plant versus lab) show the mixtures with similar linear viscoelastic characteristics (dynamic modulus and phase angle) does not necessarily have similar cracking behavior against fatigue or thermal cracking. Although, linear viscoelastic properties are important factors, but they do not seem to be sufficient for the evaluation of cracking susceptibility.
- This study supports the longer exposure time at the aging temperatures lower than 100°C. 12 days at 95°C is the long term aging level recommended for the mixtures in the climate conditions similar to New Hampshire. The aging exposure time should be adjusted for the mixtures from different regions of country.

- The binder cracking parameters from current specification or the other recently developed binder parameters are not able to accurately predict the cracking behavior of asphalt mixtures obtained from laboratory testing or numerical modeling. However, the cracking performance of field cored specimens should be monitored and evaluated to compare with experimental results, the mixture-related cracking criteria seem to be required in specifications.
- The promising trends observed in the correlation of fracture properties (from DCT testing) and the shape factors of asphalt mixtures can result in a prediction model for thermal cracking potential. There are opportunities to extend this research to develop new thresholds for cracking criteria with the consideration of aging effect in performance based specifications.
- The results of this research is important to the community, as it relates to fatigue and thermal cracking which are two major types of distresses in asphalt pavements especially in northern climate areas, and the capabilities of this study can result in cost saving to DoTs and contractors through maximizing the efficiency in selection the raw materials and design, and ultimately to taxpayers.

It should be noted that the efforts performed in this study are intended to serve as a guideline to asphalt industry with the aim of improving cracking performance of pavements. The future work is required by expanding the data base from different locations of country, evaluating the cracking criteria, and developing new parameters for fatigue and thermal cracking in performance based specifications. The results of this research will help to identify the most efficient mixtures and improve pavement service life and ride quality benefitting the asphalt industry and travelling public

LIST OF REFERENCES

"A Manual for Design of Hot Mix Asphalt with Commentary", NCHRP, Report No. 673, Transportation Research Board of the National Academics, 2012

Airey, G. D. "State of the Art Report on Ageing Test Methods for Bituminous Pavement Materials." International Journal of Pavement Engineering, 2003: 165 — 176.

American Association of State Highway and Transportation Officials, "Standard Method of Test for Determining the Dynamic Modulus and Flow Number for Hot-Mix Asphalt (HMA) Using the Asphalt Mixture Performance Tester (AMPT)," AASHTO TP 79-15, Washington, D.C., 2015.

American Association of State Highway and Transportation Officials, "Standard Method of Test for Quantitative Extraction of Asphalt Binder from Hot Mix Asphalt (HMA), AASHTO T 164-08

American Society for Testing and Materials, "Standard Practice for Recovery of Asphalt from Solution Using Toluene and the Rotary Evaporation", ASTM D 7906-14

American Association of State Highway and Transportation Officials, "Standard Specification for Performance Graded Asphalt Binder", AASHTO MP1-93

American Association of State Highway Transportation Officials (AASHTO), AASHTO TP 107, "Determining the Damage Characteristic Curve of Asphalt Concrete from Direct Tension Cyclic Fatigue Tests*"* (2014)

American Association of State Highway and Transportation Officials, "Standard Method of Test for Determining the Dynamic Modulus and Flow Number for Hot-Mix Asphalt (HMA) Using the Asphalt Mixture Performance Tester (AMPT)," AASHTO TP 79-15, Washington, D.C., 2015.

Anderson, D., Lapalu, L., Marasteanu, M., Hir, Yann, Planche J., Martin, D., 2014, "Low-Temperature Thermal Cracking of Asphalt Binders as Ranked by Strength and Fracture Properties" Journal of Transportation Research Board, volume 1766, DOI: 10.3141/1766-01

Al-Khateeb, G., Stuart, K., Mogawer, W., Gibson, N., 2008, “Fatigue Performance, Asphalt Binders versus Mixtures versus Full-Scale Pavements”, Canadian Journal of Transportation, Vol. 2, Part 1

Al-Qadi, I., Ozer, H., Lambros, J., Khatib, A., Singhvi, P., Khan, T., Rivera, J., Doll, B. (2015). “Testing Protocols to Ensure Performance of High Asphalt Binder Replacement Mixes Using RAP and RAS,” Report No. FHWA-ICT-15-017, *Illinois Center for Transportation, Rantoul, IL*.

Anderson, D.A., Christensen, D.W., Bahia, H.U., Dongré, R.N., Sharma, M.G., Antle, C.E., and Button, J., “Binder Characterization and Evaluation,” SHRP A-369, Vol. 3 Physical Characterization, Strategic Highway Research Program, National Research Council, Washington, D.C., 1994.

Anderson, M., G. King, D. Hanson, and P. Blankenship, “Evaluation of the Relationship 2 Between Asphalt Binder Properties and Non-Load Related Cracking” Journal of the Association of Asphalt Paving Technologists, Vol. 80, 2011, pp. 615-661

Aragão, F. and Y.-R. Kim (2012). "Mode I fracture characterization of bituminous paving mixtures at intermediate service temperatures." Experimental Mechanics 52(9): 1423- 1434.

Artamendi, I., and Khalid, H., “Different Approaches to Depict Fatigue of Bituminous Materials” University of Liverpool

Aschenbrener, T. and Far, N., “Influence of Compaction Temperature and Anti-Stripping Treatment on the Results from the Hamburg Wheel-Tracking Device,” Rpt # CDOT-DTDR-94-9, Colorado Department of Transportation, July 15, 1994.

Baek, J., H. Ozer, H. Wang, and I. Al-Qadi (2010). “Effects of Interface Conditions of Reflective Cracking Development in Hot-Mix Asphalt Overlays,” Road Materials and Pavement Design, 11(2), pp. 307-334.

Bahia, H. U., Hanson, D. I., Zeng, M., Zhai, H., Khatri, M. A., Anderson, R. M., 2001, “Characterization of Modified Asphalt Binders in Superpave Mix Design” NCHRP report No.459, Transportation Research Board

Bell, C. A., Y. AbWahab, R. E. Cristi, and D. Sognovske. (1994). "Selection of Laboratory Aging Procedures for Asphalt-Aggregate Mixtures." Washington, DC: Strategic Highway Research Program, National Research Council, 1994.

Bennert, T., Ericson, C., Corun, R., Fee, F., (2016), "Performance of Asphalt Binders Modified with Re-refined Engine Oil Bottoms (REOB)" Tylor & Francis Group, London, ISBN 978-1-138-02924-8

Bonaquist, R. (2011). NCHRP Report 702: Precision of the Dynamic Modulus and Flow Number Tests Conducted with the Asphalt Mixture Performance Tester. Transportation Research Board, Washington, D.C.

Brown, S. F., and Scholz, T. V. (2000). Development of Laboratory Protocols for the Aging of Asphalt Mixtures. I, pp. vol. 1, pp. 83-90. 2nd Eurasphalt and Eurobitume Congress.

Brown, E. R., Kandhal, P. S., Roberts, F. L., Kim, Y. R., Lee, D., and Kennedy, T. W., "Hot Mix Asphalt Materials, Mixture, Design, and Construction", 2009, NAPA Research and Education Foundation, Third edition

Cao, W., Norouzi, A., and Kim, Y. R. (2016), "Application of Viscoelastic Continuum Damage Approach to Predict Fatigue Performance of Binzhou Perpetual Pavements", Journal of Traffic and Transportation Engineering, Vol. 3, Pages 104-115.

Chehab, G., Kim, Y. R., Schapery, R. A., Witczak, M. W., and Bonaquist, R., (2003), "Characterization of Asphalt Concrete in Uniaxial Tension using a Viscoelastoplastic Continuum Damage Model", Journal of the Association of Asphalt Paving Technologists.

Christison, J.T., Murray, D.W. and Anderson, K.O. (1972) "Stress Prediction and Low Temperature Fracture Susceptibility of Asphaltic Concrete Pavements", Proceedings of the Association of Asphalt Paving Technologists, Vol. 41, 494-523.

Collop, A., Choi, Y., Airey, G., and Elliott, R. (2004). Development of a Combined Aging / Moisture Sensitivity Laboratory Test. Vienna: 4th Euroasphalt and Eurobitume Congress.

Cowher, K. Cumulative Damage of Asphalt Materials under Repeated-Load Indirect Tension, Research Report Number 183-3, Center for Highway Research – University of Texas at Austin, Austin, TX, 1975.

Daniel, J. S., Airey, G., Oshone., M., Rahbar-Rastegar, R., Jimenez del Barco Carrion, A., Pires, G., Bailey, H., Smith, D., 2017, "Evaluating the Impact of Laboratory Asphalt Mixture Preparation Methods during Mix Design to Simulate Plant Produced Material" 7th European Asphalt Technology Association (EATA) Conference, Zurich, Switzereland

Daniel, J. S., and Kim, Y. R. (2002), "Development of a Simplified Fatigue Test and Analysis Procedure Using a Viscoelastic, Continuum Damage Model" Journal of the Association of Asphalt Paving Technologists", V. 71, P. 619-650

Daniel J.S. and Rahbar-Rastegar, R., 2016, "Correlation between Laboratory and Plant Produced High RAP/RAS Mixtures", technical report, FHWA-NH-RD-15680R

Dave, E. V., & Buttlar, W. G. (2010). Low temperature cracking prediction with consideration of temperature dependent bulk and fracture properties. Road Materials and Pavement Design, 11(sup1), 33-59.

Dave, E.V., W.G. Buttlar, S.E. Leon, B. Behnia, and G.H. Paulino (2013). "IlliTC – Low Temperature Cracking Model for Asphalt Pavements," Road Materials and Pavement Design, 14(Sup. 2), pp. 57-78.

Dave, E. V., & Hoplin, C. (2015). Flexible pavement thermal cracking performance sensitivity to fracture energy variation of asphalt mixtures. Road Materials and Pavement Design, 16(sup1), 423-441.

Dave, E.V., C. Hoplin, B. Helmer, J. Dailey, D. Van Deusen, J. Geib, S. Dai, and L. Johanneck (2016a). Effects of Mix Design and Fracture Energy On Transverse Cracking Performance of Asphalt Pavements in Minnesota. Transportation Research Record, 2576, pp. 40-50, 2016.

Dave E.V. and B. Behnia (2016b). Cohesive Zone Fracture Modelling of Asphalt Pavements with Applications to Design of High Performance Asphalt Overlays. (article submitted for publication).

De la Roche, C., Van de Ven, M., Van den Bergh, W., Gabet, T., Dubois, V., Grenel, J., and Porot, L. (2009). Development of a Laboratory Bituminous Mixtures Aging Protocol. Advanced Testing and Characterization of Bituminous Materials 331

de Souza, F.V., J.B. Soares, D.H. Allen, and F. Evangelista, Jr. (2004). “Model for Predicting Damage Evolution in Heterogeneous Viscoelastic Asphaltic Mixtures,” Transportation Research Record, 1891, pp. 131-139.

Elwardany, M. D., Yousefi Rad, F., Castorena, C., Kim, R. Y., “Evaluation of Asphalt Mixture Laboratory Long-Term Aging Methods for Performance Testing and Prediction”, 2016, Journal of Asphalt Paving Technologists Association, in press

Eslaminia, M., Thirunavukkarasu, S., Guddati, M. N., & Kim, Y. R. (2012). Accelerated pavement performance modeling using layered viscoelastic analysis. Proceedings of the 7th international RILEM conference on cracking in pavements, Delft, The Netherlands.

Estakhri, C.K., J.W. Button, A. Alvarez Lugo, 2010. Field and Laboratory Investigation of Warm Mix Asphalt in Texas. Report 5597-2, Texas Transportation Institute, Texas A&M University, College Station, Texas.

Fernandez-Gomez, W. D., Quintana, H. A., Reyez-Lizcano, F., “A review of asphalt and asphalt mixture aging”

Finn, F., Saraf, C.L., Kulkarni, R., Nair, K., Smith, W., and Abdullah, A. (1977), User’s Manual for the Computer Program Cold, NCHRP Report 1-10B, Transportation Research Board, Washington, D.C.

Glaser, R., Schabron, J., Turner, T., Planche, J.P., Salmans, S., Loveridge, J., “Low temperature oxidation kinetics of asphalt binders”, Transp. Res. Rec. 2370 (2013) 63–68

Glover, C.J., Davison, R.R., Domke, C.H., Ruan, Y., Juristyarini, P., Knorr, D.B., and Jung, S.H., “Development of a New Method for Assessing Binder Durability with Field Validation,” Report FHWA/TX-05/1872-2, Texas Department of Transportation, Austin, TX, 2005.

Glover, C. J., Martin, A. E., Chowdhury, A., Han, R., Prapaitrakul, N., Jin, X., Lawrence, J., “Evaluation of Binder Aging and its Influence in Aging of Hot Mix Asphalt Concrete: Literature Review and Experimental Design” FHWA/Texas report, 2009

Hachiya, Y., Nomura, K., and Chen, J. (2003). Accelerated Aging Test for Asphalt Concretes. Zurich: 6th RILEM Symposium PTEBM.

Hajj, R. and Bhasin, A. (2017), "The search for a measure of fatigue cracking in asphalt binders- a review of different approaches", International Journal of Pavement Engineering, http://dx.doi.org/10.1080/10298436.2017.1279490

Haslett, K. E., Dave, E. V., Daniel, J. S., (2017), "Exploration of Temperature and Loading Rate Interdependency for Fracture Properties of Asphalt Mixtures", International Conference on Advances in Construction Materials and Systems, ICACMS

Herrington, P. R., J. E. Patrick, and G. F. Ball (1994). Oxidation of Roading Asphalts. Industrial and Engineering Chemistry Research, Vol. 33 (11), pp. 2801-2809.

Hill, C. L., Widyatmoko, I., Heslop, M. W., Elliott, R. C., Williams, J. T., (2008), "Ageing Profile and Low Temperature Control Tests", Euroasphalt & Eurobitume Congress, Copenhagen.

Hills, J.F. and Brien, D. (1966) "The Fracture of Bitumens and Asphalt Mixes by Temperature Induced Stresses", Prepared Discussion, Proceedings, the Association of Asphalt Paving Technologists, Vol. 35, 292 – 309.

Hou, T., Underwood, B. S., and Kim, Y. R., (2010), "Fatigue Performance Prediction of North Carolina Mixtures Using Simplified Viscoelastic Continuum Damage Model. Journal of the Association of Asphalt Paving Technologists", Vol. 79, 2010, pp. 35–80.

Huang, B., Shu, X., and Zuo, G., "Using Notched Semi Circular Bending Fatigue Tests to Characterize Fracture Resistance of Asphalt Mixtures," Journal of Engineering Fracture Mechanics, Vol. 109, 2013, 78-88.

Jacques, C., Daniel, J. S., Bennert, T., Reinke, G., Norouzi, AmirHossein, Ericson, C., Mogawer, W., Kim, R., 2016, "Effect of Silo Storage Time on the Characteristics of Virgin and RAP Asphalt Mixtures", Journal of Transportation Research Board, in press

Jemere, Y., (2010), "Development of A Laboratory Ageing Method for Bitumen in Porous Asphalt", M. Sc. Thesis, Delf University of Technology

Johnson, E., Johnson, G., Dai, S., Linell, D., McGraw, J., Watson, M., "Incorporation of Recycled Asphalt Shingles in Hot Mixed Asphalt Pavement Mixtures," Minnesota Department of Transportation, 2010, 83p.

Kandhal, P. S., and Koehler, W. C., 1987 "Effect of Rheological Properties of Asphalt on Pavement Cracking" American Society of Testing and Materials, pp. 99-117

Keshavarzi, B., Kim, Y.R., (2016) “A viscoelastic-based model for predicting the strength of asphalt concrete in direct tension, Construction and Building Materials”. 122, pp. 721–727

Kim, Y. and F.T.S. Aragão. (2013). “Microstructure Modeling of Rate-Dependent Fracture Behavior in Bituminous Paving Mixtures.” Finite Elements in Analysis and Design, 63, pp. 23-32.

Kim, Y. 2011, “Cohesive Zone Model to Predict Fracture in Bituminous Materials and Asphaltic Pavements: State-of-the-Art Review” International Journal of Pavement Engineering, pp.343-356

Kim, Y. R., Daniel, J. S., Wen, H., 2002, “Fatigue Performance Evaluation of WesTrack Asphalt Mixtures Using Viscoelastic Continuum Damage Approach” FHWA Report

Kim, Y., and Lee, H., (2003), “Evaluation of the Effect of Aging on Mechanical and Fatigue Properties of sand Asphalt Mixtures” KSCE Journal of Civil Engineering, Vol. 7, No. 4.

Lavin, P. G., (2003), “Asphalt Pavement, a practical guide to design, production, and maintenance for engineers and architects”, Spon Press.

Li, X. J. and M. O. Marasteanu (2009). "Using Semi Circular Bending Test to Evaluate Low Temperature Fracture Resistance for Asphalt Concrete." Experimental Mechanics 50(7): 867-876.

Lolly, R. (2013), “Evaluation of Short Term Aging Effect of Hot Mix Asphalt Due to Elevated Temperatures and Extended Aging Time” Master of Science Thesis, Arizona State University

Lytton, R. L., Roque, R., Uzan, J., Hiltunen, D. R., Fernando, E., & Stoffels, S. M. (1993). *Performance models and validation of test results* (Final Report to Strategic Highway Research Program; Asphalt Project A-005, SHRP Report A-357). Washington, DC.

Marasteanu, M., K.H. Moon, E.Z. Teshale, A.C. Falchetto, M. Turos, W. Buttlar, E. Dave and others, “Investigation of Low Temperature Cracking in Asphalt Pavements,” National Pooled Fund Study -Phase II, Report No. MN/RC 2012-23, Minnesota Department of Transportation, August 2012.

Marasteanu, M., A. Zofka, M. Turos, X. Li, R. Velasquez, X. Li, C. Williams, J. Bausano, and others (2007). "Investigation of Low Temperature Cracking in Asphalt Pavements", Report No. 776, Minnesota Department of Transportation, St. Paul, MN.

McDaniel, R. S., Soleymani, H., Shah, A., "Use of Reclaimed Asphalt Pavement (RAP) Under Superpave Specifications: A Regional Polled Fund Study" 2002, Purdue University

Mensching, D. J., Rahbar-Rastegar, R., Underwood, B. S., Daniel, J. S., (2016) "Identifying Indicators for Fatigue Cracking in Hot Mix Asphalt Pavements using Viscoelastic Continuum Damage Principles", In press, *Journal of the Transportation Research Board*

Mensching, D. J., Rowe, G. M., and Daniel, J. S., 2016, "A Mixture-Based Black Space Parameter for Low Temperature Performance of Hot Mix Asphalt" Journal of the Association of Asphalt Paving Technologists, in press

Mensching, D. J., "Developing Index Parameter for Cracking in Asphalt Pavements Through Black Space and Viscoelastic Continuum Damage Principles" 2015, University of New Hampshire

Mogawer, W., T. Bennert, A. Austerman, and C. Ericson. 2015, "Investigating the Aging Mitigation Capabilities of Rejuvenators in High RAP Mixtures Using Black Space Diagrams, Binder Rheology and Mixture Tests. Journal of the Association of Asphalt Paving Technologists, Vol. 85

Mogawer, W., T. Bennert, J.S. Daniel, R. Bonaquist, A. Austerman, and A. Booshehrian (2012), "Performance Characteristics of Plant Produced High RAP Mixtures", International Journal of Road Materials and Pavement Design Vol.13, Sup. 1, 183- 208

Mogawer, W. S., Austerman, A., Al-Qadi, I. L., Buttlar, W., Ozer, H., and Hill, B., 2017, "Using Binder and Mixture Space Diagrams to Evaluate the Effect of Re-refined Engine Oil Bottoms on Binders and mixtures after ageing" Road Materials and Pavement Design, vol. 18

Mollenhauer, K., and Mouillet, V. (2011). Re-road – End of Life Strategies of Asphalt Pavements. European Commission DG Research.

Moon, K., Marasteanu, M., and Turos, M., 2013, "Comparison of Thermal Stresses Calculated from Asphalt Binder and Asphalt Mixture Creep Tests" Journal of Materials in Civil Engineering, ASCE

Moore, R.K. and Kennedy, T. W. Tensile Behavior of Subbase Materials under Repetitive Loading, Research Report 98-12, Center for Highway Research, University of Texas at Austin, Austin, TX, 1971.

Mouillet, V., Durrieu, J. L., Kister, J., and Martin, D. (2003). Development of a New Methodology for Characterization of Polymer Modified Bitumens Aging by Infrared Microspectrometry Imaging. Zurich: The 6th International RILEM Symposium, PTEBM.

Mugler, M. (1970). Die veranderung der Bitumeneigenschaften wabrend der Verarbeitung und in Fertigen Belag. Route et Traffic, 6.

Navarro, D. and Kennedy, T. W. Fatigue and Repeated-Load Elastic Characteristics of In-service Asphalt-Treated Pavement, Research Report No.183-2, Center for Highway Research, the University of Texas at Austin, Austin, TX, 1975.

Nemati, R. and Dave, E. V., 2017, "Nominal Property Based Predictive Models for Asphalt Mixture Complex Modulus (Dynamic Modulus and Phase Angle), Journal of Construction and Building Materials, in press

Norouzi, A., Sabouri, M., and Kim, Y. R., (2016). "Fatigue Life and Endurance Limit Prediction of Asphalt Mixtures Using Energy-Based Failure Criterion," International Journal of Pavement Engineering (IJPE), pp 1-14.

Norouzi, A., Sabouri, M., and Kim, Y. R. (2014), "Evaluation of the Fatigue Performance of Asphalt Mixtures with High RAP Content", Journal of Tylor and Francis Group, pp. 1069-1077.

Nsengiyumva, G., Kim, Y., You, T., 2015, "Development of a Semicircular Bend (SCB) Test Method for Performance Testing of Nebraska Asphalt Mixtures" Report SPRP1(15) MPMC07, University of Nebraska

Petersen J. C., Harnsberger, P., Asphalt aging: dual oxidation mechanism and its interrelationships with asphalt composition and oxidative age hardening, Transp. Res. Rec. 1638 (1998) 47–55.

Rahbar-Rastegar, R., and Daniel, J., (2016), "Mixture and Production Parameters Affecting Cracking Performance of Mixtures with RAP and RAS", Proceedings of 8th RILEM International Conference on Mechanisms of Cracking and Debonding in Pavements, V. 13, pp 307-312

Rahbar-Rastegar, R., and Daniel, J., (2016b), "Laboratory versus Plant Production: Impact of Material Properties and Performance for RAP and RAS Mixtures", International Journal of Pavement Engineering, pp 1-12.

Read, J., and Whiteoak, D. (2003). The Shell Bitumen Handbook. 5th Ed. London: Thomas.

Reed, J. (2010). Evaluation of the Effects of Aging on Asphalt Rubber Pavements. Masters Thesis, PhD Dissertation., Arizona State University.

Reinke, G., Hanz, A., Anderson, R. M., Ryan, M., Engber, S., Herlitzka, D., 2016, "Impact of Re-refined Engine Oil Bottoms on Binder Properties and Mix Performance on Two Pavements in Minnesota", 6th Eurasphalt & Eurobitume Congress, Prague, Czech Republic

Rowe, G. M. Prepared Discussion for the AAPT paper by Anderson et al.: Evaluation of the Relationship between Asphalt Binder Properties and Non-Load Related Cracking, Journal of the Association of Asphalt Paving Technologists, Vol. 80, 2011, pp. 649-662.

Rowe, G. M., Baumgardner, G., and Sharrock, M., 2009, "Functional forms for master curve analysis of bituminous materials" Proceedings of the 7th International RILEM Symposium ATCBM09 on Advanced Testing and Characterization of Bituminous Materials, Rhodes, Greece

Rowe, G. (2009). Phase Angle Determination and Interrelationships within Bituminous Materials. *7th International RILEM Symposium on Advanced Testing and Characterization of Bituminous Materials, Book 1 (Edited by Loizos, Partl, Scarpas and Al-Qadi), Rhodes, Greece, pp. 43-52.*

Rowe, G. M., King, G., and Anderson, M., 2014, "The Influence of Binder Rheology on the Cracking of Asphalt Mixes in Airport and Highway Projects", ASTM Journal of Testing and Evaluation, Vol. 42, No. 5

Sabouri, M. and Kim Y. R. (2014), "Development of Failure Criterion for Asphalt Mixtures under Different Modes of Fatigue Loading", Transportation Research Record: Journal of Transportation Research Board.

Sabouri, M., Bennert, T., Daniel, J.S., and Kim, Y.R., "A Comprehensive Evaluation of the Fatigue Behavior of Plant-Produced RAP Mixtures,", Journal of Association of Asphalt Paving Technologists, Vol. 84, 2015.

Sabouri, M., T. Bennert, J.S. Daniel, and Y.R. Kim. "Evaluating Laboratory-Produced Asphalt Mixtures with RAP in Terms of Rutting, Fatigue, Predictive Capabilities, and High RAP Content Potential." Transportation Research Record: Journal of the Transportation Research Board, National Academics, Washington, D.C., 2015.

Safaei, F., Castorena, C., and Kim., Y. R., 2016, "Linking Asphalt Binder Fatigue to Asphalt Mixture Fatigue Performance using Viscoelastic Continuum Damage Modeling", Mechanics of Time-Dependent Materials, Vio. 20, Issue 3, p 299-323

Song, S. H., Paulino G. H., and Buttlar W. G., 2006 "A bilinear cohesive zone model tailored for fracture of asphalt concrete considering viscoelastic bulk material", Engineering Fracture Mechanics 73 (2006) 2829-2848

Such, C., Ballie, M., Lombardi, B., Migliori, F., Ramond, G., Samanos, J., and Simoncelli, J. P. (1997). Susceptibilite au vieillissement des bitumen - Experimentation A08. LCPC. Paris: Bitume, GNB - Groupe National.

Sui, C., Farrar, M. J., Tuminello, W. H., and Turner, T., 2010, "New Technique for Measuring Measuring Low-Temperature Properties of Asphalt Binders with Small Amounts of Material", Transportation Research Board, Journal of the Transportation Research Board, Vol. 2179

Tayebali, A.A., Rowe, G.M. and Sousa, J.B., J. Assoc. Asphalt Paving Technologists, vol. 61, 333-360, 1992.

Van Dijk, W and Visser, W., J. Assoc. Asphalt Paving Technologists, vol. 46, 1-40, 1977
Underwood, B.S., and Y.R. Kim, 2010, "Improved calculation method of damage parameter in viscoelastic continuum damage model", International Journal of Pavement Engineering, Vol. 11, p459-476

Van Deusen, D., Johanneck, L., Geib, J., Garrity, J., Hanson C. & Dave, E.V. (2015). DCT low temperature fracture testing pilot project (Final Report 2015-20). St. Paul, MN: Minnesota Department of Transportation.

Van Gooswilligen, G., De Bats, F., and Harrison, T. (1989). Quality of Paving Grade Bitumen - a Practical Approach in Terms of Functional Tests. Proc. 4th Eurobitume Symp., pp. 290-297.

Verhasselt, A. F., and Vanelstraete A. (2000), "Long-term ageing comparison between PAV and RCAT ageing tests." 2nd Proceedings of Eurasphalt & Eurobitume Congress. Barcelona, 897–905.

Wagoner, M. P., W. G. Buttlar, and G. H. Paulino. (2005) "Disk-Shaped Compact Tension Test for Asphalt Concrete Fracture," Experimental Mechanics, Vol. 45, pp. 270-277.

Wang, Y., Norouzi, A., and Kim, Y. R. (2015), "Comparison of Failure Cracking Performance Predictions in Asphalt Pavements Using Pavement ME and LVECD Programs" Transportation Research Record: Journal of the Transportation, National Academics, Washington, D.C., 2015.

Xiao, F., Putman, B., and Amirkhanian, Serji., "Plant and Laboratory Compaction Effects on Performance Properties of Plant-Foamed Asphalt Mixture Containing RAP," 2014, Journal of Materials in Civil Engineering, ASCE

Yao, H., Dai, Q., You, Z., Ye, M., Yap., Y., 2016 "Rheological Properties, Low Temperature Cracking Resistance, and Optical Performance of Exfoliated Graphite Nanoplatelets Modified Asphalt Binder" Journal of Construction and Building Materials, Volume 113, pp. 988-996

Yousefi rad, F., Elwardany, M. D., Castorena, C., and Kim, R. Y., 2017, "Investigation of Proper Long-term Laboratory Aging Temperature for Performance Testing of Asphalt Concrete" Construction and Building Materials, 147, pp 616-629

Zhu, Y., Dave, V. E., Rahbar-Rastegar, R., Daniel, J. S., and Zofka, A., (2017) "Comprehensive Evaluation of Low Temperature Fracture Indices for Asphalt Mixtures" Road Materials and Pavement Design (article in press)

Zofka, A., and Braham, A., 2009, "Comparison of Low-temperature Field Performance and Laboratory Testing of 10 Test Sections in the Midwestern United States", Journal of Transportation Research Board, volume 2127

APPENDIX

IlliTC and TCModel Models Input data

Table A- 1. Shift Factors for Different Mixtures

PG 52-34, 12.5mm, 18.9% RAP		PG 52-34, 12.5mm, 28.3% RAP		PG 52-34, 12.5mm, 18.5% RAPRAS	
$1/\log(a_T(0))$	-2.9392	$1/\log(a_T(0))$	-2.948	$1/\log(a_T(0))$	-2.9429
$1/\log(a_T(-10))$	-4.5402	$1/\log(a_T(-10))$	-4.618	$1/\log(a_T(-10))$	-4.6749
$1/\log(a_T(-20))$	-6.2812	$1/\log(a_T(-20))$	-6.468	$1/\log(a_T(-20))$	-6.6269
PG 58-28, 12.5mm, 18.9% RAP		PG 58-28, 12.5mm, 28.3% RAP		PG 58-28, 12.5mm, 18.5R RAPRAS	
$1/\log(a_T(0))$	-2.7826	$1/\log(a_T(0))$	-3.5891	$1/\log(a_T(0))$	-2.5764
$1/\log(a_T(-10))$	-4.4186	$1/\log(a_T(-10))$	-5.8411	$1/\log(a_T(-10))$	-3.7304
$1/\log(a_T(-20))$	-6.2546	$1/\log(a_T(-20))$	-8.4531	$1/\log(a_T(-20))$	-4.8444
PG 58-28, 12.5mm, 22.4% RAP		PG 58-28, 9.5mm, 21.3% RAP		PG 64-28, 9.5mm, 16.4% RAP	
$1/\log(a_T(0))$	-3.9834	$1/\log(a_T(0))$	-4.3951	$1/\log(a_T(0))$	-2.8182
$1/\log(a_T(-10))$	-6.5844	$1/\log(a_T(-10))$	-7.2931	$1/\log(a_T(-10))$	-4.3492
$1/\log(a_T(-20))$	-9.6454	$1/\log(a_T(-20))$	-10.7111	$1/\log(a_T(-20))$	-6.0002

Table A- 2. The Mixture Properties from DCT Testing

PG 58-28, 9.5mm, 21.3% RAP	
Fracture Energy (J/m2)	721.4
Tensile Strength (MPa)	4.754
Coefficient of Thermal Expansion	5.00E-05
PG 58-28, 12.5mm, 22.4% RAP	
Fracture Energy (J/m2)	604
Tensile Strength (MPa)	4.836
Coefficient of Thermal Expansion	5.00E-05
PG 64-28, 9.5mm, 16.4% RAP	
Fracture Energy (J/m2)	692.4
Tensile Strength (MPa)	3.81
Coefficient of Thermal Expansion	5.00E-05
PG 52-34, 12.5mm, 18.9% RAP	
Fracture Energy (J/m2)	703.2
Tensile Strength (MPa)	3.935
Coefficient of Thermal Expansion	5.00E-05
PG 58-28, 12.5mm, 28.3% RAP	
Fracture Energy (J/m2)	650.9
Tensile Strength (MPa)	4.308
Coefficient of Thermal Expansion	5.00E-05

Table A- 3. Creep Compliance Coefficients for Different Mixtures

	PG 52-34, 12.5mm, 18.9% RAP			PG 52-34, 12.5mm, 28.3% RAP			PG 52-34, 12.5mm, 18.5% RAPRAS		
t	D(0)	D(-10)	D(-20)	D(0)	D(-10)	D(-20)	D(0)	D(-10)	D(-20)
1	1.98E-04	8.86E-05	4.87E-05	1.79E-04	8.12E-05	5.06E-05	2.26E-04	9.36E-05	7.61E-05
2	2.39E-04	1.01E-04	5.01E-05	2.17E-04	9.12E-05	5.14E-05	2.68E-04	1.07E-04	7.63E-05
5	3.13E-04	1.19E-04	5.41E-05	2.86E-04	1.05E-04	5.37E-05	3.45E-04	1.30E-04	7.70E-05
10	3.82E-04	1.40E-04	5.99E-05	3.51E-04	1.22E-04	5.72E-05	4.20E-04	1.51E-04	7.81E-05
20	4.74E-04	1.67E-04	6.95E-05	4.38E-04	1.45E-04	6.33E-05	5.08E-04	1.76E-04	8.03E-05
50	6.33E-04	2.10E-04	8.67E-05	5.92E-04	1.82E-04	7.58E-05	6.72E-04	2.22E-04	8.65E-05
100	7.82E-04	2.56E-04	9.94E-05	7.38E-04	2.21E-04	8.64E-05	8.29E-04	2.63E-04	9.54E-05
200	9.81E-04	3.14E-04	1.12E-04	9.38E-04	2.73E-04	9.59E-05	1.02E-03	3.16E-04	1.09E-04
500	1.32E-03	4.09E-04	1.37E-04	1.29E-03	3.58E-04	1.13E-04	1.36E-03	4.11E-04	1.33E-04
1000	1.64E-03	5.10E-04	1.63E-04	1.63E-03	4.48E-04	1.33E-04	1.66E-03	4.97E-04	1.54E-04
	PG 58-28, 12.5mm, 18.9% RAP			PG 58-28, 12.5mm, 28.3% RAP			PG 58-28, 12.5mm, 18.5% RAPRAS		
t	D(0)	D(-10)	D(-20)	D(0)	D(-10)	D(-20)	D(0)	D(-10)	D(-20)
1	2.39E-04	9.97E-05	7.88E-05	1.08E-04	5.42E-05	5.25E-05	1.85E-04	1.08E-04	7.71E-05
2	2.91E-04	1.14E-04	7.92E-05	1.24E-04	5.59E-05	5.25E-05	2.19E-04	1.21E-04	8.16E-05
5	3.90E-04	1.39E-04	8.03E-05	1.53E-04	6.01E-05	5.25E-05	2.80E-04	1.46E-04	9.19E-05
10	4.89E-04	1.62E-04	8.21E-05	1.83E-04	6.56E-05	5.25E-05	3.38E-04	1.71E-04	1.03E-04
20	6.16E-04	1.93E-04	8.56E-05	2.18E-04	7.29E-05	5.26E-05	4.13E-04	2.01E-04	1.16E-04
50	8.56E-04	2.49E-04	9.48E-05	2.81E-04	8.43E-05	5.27E-05	5.45E-04	2.55E-04	1.38E-04
100	1.09E-03	3.04E-04	1.07E-04	3.44E-04	9.56E-05	5.29E-05	6.76E-04	3.07E-04	1.61E-04
200	1.39E-03	3.80E-04	1.24E-04	4.20E-04	1.10E-04	5.34E-05	8.46E-04	3.72E-04	1.88E-04
500	1.91E-03	5.12E-04	1.50E-04	5.62E-04	1.34E-04	5.46E-05	1.12E-03	4.90E-04	2.38E-04
1000	2.35E-03	6.48E-04	1.78E-04	7.04E-04	1.58E-04	5.65E-05	1.39E-03	6.04E-04	2.86E-04
	PG 58-28, 12.5mm, 22.4% RAP			PG 58-28, 9.5mm, 21.3% RAP			PG 64-28, 9.5mm, 16.4% RAP		
t	D(0)	D(-10)	D(-20)	D(0)	D(-10)	D(-20)	D(0)	D(-10)	D(-20)
1	8.12E-05	4.96E-05	4.92E-05	7.54E-05	4.81E-05	4.79E-05	1.61E-04	9.74E-05	8.20E-05
2	9.04E-05	5.00E-05	4.92E-05	8.31E-05	4.83E-05	4.79E-05	1.82E-04	1.06E-04	8.24E-05
5	1.04E-04	5.12E-05	4.92E-05	9.45E-05	4.87E-05	4.79E-05	2.18E-04	1.19E-04	8.38E-05
10	1.18E-04	5.29E-05	4.92E-05	1.05E-04	4.95E-05	4.79E-05	2.52E-04	1.32E-04	8.60E-05
20	1.34E-04	5.59E-05	4.92E-05	1.19E-04	5.09E-05	4.79E-05	2.96E-04	1.47E-04	8.99E-05
50	1.60E-04	6.23E-05	4.92E-05	1.39E-04	5.45E-05	4.79E-05	3.71E-04	1.72E-04	9.87E-05
100	1.87E-04	6.80E-05	4.92E-05	1.59E-04	5.88E-05	4.79E-05	4.47E-04	1.96E-04	1.08E-04
200	2.19E-04	7.39E-05	4.93E-05	1.83E-04	6.40E-05	4.79E-05	5.51E-04	2.26E-04	1.18E-04
500	2.73E-04	8.41E-05	4.94E-05	2.21E-04	7.11E-05	4.80E-05	7.27E-04	2.75E-04	1.34E-04
1000	3.29E-04	9.36E-05	4.96E-05	2.60E-04	7.78E-05	4.80E-05	9.06E-04	3.25E-04	1.50E-04